Status of Big Skate (*Beringraja binoculata*) Off the U.S. Pacific Coast in 2019

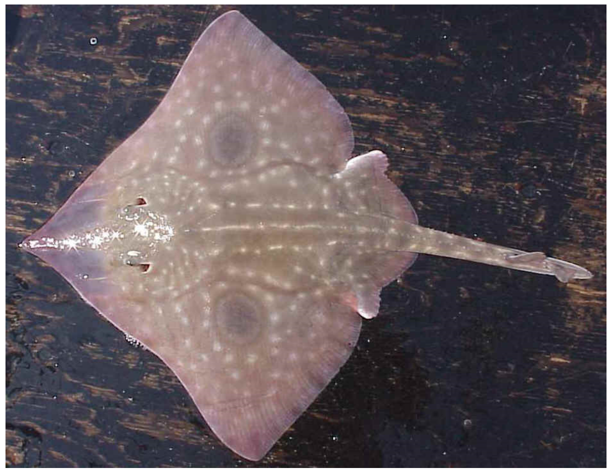

Ian G. Taylor[1]
Vladlena Gertseva[1]
Andi Stephens[2]
Joseph Bizzarro[3]

[1]Northwest Fisheries Science Center, U.S. Department of Commerce, National Oceanic and Atmospheric Administration, National Marine Fisheries Service, 2725 Montlake Boulevard East, Seattle, Washington 98112

[2]Northwest Fisheries Science Center, U.S. Department of Commerce, National Oceanic and Atmospheric Administration, National Marine Fisheries Service, 2032 S.E. OSU Drive Newport, Oregon 97365

[3]Southwest Fisheries Science Center, U.S. Department of Commerce, National Oceanic and Atmospheric Administration, National Marine Fisheries Service, 110 Shaffer Road, Santa Cruz, California 95060

This report may be cited as:

Taylor, I.G., Gertseva, V., Stephens, A. and Bizzarro, J. Status of Big Skate (*Beringraja binoculata*) Off the U.S. West Coast, 2019. Pacific Fishery Management Council, Portland, OR. Available from http://www.pcouncil.org/groundfish/stock-assessments/

Acronyms used in this Document

ABC	Allowable Biological Catch
ACL	Annual Catch Limit
AFSC	Alaska Fisheries Science Center
CDFW	California Department of Fish and Wildlife
DFO	Canada's Department of Fisheries and Oceans
DW	Disk Width
IFQ	Individual Fishing Quota
IPHC	International Pacific Halibut Commission
ISW	Interspiracular Width
NMFS	National Marine Fisheries Service
NWFSC	Northwest Fisheries Science Center
ODFW	Oregon Department of Fish and Wildlife
OFL	Overfishing Limit
OY	Optimum Yield
PacFIN	Pacific Fisheries Information Network
PFMC	Pacific Fishery Management Council
SPR	Spawning Potential Ratio
SSC	Scientific and Statistical Committee
SWFSC	Southwest Fisheries Science Center
TL	Total Length
VAST	Vector Autoregressive Spatio-Temporal Package
WCGBT	West Coast Groundfish Bottom Trawl Survey
WCGOP	West Coast Groundfish Observer Program
WDFW	Washington Department of Fish and Wildlife

Status of Big Skate (*Beringraja binoculata*) Off the U.S. Pacific Coast in 2019

Contents

References

Executive Summary

Stock

This assessment reports the status of the Big Skate (*Beringraja binoculata*) resource in U.S. waters off the West Coast using data through 2018. A map showing the area of the U.S. West Coast Exclusive Economic Zone covered by this stock assessment is provided in Figure a.

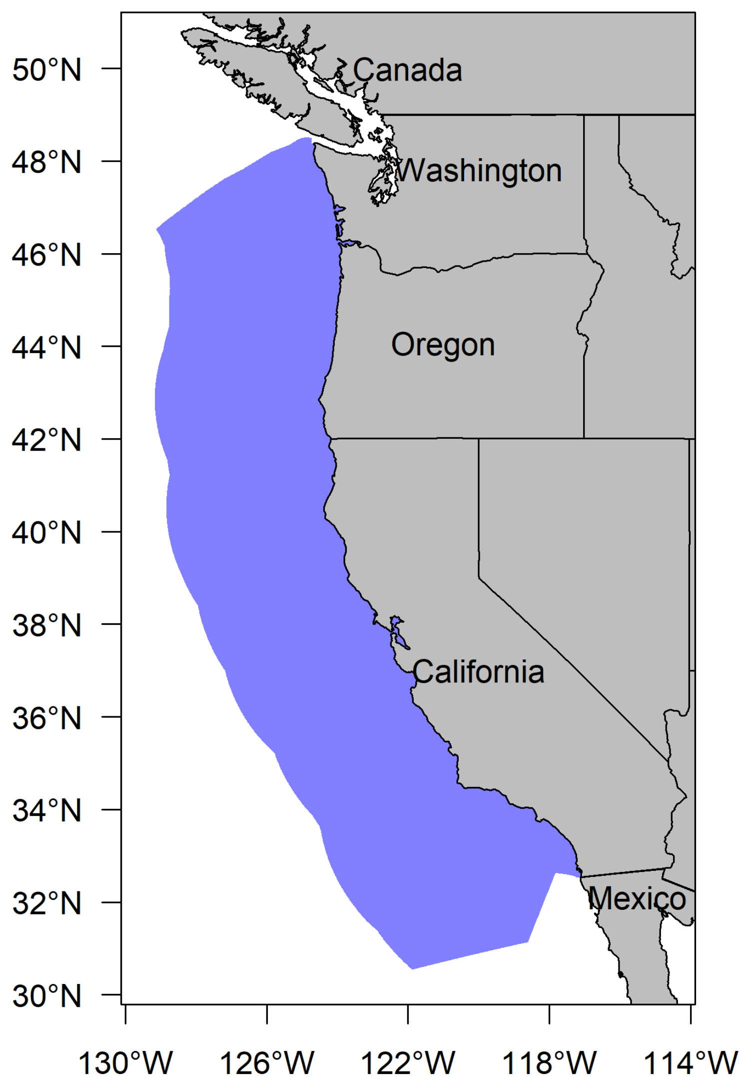

Figure a: U.S. West Coast Exclusive Economic zone covering the area in which this stock assessment is focused.

Catches

Landings and estimated discards of Big Skate were reconstructed for this assessment from historical records of other species and from species composition data collected in the recent fishery. These reflect the fishery from 1916-1994. The current fishery started in 1995. For records from 1995-2017, Big Skate landings were estimated from species-composition samples and the landings of "Unspecified Skates". Beginning in 2017, Big Skate have been recorded in species-specific landings.

In the current fishery (since 1995), annual total landings of Big Skate have ranged between 135-528 mt, with landings in 2018 totaling 173 mt.

Table a: Recent Big Skate landings (mt)

Year	Landings
2008	366.00
2009	205.70
2010	196.20
2011	268.40
2012	269.60
2013	135.00
2014	372.40
2015	331.50
2016	411.50
2017	277.60
2018	172.60

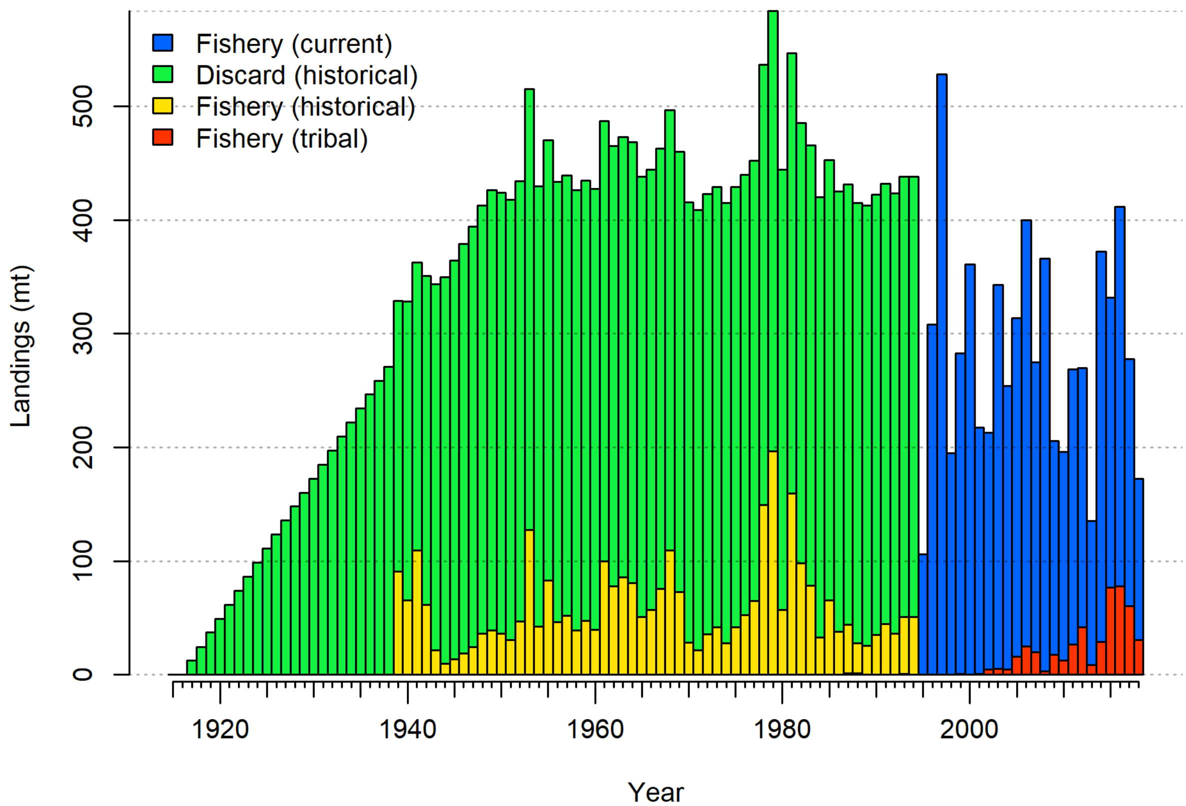

Figure b: Catch history of Big Skate in the model.

Data and Assessment

This the first full assessment for Big Skate. It is currently managed using an OFL which was based on a proxy for F_{MSY} and a 3-year recent average of survey biomass. This assessment uses the newest version of Stock Synthesis (3.30.13). The model begins in 1916, and assumes the stock was at an unfished equilibrium that year.

The assessment relies on two bottom trawl survey indices of abundance, the Triennial Survey from an index covering the period 1980–2004 was used here and the West Coast Groundifish Bottom Trawl (WCGBT) Survey, which began in 2003 and for which data is available through 2018. The triennial survey shows an increasing trend over the 25 year period it covers, which the model is not able to fit as this includes the peak period of the fishery when the stock would have been expected to be declining. The WCGBT Survey also shows an increasing trend, with the 5 most recent observations (2014–2018) all falling in the top 6 ever observed (2004 was the 5th highest observation). The model estimates an increasing trend during this period but the slope is more gradual than the trend in the survey. The misfit to these survey indices could be due to some combination of incorrect estimation of the catch history, variability in recruitment which is not modeled here, or biological or ecological changes for which data are not available.

Length composition data from the fishery is available starting in 1995 but is sparse until the past decade. Most of the ages are also from 2008 onward. This limits the ability of the model to estimate any changes composition of the population during the majority of the history of the fishery. Estimates of discard rates and mean body weight of discards are available for the years 2002 onward and discard length compositions are available starting in 2010.

The age and length data provide evidence for growth patterns and sex-specific differences in selectivity that are unusual among groundfish stocks that have been assessed within the U.S. West Coast and are not found in Longnose Skate where the data show little difference between the sexes. Growth appears to be almost linear and similar between females and males up to about age 7 or over 100 cm at which point male growth appears to stabilize while females continue to grow. However, in spite of the similar growth pattern for ages prior to 7, males are observed more frequently, with the 70–100 cm length bins often showing 60% males. Sex-specific differences in selectivity were included in the model in order to better match patterns in the sex ratios in the length composition data. The length and age data do not cover enough years or show enough evidence of distinct cohorts to reliably estimate deviations in recruitment around the stock-recruit curve.

The scale of the population is not reliably informed by the data due to the combination of surveys that show trends which can't be matched by the structure of the model and length and age data which inform growth and selectivity but provide relatively little information about changes in stock structure over time. Therefore, a prior on catchability of the WCGBT Survey (centered at 0.83) was applied in order to provide more stable results.

Although the assessment model requires numerous simplifying assumptions, it represents an improvement over the simplistic status-quo method of setting management limits, which relies on average survey biomass and an assumption about F_{MSY}. The use of an age-structured model with estimated growth, selectivity, and natural mortality likely provide a better estimate of past dynamics and the impacts of fishing in the future.

Stock Biomass

The 2018 estimated spawning biomass relative to unfished equilibrium spawning biomass is above the target of 40% of unfished spawning biomass at 75.0% (95% asymptotic interval: $\pm$ 63.9%-86.0%) (Figure ??). Approximate confidence intervals based on the asymptotic variance estimates show that the uncertainty in the estimated spawning biomass is high, although even the lower range of the 95% interval for %unfished is above the 40% reference point, and all sensitivity analyses explore also show the stock to be at a high level.

Table b: Recent trend in beginning of the year spawning output and (spawning biomass relative to unfished equilibrum spawning biomass)

Year	Spawning Output (mt)	~ 95% confidence interval	Estimated %unfished	~ 95% confidence interval
2010	1603.690	(726.67-2480.71)	0.721	(0.6-0.842)
2011	1617.560	(738.18-2496.94)	0.727	(0.608-0.847)
2012	1625.610	(745.16-2506.06)	0.731	(0.613-0.849)
2013	1634.790	(753.17-2516.41)	0.735	(0.618-0.852)
2014	1657.340	(772.22-2542.46)	0.745	(0.631-0.859)
2015	1657.020	(772.35-2541.69)	0.745	(0.632-0.859)
2016	1659.820	(774.79-2544.85)	0.746	(0.634-0.859)
2017	1652.180	(768.4-2535.96)	0.743	(0.63-0.856)
2018	1655.400	(770.86-2539.94)	0.744	(0.632-0.857)
2019	1667.190	(780.42-2553.96)	0.750	(0.639-0.86)

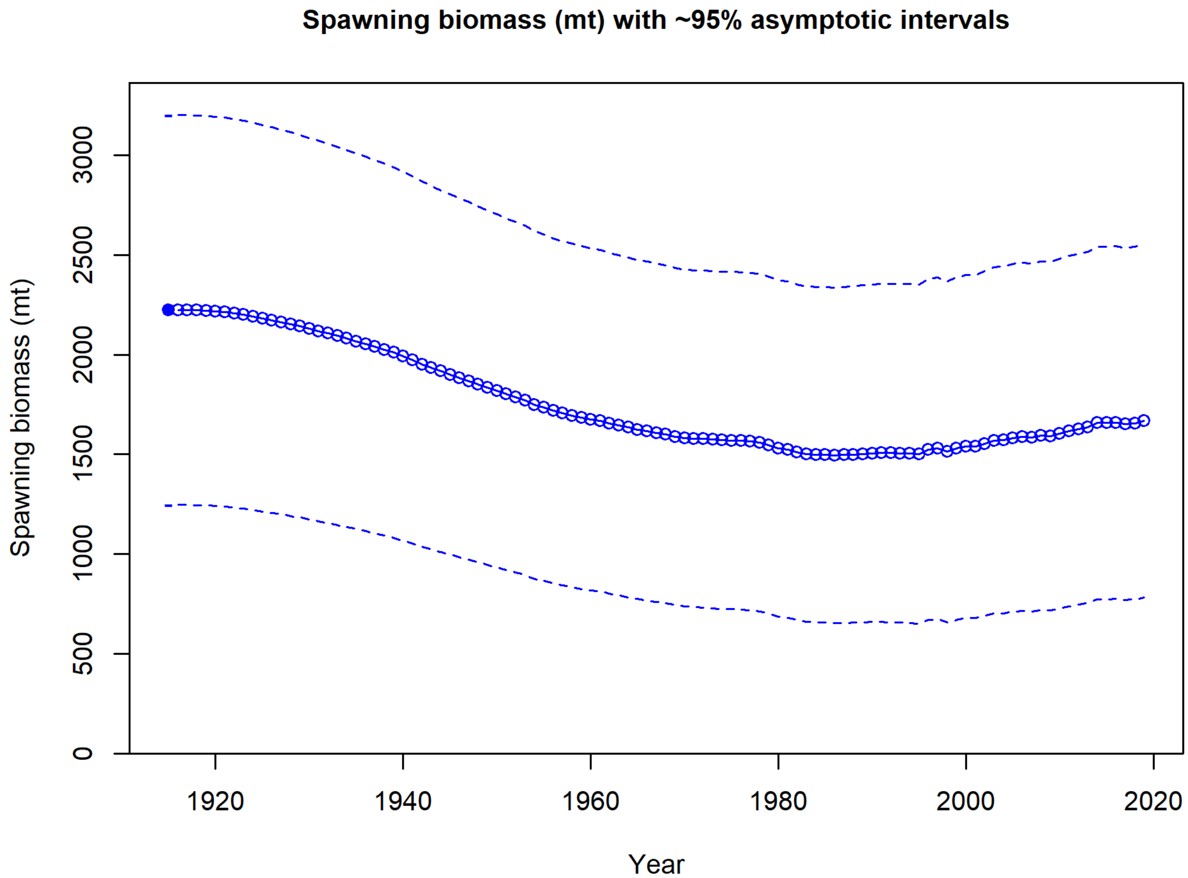

Figure c: Time series of spawning biomass trajectory (circles and line: median; light broken lines: 95% credibility intervals) for the base case assessment model.

Recruitment

Recruitment was assumed to follow the Beverton-Holt stock recruit curve, so uncertainty in estimated recruitment is due to uncertainty in spawning biomass and the unfished equilibrium recruitment R_0 (Figure d and Table c).

Table c: Recent recruitment for the model.

Year	Estimated Recruitment (1,000s)	~ 95% confidence interval
2010	5393.54	(2966.19 - 9807.3)
2011	5414.62	(2982.16 - 9831.17)
2012	5426.77	(2991.46 - 9844.65)
2013	5440.55	(3002 - 9859.94)
2014	5474.01	(3027.33 - 9898.09)
2015	5473.54	(3027.82 - 9894.77)
2016	5477.66	(3031.98 - 9896.09)
2017	5466.40	(3024.88 - 9878.58)
2018	5471.15	(3029.62 - 9880.26)
2019	5488.48	(3043.55 - 9897.46)

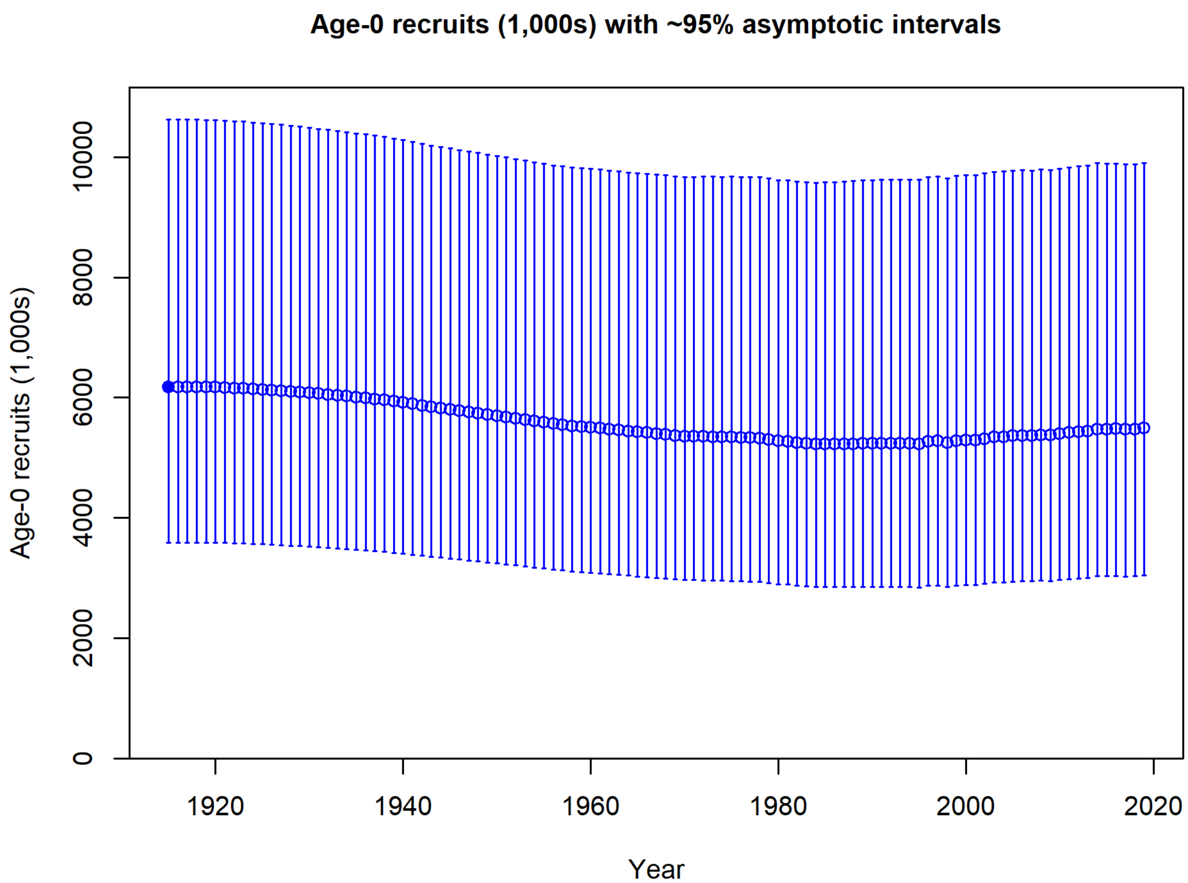

Figure d: Time series of estimated Big Skate recruitments for the base-case model with 95% confidence or credibility intervals.

Exploitation Status

Harvest rates estimated by the base model indicate catch levels have been below the limits that would be associated with the SPR = 50% target (Table d and Figure e).

Table d: Recent trend in spawning potential ratio and exploitation for Big Skate in the model. Relative fishing intensity is (1-SPR) divided by 50% (the SPR target) and exploitation is catch divided by age 2+ biomass.

Year	Relative fishing intensity	~ 95% confidence interval	Exploitation rate	~ 95% confidence interval
2009	0.21	(0.12-0.3)	0.01	(0.01-0.02)
2010	0.20	(0.11-0.29)	0.01	(0.01-0.02)
2011	0.26	(0.15-0.38)	0.01	(0.01-0.02)
2012	0.26	(0.15-0.38)	0.01	(0.01-0.02)
2013	0.14	(0.08-0.2)	0.01	(0-0.01)
2014	0.36	(0.21-0.5)	0.02	(0.01-0.03)
2015	0.32	(0.19-0.45)	0.02	(0.01-0.03)
2016	0.39	(0.23-0.55)	0.02	(0.01-0.03)
2017	0.28	(0.16-0.39)	0.02	(0.01-0.02)
2018	0.18	(0.1-0.25)	0.01	(0.01-0.01)

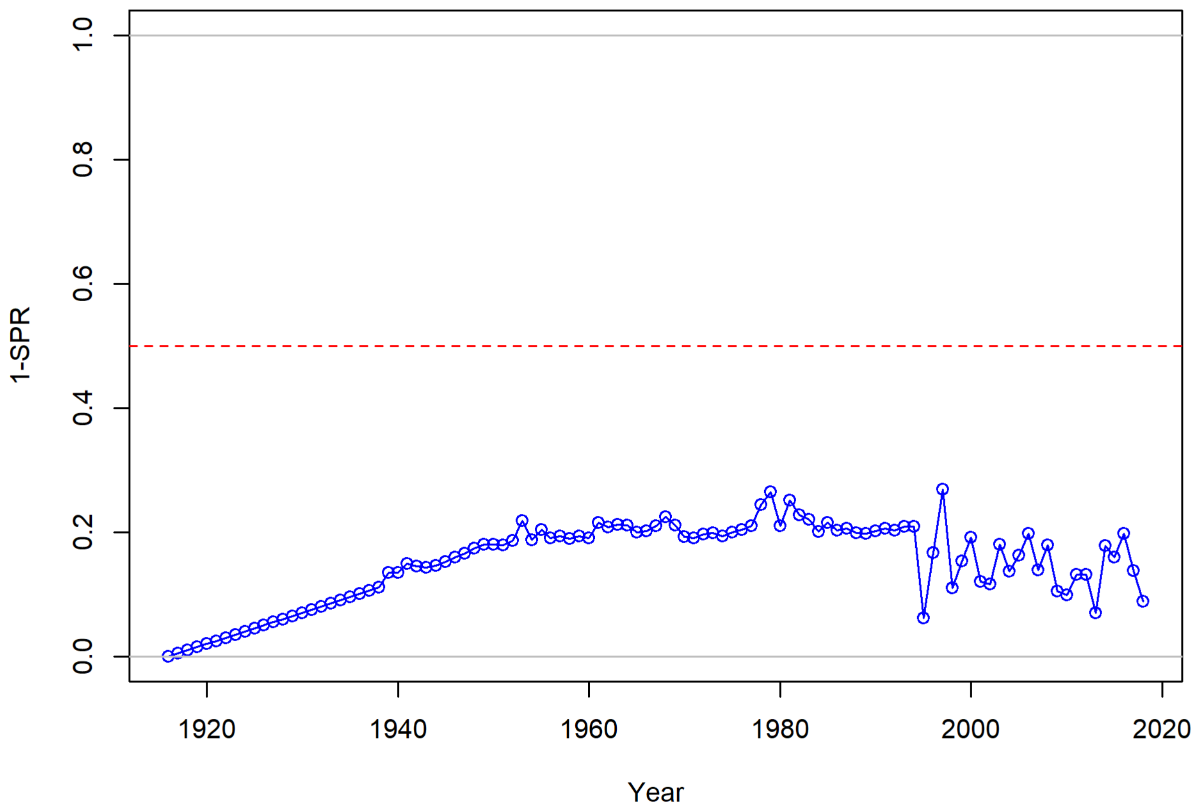

Figure e: Estimated spawning potential ratio (SPR) for the base-case model. One minus SPR is plotted so that higher exploitation rates occur on the upper portion of the y-axis. The management target is plotted as a red horizontal line and values above this reflect harvests in excess of the overfishing proxy based on the $SPR_{50\%}$ harvest rate. The last year in the time series is 2018.

Reference Points

This stock assessment estimates that Big Skate in the model is above the biomass target ($SB_{40\%}$), and well above the minimum stock size threshold ($SB_{25\%}$). The estimated %unfished level for the base model in 2019 is 75.0% (95% asymptotic interval: ± 63.9%-86.0%, corresponding to an unfished spawning biomass of 1667.19 mt (95% asymptotic interval: 780.42-2553.96 mt) of spawning biomass in the base model (Table e). Unfished age 2+ biomass was estimated to be 2,523 mt in the base case model. The target spawning biomass ($SB_{40\%}$) is 890 mt, which corresponds with an equilibrium yield of 602 mt. Equilibrium yield at the proxy F_{MSY} harvest rate corresponding to $SPR_{50\%}$ is 507 mt (Figure f).

Table e: Summary of reference points and management quantities for the base case model.

Quantity	**Estimate**	**Low 2.5% limit**	**High 2.5% limit**
Unfished spawning output (mt)	2,224	1,246	3,202
Unfished age 2+ biomass (mt)	2,523	1,705	3,341
Unfished recruitment (R_0)	6,176	2,760	9,592
Spawning output(2018 mt)	1,655	771	2,540
Depletion (2018)	0.744	0.632	0.857
Reference points based on $\mathbf{SB_{40\%}}$			
Proxy spawning output ($B_{40\%}$)	890	498	1,281
SPR resulting in $B_{40\%}$ ($SPR_{B40\%}$)	0.625	0.625	0.625
Exploitation rate resulting in $B_{40\%}$	0.048	0.042	0.055
Yield with $SPR_{B40\%}$ at $B_{40\%}$ (mt)	602	395	810
Reference points based on SPR proxy for MSY			
Spawning output	445	249	640
SPR_{proxy}	0.5		
Exploitation rate corresponding to SPR_{proxy}	0.071	0.061	0.08
Yield with SPR_{proxy} at SB_{SPR} (mt)	507	333	681
Reference points based on estimated MSY values			
Spawning output at MSY (SB_{MSY})	833	458	1,207
SPR_{MSY}	0.609	0.604	0.614
Exploitation rate at MSY	0.051	0.045	0.057
Dead Catch MSY (mt)	604	396	812
Retained Catch MSY (mt)	559	367	750

Ecosystem Considerations

In this assessment, neither environmental nor ecosystem considerations were explicitly included in the analysis. This is primarily due to a lack of relevant data or results of analyses that could contribute ecosystem-related quantitative information for the assessment.

Management Performance

Table f: Recent trend in total catch (mt) relative to the management guidelines. Big skate was managed in the Other Species complex in 2013 and 2014, designated an Ecosystem Component species in 2015 and 2016, and managed with stock-specific harvest specifications since 2017.

Year	OFL (mt; ABC prior to 2011)	ABC (mt)	ACL (mt; OY prior to 2011)	Estimated total catch (mt)
2009				205.70
2010				196.20
2011				268.40
2012				269.60
2013	458.00	317.90	317.90	135.00
2014	458.00	317.90	317.90	372.40
2015				331.50
2016				411.50
2017	541.00	494.00	494.00	277.60
2018	541.00	494.00	494.00	172.60
2019	541.00	494.00	494.00	
2020	541.00	494.00	494.00	

Unresolved Problems and Major Uncertainties

The data provide little information about the scale of the population, necessitating the use of a prior on catchability to maintain stable model results. The prior was developed for the 2007 Longnose Skate stock assessment and has not been revised to account for any differences between the two species.

There is little evidence that the population is overfished or experiencing overfishing, but forecasts of overfishing limits vary considerably among the sensitivity analyses explored (though all remain well above the recent average catch).

The fit to the length data was significantly improved by estimating a difference between female and male selectivity, with females having a lower maximum selectivity than males, but the behavioral processes that might contribute to this difference are not understood.

Decision Table

Template in Table h and associated discussion to be filled in during the STAR panel

Projected Landings, OFLs and Time-varying ACLs

Potential OFLs projected by the model are shown in Table g. These values are based on an SPR target of 50%, a P* of 0.45, and a time-varying Category 2 Sigma which creates the buffer shown in the right-hand column.

Table g: Projections of landings, total mortality, OFL, and ACL values.

Year	Landings (mt)	Estimated total mortality (mt)	OFL (mt)	ACL (mt)	Buffer
2019	313.16	336.35	541.00	494.00	1.00
2020	313.16	336.32	541.00	494.00	1.00
2021	1042.23	1119.74	1275.51	1119.75	0.87
2022	987.51	1062.58	1222.62	1062.58	0.86
2023	942.80	1015.91	1179.51	1015.91	0.86
2024	906.41	977.59	1145.41	977.59	0.85
2025	876.49	945.64	1118.21	945.64	0.84
2026	850.59	917.76	1095.36	917.76	0.83
2027	828.05	893.39	1075.04	893.39	0.83
2028	805.87	869.37	1056.06	869.37	0.82
2029	784.60	846.33	1037.94	846.33	0.81
2030	764.95	825.07	1020.44	825.07	0.80

Table h: Summary of 10-year projections beginning in 2020 for alternate states of nature based on an axis of uncertainty for the model. Columns range over low, mid, and high states of nature, and rows range over different assumptions of catch levels. An entry of "–" indicates that the stock is driven to very low abundance under the particular scenario.

			States of nature					
			Low State		Base State		High State	
	Year	Catch	Spawning Output	Depletion	Spawning Output	Depletion	Spawning Output	Depletion
Default harvest, for Low State	2019	-	-	-	-	-	-	-
	2020	-	-	-	-	-	-	-
	2021	-	-	-	-	-	-	-
	2022	-	-	-	-	-	-	-
	2023	-	-	-	-	-	-	-
	2024	-	-	-	-	-	-	-
	2025	-	-	-	-	-	-	-
	2026	-	-	-	-	-	-	-
	2027	-	-	-	-	-	-	-
	2028	-	-	-	-	-	-	-
Default harvest, for Base State	2019	-	-	-	-	-	-	-
	2020	-	-	-	-	-	-	-
	2021	-	-	-	-	-	-	-
	2022	-	-	-	-	-	-	-
	2023	-	-	-	-	-	-	-
	2024	-	-	-	-	-	-	-
	2025	-	-	-	-	-	-	-
	2026	-	-	-	-	-	-	-
	2027	-	-	-	-	-	-	-
	2028	-	-	-	-	-	-	-
Default harvest, for High State	2019	-	-	-	-	-	-	-
	2020	-	-	-	-	-	-	-
	2021	-	-	-	-	-	-	-
	2022	-	-	-	-	-	-	-
	2023	-	-	-	-	-	-	-
	2024	-	-	-	-	-	-	-
	2025	-	-	-	-	-	-	-
	2026	-	-	-	-	-	-	-
	2027	-	-	-	-	-	-	-
	2028	-	-	-	-	-	-	-
Average Catch	2019	-	-	-	-	-	-	-
	2020	-	-	-	-	-	-	-
	2021	-	-	-	-	-	-	-
	2022	-	-	-	-	-	-	-
	2023	-	-	-	-	-	-	-
	2024	-	-	-	-	-	-	-
	2025	-	-	-	-	-	-	-
	2026	-	-	-	-	-	-	-
	2027	-	-	-	-	-	-	-
	2028	-	-	-	-	-	-	-

Table i: Base case results summary.

Quantity	2010	2011	2012	2013	2014	2015	2016	2017	2018	2019
Landings (mt)	313.160	313.160	1042.228	987.509	942.796	906.409	876.485	850.594	828.055	805.865
Total Est. Catch (mt)	336.345	336.325	1119.745	1062.581	1015.907	977.592	945.644	917.761	893.393	869.365
OFL (mt)	541.00	541.00	1275.51	1222.62	1179.51	1145.41	1118.21	1095.36	1075.04	1056.06
ACL (mt)	494.000	494.000	1119.750	1062.580	1015.910	977.592	945.643	917.762	893.393	869.365
(1-SPR)(1-$SPR_{50\%}$)	0.20	0.26	0.26	0.14	0.36	0.32	0.39	0.28	0.18	
Exploitation rate	0.01	0.01	0.01	0.01	0.02	0.02	0.02	0.02	0.01	
Age 2+ biomass (mt)	18810.9	18968.2	19113.5	19171.0	19221.9	19394.4	19315.6	19300.1	19211.4	19275.8
Spawning Output	1603.7	1617.6	1625.6	1634.8	1657.3	1657.0	1659.8	1652.2	1655.4	1667.2
95% CI	(726.67-2480.71)	(738.18-2496.94)	(745.16-2506.06)	(753.17-2516.41)	(772.22-2542.46)	(772.35-2541.69)	(774.79-2544.85)	(768.4-2535.96)	(770.86-2539.94)	(780.42-2553.96)
Depletion	0.7	0.7	0.7	0.7	0.7	0.7	0.7	0.7	0.7	0.7
95% CI	(0.6-0.842)	(0.608-0.847)	(0.613-0.849)	(0.618-0.852)	(0.631-0.859)	(0.632-0.859)	(0.634-0.859)	(0.63-0.856)	(0.632-0.857)	(0.639-0.86)
Recruits	5393.54	5414.62	5426.77	5440.55	5474.01	5473.54	5477.66	5466.40	5471.15	5488.48
95% CI	(2966.19 - 9807.3)	(2982.16 - 9831.17)	(2991.46 - 9844.65)	(3002 - 9859.94)	(3027.33 - 9898.09)	(3027.82 - 9894.77)	(3031.98 - 9896.09)	(3024.88 - 9878.58)	(3029.62 - 9880.26)	(3043.55 - 9897.46)

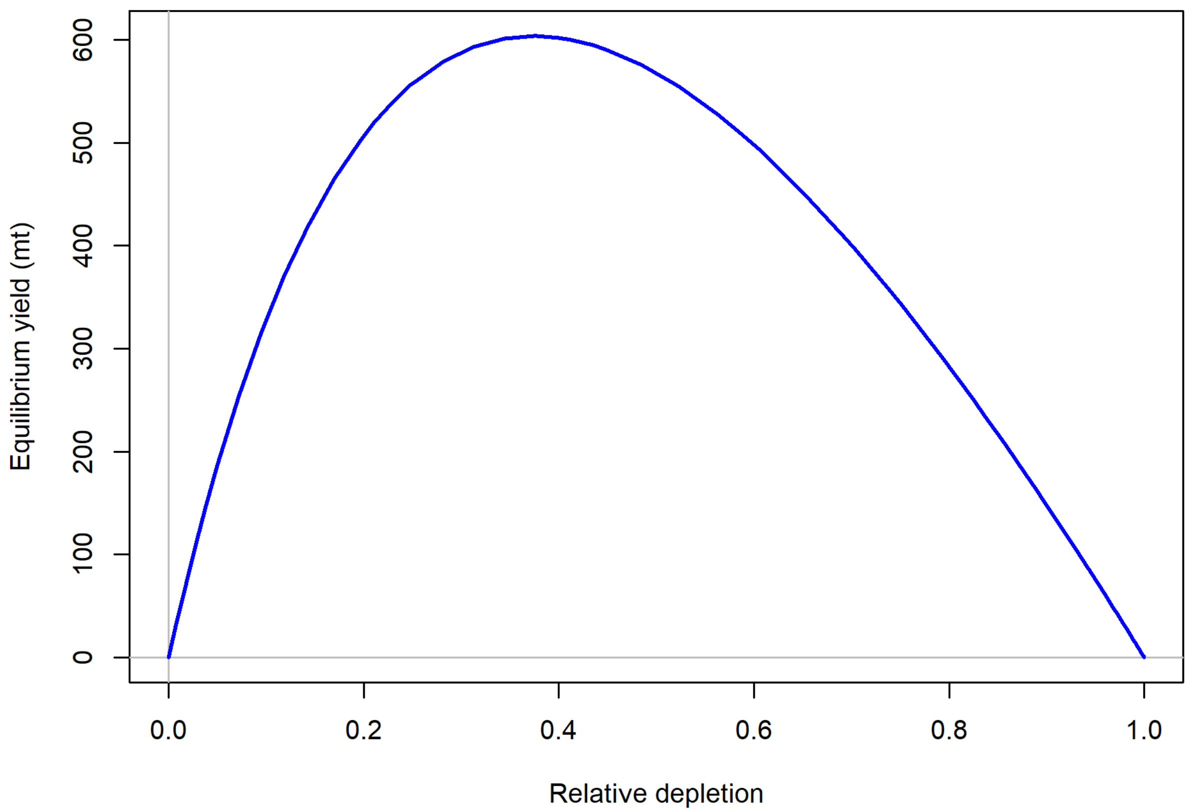

Figure f: Equilibrium yield curve for the base case model. Values are based on the 2018 fishery selectivity and with steepness fixed at 0.718.

Research and Data Needs

We recommend the following research be conducted before the next assessment:

1. **Data!**:
2. **xxxx**:
3. **xxxx**:
4. **xxxx**:
5. **xxxx**:

To be continued

1 Introduction

Skates are the largest and most widely distributed group of batoid fish with approximately 245 species ascribed to two families (Ebert and Compagno (2007), McEachran and Miyake (1990)). Skates are benthic fish that are found in all coastal waters but are most common in cold temperatures and polar waters (Ebert and Compagno 2007).

There are eleven species of skates in three genera (Amblyraja, Bathyraja, and Raja) present in the Northeast Pacific Ocean off California, Oregon and Washington (Ebert 2003). Of that number, just three species (Longnose Skate, *Raja rhina*; Big Skate, *Raja binoculata*; and Sandpaper Skate, *Bathyraja interrupta*) make up over 95 percent of West Coast Groundfish Bottom Trawl Survey (WCGBTS) catches in terms of biomass and numbers, with the Longnose Skate leading in both categories (with 62 percent of biomass and 56 percent of numbers).

Big Skate (*Raja binoculata*) is the largest of the skate species in North America with a documented maximum length of 244 cm total length and a maximum weight of 91 kg (Eschmeyer and Herald 1983). The species name "binoculata" (two-eyed) refers to the prominent ocellus at the base of each pectoral fin. Big Skates are usually seen buried in sediment with only their eyes showing.

1.1 Biology

Big Skate is oviparious, and is one of two skate species that have multiple embryos per egg case (Ebert et al. 2008). From 1–8 embryos can be contained in a single, large egg capsule, but most have 3–4 (DeLacy and Chapman 1935, Hitz 1964, Ford 1971). Eggs are deposited year-round on sand or mud substrates at depths of ˜50–150 m (Hitz 1964, Ebert and Compagno 2007). Embryos hatch from eggs after 6–20 months, with shorter developmental periods associated with warmer temperatures (Hoff, GR 2009). In captivity, Big Skate females may produce > 350 eggs/year (average of 2 embryos/egg case; Chiquillo, Kelcie L and Ebert, David A and Slager, Christina J and Crow, Karen D (2014)) from long-term sperm storage . Size at birth is 18–23 cm TL (Ebert 2003). Maximum size is 244 cm TL [Eschmeyer and Herald (1983), with females growing to larger sizes.

Size at maturity has been variably estimated for Big Skate populations off California, British Columbia, and Alaska. Off central California, Zeiner and Wolf (1993) reported sizes at first maturity of ˜129 cm TL (females) and ˜100 cm TL (males). A similar size at maturity was estimated for females from the Gulf of Alaska (first = 126 cm TL, 50% = 149 cm TL), but male estimates were considerably greater (first = 124 cm TL, 50% = 119 cm TL; Ebert et al. (2008)). Much smaller sizes at first (female = 60 cm TL, male = 50 cm TL) and 50% (female = 90 cm TL, male = 72 cm TL) maturity were generated for the Longnose Skate populations off British Columbia (McFarlane GA and King JR 2006); however, maturity evaluation criteria were flawed (subadults were considered to be mature), and these results are therefore not considered valid.

Age and growth parameters have been established from California, British Columbia, and the Gulf of Alaska. Maximum ages off central California (females = 12, males = 11; Zeiner, S.J. and P. Wolf. (1993)) and in the Gulf of Alaska (females = 14, males = 15; Gburski et al. 2007) were similar, but estimates off British Columbia were much greater (females = 26, males = 25; McFarlane and King 2006). It is important to note that age estimates are based on an unvalidated method and geographic differences in size or age may reflect differences in sampling or ageing criteria. In the Gulf of Alaska, Big Skates reach 50% maturity at 10 years and 7 years for females and males, respectively (Gburski, C.M. and Gaichas, S.K. and Kimura, D.K. (2007), Ebert et al. (2008)). Generation length estimates range from 11.5 (Zeiner, S.J. and P. Wolf. 1993) to 17 years (McFarlane GA and King JR 2006).

Table 1: Regional comparison of life history parameter estimates.

	California		British Columbia		Gulf of Alaska	
	Female	Male	Female	Male	Female	Male
1st Maturity (TL cm)	129	100	60	50	126	124
50% Maturity (TL cm)			90	72	149	119
Max Age (year)	12	11	26	25	14	15
1st Maturity (year)	12	10	6	5	7	9
50% Maturity (year)			8	10	10	7

1.2 Distribution and Life History

The Big Skate is most common in soft-sediment habitats in coastal waters of the continental shelf (Bizzarro, JJ and Broms, KM and Logsdon, MG and Ebert, DA and Yoklavich, MM and Kuhnz, LA and Summers, AP (2014), Farrugia et al. (2016)). Use of mixed substrate (e.g., mud with boulders) increases with ontogeny but hard substrates are largely avoided (Bizzarro (2015)). In the GOA, the Big Skate is the most commonly encountered skate species in continental shelf waters at 100–200 m depth, and is most abundant in the central and western areas of the GOA (Stevenson, DE and Orr, JW and Hoff, GR and McEachran, JD (2008); Bizzarro, JJ and Broms, KM and Logsdon, MG and Ebert, DA and Yoklavich, MM and Kuhnz, LA and Summers, AP (2014)). Off the U.S. Pacific Coast, the Big Skate is most densely distributed on the inner continental shelf (< 100 m; Bizzarro, JJ and Broms, KM and Logsdon, MG and Ebert, DA and Yoklavich, MM and Kuhnz, LA and Summers, AP (2014)). Eggs are mainly deposited between 70–90 m on sand or mud substrates (Hitz (1964); NMFS-NWFSC-FRAM, unpub. data). Juveniles typically occur in shallower waters than adults (Bizzarro (2015)). Core habitat regions of Big Skate off the U.S. Pacific Coast and in the Gulf of Alaska are spatially segregated from those of other species (Bizzarro, JJ and Broms, KM and Logsdon, MG and Ebert, DA and Yoklavich, MM and Kuhnz, LA and Summers, AP (2014)).

Big Skates are highly mobile and capable of long range (> 2000 km) movements (KingandMcF2010; Farrugia et al. (2016)). For example, in British Columbia, a study revealed that ˜75% of tagged individuals were recaptured within 21 km of the tagging locations, but 15 of the tagged individuals (0.1%) moved over 1,000 km (max = 2340 km; King, JR and McFarlane, GA (2010)). In the Gulf of Alaska, a year of satellite tag data showed that six of twelve tagged individuals moved over 100 km, with one skate moving > 2,000 km (Farrugia et al. 2016). Although primarily benthic, Big Skates utilize the entire water column including surface waters (Farrugia et al. (2016)). They have broad thermal tolerances 2–19º C that enable their occurrence from boreal to subtropical latitudes (Love, Milton S (2011); Farrugia et al. (2016)).

The Big Skate is broadly distributed, occurring from the southeastern Bering Sea (Mecklenburg, CW and Mecklenburg, TA and Thorsteinson, LK 2002) to southern Baja California (22.90º N, 110.03º W; (Castro-Aguirre et al. 1993)) and the Gulf of California (Castro-Aguirre and Pérez 1996). It has been reported at depths of 2–501 m (min: Miller et al. (1980); max: Farrugia et al. (2016)) but is most common on the inner continental shelf (< 100 m; (Love, Milton S 2011); (Bizzarro 2015)). Big Skates are highly mobile and capable of long range (> 2000 km) movements ((King and McFarlane 2009); (Farrugia et al. 2016)).

In 2012, the Big Skate was moved from genus *Raja* to the new genus *Beringraja* together with the Mottled Skate (*B. pulchra*) (Ishihara et al. 2012). These are the only two skates with multiple embryos per egg case, and they are very similar mophologically and genetically (Bizzarro, J. 2019).

1.3 Ecosystem Considerations

Big Skates are opportunistic, generalist mesopredators with highly variable spatio-temporal trophic roles (Ebert and Compagno (2007); Bizzarro (2015)). Off central California, diet of Big Skates is composed mainly of fishes, shrimps, and crabs (in descending order), with larger skates incorporating more fishes (Bizzarro et al. (2007)); however, in the Gulf of Alaska, Big Skate diet consists mainly of crabs (esp. Tanner Crabs) throughout ontogeny, with relatively small portions of fishes and shrimps (Bizzarro (2015)). Correspondingly, trophic level and general diet composition estimates differ significantly between California and Gulf of Alaska Big Skate populations (Bizzarro (2015)).

Big Skates and their egg cases are preyed upon by a variety of vertebrates and invertebrates. Snails and other molluscs bore holes in egg cases to feed on developing embryos and especially their protein rich yolk-sacs (Bizzarro, pers. obs; Hoff, GR (2009)). Sevengill Sharks, Brown Rockfish, and Stellar Sea Lions are known predators of juvenile and adult Big Skates (Ebert (2003), Love, Milton S (2011)). Northern Sea Lions consume free-living Big Skates and their egg cases (Ebert (2003), Love, Milton S (2011)).

In this assessment, neither environmental nor ecosystem considerations were explicitly included in the analysis. This is primarily due to a lack of relevant data or results of analyses that could contribute ecosystem-related quantitative information for the assessment.

1.4 Fishery Information

Big Skate are caught in commercial and recreational fisheries on the West Coast using line and trawl gears. There is a limited market for pectoral fins (skate wings).

The history of Big Skate is not well documented. They were used as a food source by the native Coastal and Salish Tribes (Batdorf, C 1990) long before Europeans settled in the Pacific Northwest and then as fertilizer by the settlers (Bowers, G. M. 1909). No directed fishery for Big Skate has been documented; rather, they were taken along with other skates and rays as "scrap fish" and used for fertilizer, fish meal and oil (Lippert 2019).

Skates have been regarded as a predator on desirable market species such as Dungeness crab, and were thought of as nuisance fish with no appeal as a food item save for small local markets. They had been discarded or harvested at a minimal level until their livers became valued along with those of other cartilaginous fishes for the extraction of vitamin A in the 1940s. Chapman (Chapman, W.M. 1944) recorded that "At present they are being fished heavily, in common with the other elasmobranchs of the coast, for the vitamins in their livers. The carcasses are either thrown away at sea or made into fish meal. Little use is made of the excellent meat of the wings".

Little information is available about the historic Washington fishery for Big Skate. In records before 2000, they are lumped together with other skates or in market categories (Lippert 2019); this necessitates considerable attention to reconstructing the fishery by observing the composition of skate catches in the modern fishery and applying those to the recently reconstructed historical records.

Very little information is known about the Big Skate historical fishery in Oregon. The information we do have is mainly from historical landing data and species composition samples starting in the mid-nineties. The bulk of the catch is from the bottom trawl and longline fisheries, with smaller amounts as by-catch in mid-water trawl and the shrimp trawl fishery. Big Skate was lumped into the nominal "Skate" category until 2015 when it was separated into its own market category. Species composition data have been vitally important in reconstructing the pre-2015 historical catch (Calavan 2019).

1.5 Stock Status and Management History

The history of Big Skate management is documented in (Pacific Fishery Management Council 2018), reproduced here.

Big Skate were managed in the "Other Fish" complex until 2015 when they were designated an Ecosystem Component (EC) species. Catches of Big Skate are estimated to have averaged 95 mt from 2007–2011, along with large landings of "Unspecified Skate". Analysis of Oregon port-sampling data indicates that about 98 percent of the recent Unspecified Skate landings in Oregon were comprised of Big Skate. Such large landings indicates targeting of Big Skate has occurred and an EC designation was not warranted. Based on this evidence, Big Skate was redesignated as an actively-managed species in the fishery. Big skate have been managed with stock-specific harvest specifications since 2017.

The recent OFL of 541 mt was calculated by applying approximate MSY harvest rates to estimates of stock biomass from the Northwest Fisheries Science Center (NWFSC) West Coast Groundfish Bottom Trawl Survey. This survey-based biomass estimate is likely underestimated since Big Skate are distributed all the way to the shoreline and no West Coast trawl surveys have been conducted in water shallower than 55 meters. This introduces an extra source of uncertainty to management and suggests that increased precaution is needed to reduce the risk of overfishing the stock.

There has been consideration for managing Big Skate in a complex with Longnose Skate, the other actively-managed West Coast skate species, but the two species have disparate distributions and fishery interactions (Longnose Skate is much more deeply distributed than Big Skate) and that option was not endorsed. The Pacific Fishery Management Council has chosen to set the Annual Catch Limit (ACL) equal to the Allowable Biological Catch (ABC) with a buffer for management uncertainty (P*) of 0.45.

1.6 Fisheries Off Alaska, Canada and Mexico

1.6.1 Alaska

In Alaska, skates were primarily taken as bycatch in both longline and trawl fisheries until 2003, when a directed skate fishery developed in the Gulf of Alaska, where Longnose and Big skates comprise the majority of the skate biomass.

The Gulf of Alaska (GOA) skate complex is managed as three units. Big skates and Longnose Skates each have separate harvest specifications, with acceptable biological catches (ABCs) specified for each GOA regulatory area (western, central, and eastern). A single gulfwide overfishing level (OFL) is specified for each stock. All remaining skate species are managed as an "Other Skates" group with gulfwide harvest specifications. All GOA skates are managed as Tier 5 stocks, where OFL and ABC are based on survey biomass estimates and natural mortality rate (Alaska Fisheries Science Center 2018).

In the Bering Sea and Aleutian Islands, skates are assessed as a group rather than as separate species.

1.6.2 Canada

In Canada historic information regarding skate catches goes back to the 1950's. Prior to 1990's skates were taken mostly as bycatch and landings were reported as part of a skate complex (not by species). As with the West Coast, the trawl fishery is responsible for the largest amount of bycatch. Skate catches off British Columbia accelerated in the early 1990's, partly due to emerging Asian markets. Since 1996, longnose skate has been targeted by the B.C. trawl fishery and, as a result, catches have been more accurately reported.

Assessments of Longnose Skate and Big Skate were conducted by Canada's Division of Fisheries and Oceans in 2015(King, J.R., Surry, A.M., Garcia, S., and P.J. Starr 2015). For Big Skate, a Bayesian surplus production model failed to provide plausible results, and two data-limited approaches were investigated: Depletion-Corrected Average Catch Analysis (DCAC), and a Catch-MSY (maximum sustainable yield) Approach.

DCAC produced a range of potential yield estimates that were above the long-term average catch, with an upper bound that was three orders of magnitude larger than the long-term average catch. The Catch-MSY approach was found to be quite sensitive to assumptions and was not recommended as the sole basis of advice to managers.

The recommendation for management for both skate species was that they should be managed with harvest yields based on mean historic catch, with consideration given to survey trends and to the ranges of maximum sustainable yield estimates identified by the Catch-MSY Approach. However, the analysis found no significant trends in abundance indices for Big Skate, and mean historical catches were below the maximum MSY estimate from the catch-MSY results.

1.6.3 Mexico

No information is available on any fishery for Big Skate in Mexican waters, where they rarely occur, however they may be taken in the artisanal fishery.

2 Fishery Data

2.1 Data

Data used in the Big Skate assessment are summarized in Figure 1. Descriptions of the data sources are in the following sections.

2.2 Fishery Landings and Discards

Catch information for Big Skate is very limited, in part because the requirement to sort landings of Big Skate in the shore-based Individual Fishing Quota fishery from landings in the "Unidentified Skate" category was not implemented until June 2015. The historical catch of Big Skate therefore relies on the historical reconstruction of the landings of all skates as well as an analysis of discards of Longnose Skate. The estimated landings for each state and the tribal fishery are provided in Table 2 and shown in Figure 3.

2.2.1 Washington Commercial Skate Landings Reconstruction

Estimates of landings of Big Skate in Washington state were estimated as a fraction of total skate landings as described in (Gertseva, V. 2019). The approached relied on trawl survey estimates of depth distributions for each species, combined with logbook estimates of fishing depths in each year.

The WCGBT Survey data was used to estimate proportions of longnose and big skates by depth (aggregated into 100m bins) and year for the period of the survey (between 2003 and 2018). Big Skate were primarily found in the 0–100m and 100–200m. Trawl logbook data include information on the amount of retained catch of skate (all species combined) within each haul as well depth of catch. The proportion of Big Skate for each depth bin was assigned to the skate catch for each haul within those depth bins and summed to get a total for each year. When survey skate information was available (2003-2018), survey skate proportions were applied by depth and year to account for inter-annual variability in those proportions. Prior to 2003, average proportions from 2003-2007 within each depth bin were applied.

These estimated annual proportion of Big Skate relative to all skates from the logbook analysis was then applied to total Washington skate landings by year (provided by WDFW) to account for landings that weren't included in the available logbook data. Prior to 1987 (when no logbook data were available), the average proportion Big Skate within the combined skate category, calculated from 1987-1992 logbook data, was applied to total skate landings in Washington. Estimated Big Skate landings provided by WDFW were used for the period from 2004 forward.

2.2.2 Oregon Commercial Skate Landings Reconstruction

Oregon Department of Fish and Wildlife (ODFW) provided newly reconstructed commercial landings for all observed skate species for the 2019 assessment cycle (1978 – 2018). In addition, the methods were reviewed at a pre-assessment workshop. Historically, skates were landed as a single skate complex in Oregon. In 2009, longnose skates were separated into their own single-species landing category, and in 2014, big skates were also separated. The reconstruction methodology differed by these three time blocks in which species composition collections diverged (1978 – 2008; 2009 – 2014; 2015 – 2018).

Species compositions of skate complexes from commercial port sampling are available throughout this time period but are generally limited, which precluded the use of all strata for reconstructing landings. Quarter and port were excluded, retaining gear type, PMFC area, and market category for stratifying reconstructed landings within the three time blocks. Bottom trawl gear types include multiple bottom trawl gears, and account for greater than 98% of skate landings . Minor gear types include primarily bottom longline gear, but also include mid-water trawl, hook and line, shrimp trawl, pot gear and scallop dredge.

For bottom trawl gears, trawl logbook areas and adjusted skate catches were matched with strata-specific species compositions. In Time Block 1 (1978 – 2008), all bottom trawl gear types were aggregated due to a lack of specificity in the gear recorded on the fish tickets. However, in Time Blocks 2 and 3, individual bottom trawl gear types were retained. Some borrowing of species compositions was required (31% of strata) and when necessary, borrowed from the closest area or from the most similar gear type . Longline gear landings were reconstructed in a similar fashion as to bottom trawl and required some borrowing among strata as well (25%).

Due to insufficient species compositions, mid-water trawl landings were reconstructed using a novel depth-based approach. Available compositions indicate that the proportion by weight of big skates within a composition drops to zero at approximately 100 fathoms, and an inverse relationship is observed for longnose skate, where the proportion by weight is consistently one beyond 100 – 150 fathoms . Complex-level landings were assigned a depth from logbook entries and these species specific depth associations were used to parse out landings by species. The approach differed somewhat by time block . Landings from shrimp trawls were handled using a similar methodology. Finally, very minor landings from hook and line, pot gear and scallop dredges were assigned a single aggregated species composition, as they lack any gear-specific composition samples. Landings from within a time block were apportioned by year using the proportion of the annual ticket landings.

Results indicate that the species-specific landings from this reconstruction are very similar to those from Oregon's commercial catch reconstruction (Karnowski et al. 2014) during the overlapping years but cover a greater time period with methodology more applicable to skates in particular. ODFW intends to incorporate reconstructed skate landings into PacFIN in the future (A. Whitman, ODFW; pers. comm.).

2.2.3 California Catch Reconstruction

A reconstruction of historical skate landings from California waters was developed for the 1916–2017 time period using a combination of commercial catch data (spatially explicit block summary catches and port sample data from 2009-2017) and fishery-independent survey data (Bizzarro, J. 2019). Virtually all landings in California were of “unspecified skate” until species-composition sampling of skate market categories began in 2009.

From 2009 through 2017, catch estimates were based on these market category species-composition samples, and the average of those species-compositions was hindcast to 2002, based on the assumption that those data were representative of the era of large area closures in the post-2000 period.

For the period from 1936-1980, spatially explicit landings data (the California Department of Fisheries and Wildlife (CDFW) block summary data) were merged with survey data to provide species-specific estimates.

For years 1981-2001, a “blended” product of these two approaches was taken, in which a linear weighting scheme blended the two sets of catch estimates through that period. Landings estimates were also scaled upwards by an expansion factor for skates landed as “dressed” based on fish ticket data. Prior to 1981 these data had not been reported and skate landings were scaled by the “average” percentage landed as dressed in the 1981-1985 time period, but by the late 1980s nearly all skates were landed round.

As no spatial information on catch is available from 1916-1930, and the block summary data were very sparse in the first few years of the CDFW fish ticket program (1931–1934), spatial information from the late 1930’s was used to hindcast to the 1916–1935 time period. However, since Washington and Oregon did not have catch estimates for this year period, the California estimates of catch prior to 1938 were not used as they were subsumed into an estimated of the total catch across all states increasing linearly from 1916 to 1950.

2.2.4 Tribal Catch in Washington

Tribal catch of Big Skate was provided by WDFW as all landings took place in Washington State. The landings were estimated from limited state sampling of species compositions in combined skate category. Anecdotal evidence suggest that most of the catch in tribal fishery is retained, and discard is minimal.

2.2.5 Fishery Discards

Fishery discards of Big Skate are highly uncertain. The method used to estimate discards for Longnose Skate was based on a strong correlation ($R^2 = 95.7\%$) between total mortality of that species, and total mortality of Dover Sole for the years 2009–2017 during which Longnose were landed separately from other skates. In contrast, the sorting requirement for Big Skate occurred too recently to provide an adequate range of years for this type of correlation. Furthermore, there is greater uncertainty in the total mortality for the shallow-water species with which Big Skate most often co-occurs, such as Sand Sole and Starry Flounder, than there is for Dover Sole, which has been the subject of recurring stock assessments.

Both what discard rate information is available and anecdotal information from those involved in the fishery for both skate species indicate that discarding for Big Skate and Longnose Skate in the years prior to 1995 were driven by the same market forced and the discard rates were similar. Therefore, the discard rate for Longnose Skate was used as a proxy for the discards of Big Skate in order to estimate Big Skate discards.

The reconstructed landings of Big Skate for the period 1950–1995 had a mean of 63.1 t with no significant trend (a linear model fit to the data increased from 62.8 t in 1950 to 63.5 in 1995. The estimated tribal catch prior to 1995 averaged less than 1 t and was not included in this analysis of Big Skate discards for the years prior to 1995.

The mean discard rate for LN was 92.46%, also with no significant linear trend (the linear fit decreased from 92.8% in 1950 to 92.1% in 1995). An estimate of the mean annual discard amount can therefore be calculated as from the mean discard rate and the mean landings as $\bar{L}/(1-\bar{d})$ where $\bar{L}$ is the mean landings across that time period and $\bar{d}$ is the mean discards (Figure **??**).

Two alternative methods were used to estimate the mean annual discard amount: applying the annual LN discard rates to the annual BS catch, and applying 3-year moving averages of these two quantities. The use of the annual values resulted in an implausibly high degree of annual variability among the estimates, with the most extreme being a spike of 2146.4 in 1979 compared to 1032.7 t the year before and 654.0 the year after. The use of the 3-year moving average dampened this variability and these estimates were retained for a sensitivity analysis (Figure 4).

A discard mortality rate of 50 percent was assumed for all discards, following the assumption used for the Longnose Skate assessment conducted for the U.S. West Coast in 2007 (Gertseva, V and Schrippa, MJ 2007) The same rate has been used for skates in the trawl fishery in British Columbia, based on an approximate average of these reported rates. In 2015, PFMC's Groundfish Management Team (GMT) conducted a comprehensive literature review of skate discard mortality, and concluded that the current assumption regarding Big Skate discard mortality is consistent with existing reported rates for other similar species.

Estimation of discard rates (discards amount relative to total catch) during the period of the West Coast Groundfish Observer Program (WCGOP), which began in 2002, was hindered by the landings of Big Skate primarily occurring in the "unspecified skate" category prior to 2015. Therefore, a discard rate was computed using the combination of Big Skate and unspecified skate under the assumption that the vast majority of the unspecified skates were

Big Skate. A coefficient of variation was calculated for the by bootstrapping vessels within ports because the observer program randomly chooses vessels within ports to be observed. For the years after the catch share program was implemented in 2011, the trawl fishery was subject to 100% observer coverage and discarding is assumed to be known with minimal error (CV = 0.01).

The mean body weight of discarded Big Skates, calculated from the weight and count of baskets of discarded Big Skate, was available for the years 2002–2017.

3 Fishery-Independent Data Sources

3.1 Indices of abundance

3.1.1 Alaska Fisheries Science Center (AFSC) Triennial Shelf Survey

Research surveys have been used since the 1970s to provide fishery-independent information about the abundance, distribution, and biological characteristics of Big Skate. A coast-wide survey was conducted in 1977 (Gunderson, Donald Raymond and Sample, Terrance M. 1980) by the Alaska Fisheries Science Center, and repeated every three years through 2001. The final year of this survey, 2004, was conducted by the NWFSC according to the AFSC protocol. We refer to this as the **Triennial Survey**.

The survey design used equally-spaced transects from which searches for tows in a specific depth range were initiated. The depth range and latitudinal range was not consistent across years, but all years in the period 1980-2004 included the area from 40° 10'N north to the Canadian border and a depth range that included 55-366 meters, which spans the range where the vast majority of Big Skate encountered in all trawl surveys. Therefore the index was based on this depth range. The survey as conducted in 1977 had incomplete coverage and is not believe to be comparable to the later years, and is not used in the index.

3.1.2 Northwest Fisheries Science Center West Coast Groundfish Bottom Trawl Survey

In 2003, the NWFSC took over an ongoing slope survey the AFSC had been conducting, and expanded it spatially to include the continental shelf. This survey, referred to in this document as the "WCGBT Survey" or "WCGBTS", is conducted annually. It uses a random-grid design covering the coastal waters from a depth of 55 m to 1,280 m from late-May to early-October (Bradburn, M.J. and Keller, A.A and Horness, B.H. 2011 , Keller, A.A. and Wallace, J.R. and Methot, R.D. 2017). Four chartered industry vessels are used each year (with the exception of 2013 when the U.S. federal-government shutdown curtailed the survey).

3.1.3 Index Standardization

The index standardization methods for the two bottom trawl surveys matched that used for Longnose Skate and additional detail is provided in (Gertseva, V. 2019). The data from both surveys was analyzed using a spatio-temporal delta-model (Thorson, J. T. and Shelton, A. O. and Ward, E. J. and Skaug, H. J. 2015), implemented as an R package VAST (Thorson, James T. and Barnett, Lewis A. K. 2017) and publicly available online (https://github.com/James-Thorson/VAST). Spatial and spatio-temporal variation is specifically included in both encounter probability and positive catch rates, a logit-link for encounter probability, and a log-link for positive catch rates. Vessel-year effects were included for each unique combination of vessel and year in the database for the WCGBT Survey but not the Triennial survey. Further details regarding model structure are available in the user manual (https://github.com/James-Thorson/VAST/blob/master/examples/VAST_user_manual.pdf).

Spatial patterns in the survey estimates show Big Skate widely distributed along the coast, with higher densities in the central and more northern areas and closer to shore 7.

3.1.4 Internation Pacific Halibut Commission Longline Survey

The IPHC has conducted an annual longline survey for Pacific Halibut off the coast of Oregon and Washington since 1997 (no surveys were performed in 1998 or 2000). Beginning in 1999, this has been a fixed station design, with 84 locations in this area (station locations differed in 1997, and are therefore not comparable with subsequent surveys). 400 to 800 hooks have been deployed at each station in 100-hook groups (typically called "skates" although that term will be avoided here to avoid confusion). The gear used to conduct the survey was designed to efficiently sample Pacific Halibut and used 16/0 (#3) circle hooks baited with Chum Salmon.

In some years from 2011 onward, additional stations were added to the survey to sample Yelloweye Rockfish. These stations were excluded from the analysis, as were additional stations added in 2013, 2014, and 2017, off the coast of California (south of 42 degrees latitude). Some variability in exact sampling location is practically unavoidable, and leeway is given in the IPHC methods to center the set on the target coordinates while allowing wind and currents to dictate the actual direction in which the gear is deployed. This can result in different habitats being accessed at each fixed deployment location across years. One station that was very close to the U.S. Canada border had the mid-point of the set in Canada in 2 out of the 19 years of the survey. For consistency among years, all samples from this station were included in the analysis, including those in Canada.

In most years, bycatch of non-halibut species has been recorded during this survey on the first 20 hooks of each 100-hook group, although in 2003 only 10% of the hooks were observed for bycatch, and starting in 2012, some stations had 100% of the hooks observed for bycatch. Combining these observation pattern with the number of hooks deployed each year, resulted in most stations having 80, 100, 120, 140, or 160 hooks observed, with a mean of 144 hooks and a maximum of 800 hooks observed. The depth range of the 84 stations considered was 42—530 m, thus extending beyond the range of Big Skate, but 74% of the stations were shallower than 200 m. Big Skate have been observed at 51 of the 84 the standard stations that were retained for this analysis, but no station had Big Skates observed in more than 12 out of the 19 years of survey data, and only 10% of the station/year combinations had at least one observed Big Skate (Figure X). Of those station/year combinations with at least one Big Skate observed, the Big Skates were observed on an average of 1.3% of the hooks observed. The highest proportion was 10 Big Skates out of 81 hooks observed at one station.

The IPHC longline survey catch data were standardized using a Generalized Linear Model (GLM) with binomial error structure. Catch-per-hook was modeled, rather than catch per station due to the variability in the number of hooks deployed and observed each year. The binomial error structure was considered logical, given the binary nature of capturing (or not) a Longnose Skate on each longline hook. The modeling approach is identical to that which has been applied in the past for Yelloweye Rockfish (Stewart et al. 2009), and Spiny Dogfish (Gertseva and Taylor 2011). MCMC sampling of the GLM parameters was used to estimate the variability around each index estimate. The median index estimates themselves were approximately equal to the observed mean catch rate in each year (Figure Y). In recent years, the IPHC standardization of the index of halibut abundance has included an adjustment to account for missing baits on hooks returned empty in an effort to account for reduced catchability of the gear that may result from the lost bait. This adjustment was not included in the analysis for Big Skate although it could be considered in future years.

4 Biological Parameters and Data

4.1 Measurement Details and Conversion Factors

Some size measurements were taken as either disc width or inter-spiracle width rather than total length. A conversion from disc width to total length was estimated as $L = 1.3399 * W$ based on from 95 samples from WCGBT Survey where both measurements collected (R-squared = 0.9983). Little sex difference observed, so using single relationship for both sexes (Figure 15). This estimate is similar to the conversion estimated by Ebert (2008) for Big Skate in Alaska. The inter-spiracle width to total length was converted based on estimates from Downs & Cheng (2013):

$$L = 12.111 + 9.761 * ISW \text{ (females)},$$

$$L = 3.824 + 10.927 * ISW \text{ (males)}.$$

4.2 Fishery dependent length and age composition data

Fishery length composition data was available from PacFIN were available for the years 1995–2018 (with the exception of 2000) as shown in Table 4. Ages were available from only 2004, 2008-2012, and 2018. These were all represented as conditioned on length in order to provide more detailed information about the relationship between age and length, to reduce any influence of size-based selectivity on the age composition, and to ensure independence from the length samples. Furthermore, the samples from Washington in 2009 were sampled using a length-stratified system, so should only be treated as conditioned on length.

Length compositions of Big Skate discarded in commercial fisheries measured by the West Coast Groundfish Observer program were available for the years 2010–2017.

The input sample sizes for the length compositions were calculated via the Stewart Method (Ian Stewart, personal communication, IPHC):

$$\text{Input N} = N_{\text{hauls}} + 0.138 * N_{\text{fish}} \text{ if } N_{\text{fish}}/N_{\text{hauls}} \text{ is} < 44,$$

$$\text{Input N} = 7.06 * N_{\text{hauls}} \text{ if } N_{\text{fish}}/N_{\text{hauls}} \text{ is} \geq 44.$$

However, no haul had greater than 44 Big Skate sampled, so only the first formula was used.

4.3 Survey length and age composition data

Lengths of Big Skate were only collected form the Triennial survey in 1998, 2001, and 2004, but 1998 had only 3 samples and were excluded from this analysis. Length compositions were available for all years of the WCGBT Survey. Sample sizes for both surveys are provided in Table 5. The WCGBT Survey used disc width for the years 2006 and 2007 and total length in all other years. Those samples where only disc width was measured were converted to total length using the formula above.

The length compositions from the fishery and each of the two surveys aggregated across all years is shown in Figure 9.

Ages were available from the WCGBT Survey in the years 2009, 2010, 2016, 2017, and 2018. No ages were available from the Triennial Survey.

Ageing Precision and Bias

Ages of Big Skate were all estimated based on growth band counts of sectioned vertebrae. Ageing precision and bias were estimated using double-reads of 518 Big Skate vertebrae using the approach of Punt et al. (2008). The results showed strong agreement among readers (Figure 13), with a standard deviation of the ageing error increasing from about 0.4 at age 0 to 1.6 years at age 15 (Figure 14).

Weight-Length

The mean weight as a function of length was estimated from 1159 samples from the WCGBT Survey using a linear regression on a log-log scale. Sex was not found to be a significant predictor, so a single relationship was estimated: $Weight = 0.00000749 * Length^{2.9925}$ (Figure 15).

Sex Ratio, Maturity, and Fecundity

The female maturity relationship was based on visual maturity estimates from port samplers (n = 278, of which 241 were from Oregon and 37 from Washington, with 24 mature specimens) as well as 55 samples from the WCGBT Survey (of which 4 were mature). The resulting relationship was $L_{50\%} = 148.245$ with a slope parameter of $Beta = -0.13155$ in the relationship $M = (1 + Beta(L - L_{50\%}))^{-1}$ (Figure 16). This result is consistent with the estimated maturity of Big Skate in Alaska (Table 1).

4.4 Environmental or Ecosystem Data Included in the Assessment

In this assessment, neither environmental nor ecosystem considerations were explicitly included in the analysis. This is primarily due to a lack of relevant data or results of analyses that could contribute ecosystem-related quantitative information for the assessment.

5 Assessment

5.1 Previous Assessments

No previous stock assessment has been conducted for Big Skate. The current management is based on an OFL estimate calculated from a proxy for F_{MSY} and average survey biomass from the WCGBT Survey during the years 2010–2012 (Taylor IG and Cope, J and Hamel O and Thorson, J 2013). The F_{MSY} estimate was based on the product of an assumed F_{MSY}/M ratio and an M estimate of 0.162 based on the maximum age of 26 reported by McFarlane and King (McFarlane GA and King JR 2006). Values were sampled from an assumed distribution around all these quantities to develop a measure of uncertainty around the OFL estimate.

5.2 Model Description

5.2.1 Modeling Software

The STAT team used Stock Synthesis version 3.30.13 (Methot, Richard D. and Wetzel, Chantell R. (2013), Methot, RD Jr. and Wetzel, CR and Taylor, IG (2019)). The r4ss package version 1.35.1 (Taylor et al. 2019) was used to post-process the output data from Stock Synthesis.

5.2.2 Summary of Data for Fleets and Areas

Catch is divided among 4 fleets in the base model:

- Fishery (current) combines all non-tribal sources of catch for the years 1995 onward,
- Discard (historical) includes the estimated discard amount calculated from the estimated Longnose Skate discard rate as described above. The input catch for this fleet was 50
- Fishery (historical) includes the reconstructed landings estimates from each of the three states for 1916–1994.
- Tribal includes the estimates of catch of Big Skate by treaty tribes.

5.2.3 Other Specifications

This assessment covers the U.S. West Coast stock of Big Skate in off the coasts of Washington, Oregon and California, the area bounded by the U.S.-Canada border to the north, and the U.S.-Mexico border to the south. The population is treated as a single coastwide stock with no net movement in or out of the area. Females and males are modeled separately as there is evidence for differences in growth based on both the age and length data, as well as patterns in the sex ratios associated with the length composition data. Natural Mortality is estimated within the model using a natural mortality prior developed by Hamel (2015). A Beverton-Holt stock-recruit function is assumed with no deviations from the spawner-recruit curve estimated.

The length composition data are stratified into 37 5-cm bins, ranging between 20 and 200 cm and the age data are stratified into ages 0–15+, conditioned on the same length bin structure. The population dynamics are computed over a larger range of lengths-at-age, with the 5-cm length bins extending up to 250 cm and the numbers-at-age computed up to age 20.

5.2.4 Data Weighting

The Francis (2011) data weighting method "TA1.8" as implemented in the r4ss package was used for all length and age composition data.

5.2.5 Priors

Natural Mortality A log-normal prior for natural mortality was based on a meta-analysis completed by Hamel (2015). The Hamel prior for M is lognormal(ln(5.4/max age), .438), which based on the single 15-year-old fish observed out of 1034 ages from the WCGBT Survey. This results in lognormal(log(0.36) = –1.021651, 0.438) prior.

Survey Catchability The lack of contrast in the data resulted in unstable model results under a variety of configurations. To keep biomass estimates within a plausable range, the assessment uses a prior on the WCGBTS survey catchability parameter (q) that was originally developed for the 2007 Longnose Skate assessment (Gertseva, V and Schrippa, MJ 2007 p. @Dorn2007), and is being used for the concurrent Longnose Skate assessment (Gertseva, V. 2019). The prior for the WCGBT Survey was derived as follows.

The prior is based on consideration of the availability of longnose skate to the survey gear and the probability that a skate in the path of the gear would be caught and retained by the gear. The methodology for developing the prior involves specifying the potential range in the proportion of fish that are available to the gear and the potential range in the vulnerability to the gear, and "best guesses" for the individual probabilities. These values are translated into a lognormal prior where the median of the lognormal is the "best guess" and the range of plausible values covers 99% of the lognormal distribution.

Several factors inform catchability in the survey. The WCGBT Survey covers the full latitudinal range of Longnose Skate modeled in the assessment, and thus, the latitudinal availability factor was assumed to be one (complete latitudinal coverage). The survey coverage exceeds the maximum depth distribution of Longnose Skates but doesn't fully cover the shallow end of the skate distribution. A range of 95 to 100 percent was assumed for the depth availability. A range of 75 to 95 percent was assumed for vertical availability on the basis that skates are known to bury in the mud, and therefore some may be unavailable to the bottom trawl gear.

The largest bounds were placed on the probability of capture, given that a fish is in the net path. It is known that flatfish can be herded by trawl gear, and it is possible that this could also occur for skates. However, it is also possible that skate could avoid the trawl nets. For capture probability, a range of 75 to 150 percent was assumed. The best estimates for each of these factors were set at the midpoint of the range for individual factors, except for the probability of capture, which was given a value of one. The overall estimate for the survey catchability was the product of the best estimates, 0.83. The bounds on catchability are the products of the low and high values for factor ranges, respecively, which are 0.53 and 1.43. The best guess was equated to the median of a lognormal distribution and the bounds to 99% of that distribution. This gave a normal prior on $log(q)$, with mean –0.188 and standard deviation 0.187.

5.2.6 Estimated Parameters

A full list of all estimated and fixed parameters is provided in Tables 7.

The base model has a total of 44 estimated parameters in the following categories:

- 1 natural mortality parameter applied to both sexes,
- 6 parameters related to female growth and the variability in length at age
- 2 parameters relating male growth to female growth,
- 1 stock-recruit parameter ($log(R_0)$ controlling equilibrium recruitment)
- 3 catchability parameters (1 for the WCGBT Survey and 1 each for the early and late periods of the Triennial Survey)
- 2 extra standard deviation parameters (1 for each survey)
- 29 selectivity parameters, including 16 related to time-varying retention rate

The estimated parameters are described in greater detail below and a full list of all estimated and parameters is provided in Table 7.

Growth. Examination of patterns of age-at-length and length-at-age indicated unusual patterns of growth for Big Skate. The youngest fish show near-linear growth, and average size for both sexes is similar. However, older fish show considerable sex-based differences in size. This led to the choice to model growth using the "growth cessation model" recently developed by Maunder et al. (2018). The estimated growth curves are shown in Figure 17. The growth cessation model provided two key advantages over the more common von Bertalanffy growth model in the case of Big Skate: it allowed essentially linear growth for the early years and it allowed growth for the earlier ages to be similar between females and males while diverging at older ages. The growth cessation model also improve the negative log-likelihood by 45 units relative to the von Bertalanffy growth model.

Natural Mortality. Male natural mortality was assumed equal to the value estimated for females. Sensitivity analyses were used to test the impact of both the the prior on natural mortality and the assumption of equal natural mortality for both sexes.

Selectivity.
A double-normal selectivity function was used for all fleets to allow consideration of both asymptotic and dome-shaped patterns. For the fishery and the Triennial survey, the difference in likelihood between dome-shaped and asymptotic patterns was very small and in the case of the Triennial survey, the dome-shape occurred at a length beyond almost all observations, indicating that this shape was likely driven by fit to other data sources, such as the index, rather than the length composition data. The WCGBT Survey was allowed to remain dome-shaped as this survey had the selectivity peak at a smaller length than the other fleets and the likelihood was improved by the dome-shape. The WCGBT Survey also has the shortest hauls, with 15 minutes or less of bottom contact, so larger skates may be better able to escape the net.

In order to fit a strong skew in the sex ratios toward males for the length bins in which the majority of the samples were found, it was necessary to estimate a sex-specific offset of selectivity. Two offset parameters were estimated for all fleets, one for the difference in length at peak selectivity and another for the maximum selectivity at that peak (allowing one sex to have a maximum of 1.0 at the peak and the other to have a maximum less than 1.0). The ascending slope was assumed equal in all cases, as was the descending slope for the WCGBT Survey.

5.2.7 Fixed Parameters

The steepness of the Beverton-Holt stock-recruit curve was fixed at 0.4. The same value was used in the 2007 Longnose Skate assessment (Gertseva, V and Schrippa, MJ 2007) and is being considered for the ongoing 2019 Longnose Skate assessment. This value reflects a

K-type reproductive strategy associated with elasmobranchs in general. The influence of the assumption of $h = 0.4$ on model output was explored via a likelihood profile analysis.

5.3 Model Selection and Evaluation

5.3.1 Key Assumptions and Structural Choices

To be added prior to May 20 CIE pre-review deadline.

5.3.2 Alternate Models Considered

To be added prior to May 20 CIE pre-review deadline.

5.3.3 Convergence

One hundred sets of jittered starting values were generated using the jitter function built into Stock Synthesis, with used with jitter input = 0.1. The same likelihood as the base model was returned by 51 out of the 100 runs, while the others all had worse total likelihood.

5.4 Response to the Current STAR Panel Requests

Request No. 1:

Rationale: xxx

STAT Response: xxx

Request No. 2:

Rationale: xxx

STAT Response: xxx

Request No. 3:

Rationale: x.

STAT Response: xxx

Request No. 4:

Rationale: xxx

STAT Response: xxx

Request No. 5:

Rationale: xxx

STAT Response: xxx

5.5 Base Case Model Results

The following description of the model results reflects a base model that incorporates all of the changes made during the STAR panel (see previous section). The base model parameter estimates and their approximate asymptotic standard errors are shown in Table 7. Estimates of derived reference points and approximate 95% asymptotic confidence intervals are shown in Table e. Time-series of estimated stock size over time are shown in Table 13.

5.5.1 Parameter Estimates

Values of all estimated parameters are provided in Table 7. A few key parameters of note include natural mortality estimated at 0.445, slightly above the 0.36 median of the prior and with much narrower uncertainty than the prior (Figure 18), L-infinity at 175.67 for females and 120.97 for males (based on an exponential offset of -0.373). The $log(R_0)$ parameter was estimated at 8.728, corresponding to an unfished equilibrium recruitment of 6.18 million.

Catchability from the WCGBT Survey was estimated at 0.81, close the median of the prior applied to this parameter, with uncertainty estimated as very similar to the uncertainty in the prior (Figure 18).

Selectivity was estimated to be asymptotic for the WCGBT Survey (the only fleet for which it was allowed to be dome-shaped), with the peak selectivity occurring at 76 cm, below the peak of the fishery selectivity at 94 cm (Figure 19). These two fleets had a similar estimate for the lower maximum selectivity for females than males, at 0.696 for the survey and 0.744 for the fishery. Selectivity for the Triennial survey was substantially different from the other two, with an additional parameter estimated for the initial selectivity of the smallest sizes necessary to fit the very flat length compositions from the two years of data available, and a peak occurring at 188 cm, far higher than the other two curves. When converted to age, the selectivity peaked at about age-4 for the WCGBT Survey, age-5 for the fishery, and age 7 and 12 for males and females in the Triennial Survey, respectively (Figure 20).

5.5.2 Fits to the Data

Indices. The observed indices show much more variability than the model expectation, with the fit to the WCGBT Survey essentially a flat line (Figure 23) and the fit to the Triennial Survey only showing a noticeable change over time due to the separate catchability parameter estimated for the early and late periods (Figure 24).

Length Data. The fits to the length data were reasonably good (Figures 25–26 and A54–A57). The observed length compositions for males in both the fishery and the WCGBT Survey is bimodal, with modes in the 80 cm and 115 cm length bins for the fishery, and in the 60 cm and 115 cm bins for the survey. The model expectation has modes in similar locations in both cases, where the first mode is close to the estimated peak selectivity value and the second is close to the estimated male L-infinity parameter. However, the second mode in the model expectation is less pronounced than in the observed data (Figure 25). The residual patterns in the fit to the length compositions don't show strong patterns, with the WCGBT Survey data especially well fit. The residuals in the fit to the fishery length compositions show a few large residuals in the early years as a few years where there were observations of small (under 50 cm) fish in the retained fishery catch which the model expected would have been discarded (Figure 26). The fit to the length data in alternative models that lacked either the growth cessation model or the sex-specific offsets to selectivity were less good.

Conditional Age-at-Length. The conditional age-at-length data is likewise fit reasonably well, with some patterns in residuals showing variability among years, but no clear pattern that is consistent across years (Figures 27 and 28).

Sex Ratios. Sex ratio data is not included in the likelihood as such, but as a part of the length composition likelihood. The proportions of females and males are compiled into a single vector that is compared to the model expectations in the multinomial likelihood. The patterns in sex ratio by length bin show fewer females than males for the middle range of sizes (70–120 cm), with a shift to almost 100% females for the largest size bins (over 130 cm). These patterns are shown in Figures 29 and 30. The approximate uncertainty associated with the observed ratios is represnted using a Jeffreys interval (Brown et al. 2001) based on the combination of the proportion of the lengths with each length bin and the adjusted input sample size. The use of sex-specific growth curves was adequate to fit the ratios for the largest bins, but ratio skews toward males at lengths where the mean ages are similar for females and males. The fit to this part of the sex ratio pattern required an offset in selectivity.

Discards Rates and Mean Weight of the Discards. Fit to the discard fraction estimates (Figure 31) and the mean weight of the discards (Figure 32) show reasonably good fits. The model expectation is able to match the trend of decreasing discard fractions and decreasing mean weights over the years 2002–2010 by estimating an increasing trend in the asymptotic retention rate from 2004 to 2008 with a peak at close to 100%, followed by a decreasing trend from 2012 onward (Figures 21 and 22). The years 2008–2012 with the highest asymptotic retention rates have little retention of large fish leading to lower discard rates and smaller mean weight of the discarded fish. The period from 2011 onward had observer coverage increased to 100% for the catch-shares trawl fishery, leading to more precise data and consistent patterns in the two data types. The first few years (which form the basis for the estimates going back to 1995), are more uncertain and less well fit, with the discard rates over 30% inconsistent with the mean weight under 1.5 kg in 2003 and 2004.

5.5.3 Uncertainty and Sensitivity Analyses

A number of sensitivity analyses were conducted, including:

- Allowing all selectivity curves to be dome-shaped
- Removing the sex-specific offset on the selectivity curves
- Removing the prior on catchability for the WCGBT Survey
- Estimating a single catchability for all years in the Triennial Survey
- Estimating separate natural mortality parameters for males and females
- Removing the prior on natural mortality
- Using the von Bertalanffy growth model
- Using the Richards growth model
- Tuning the sample sizes using the McAllister-Ianelli method
- Estimating historic discards based on 3yr average of discard rates and landings
- Changing discard mortality from 0.5 to 0.4
- Changing discard mortality from 0.5 to 0.6
- Estimating multipliers on historical discards over blocks of time

Results of these sensitivities are shown in Figures 38 to 43, and Tables 8 to 10.

Selectivity and catchability

Allowing the selectivity for all fleets to be dome-shaped resulted in domed selectivity for all fleets, but only improved the total negative log-likelihood by 0.9 units, mostly through a slightly improved fit to the length compositions, although the fit to the surveys was slightly worse (Table 8). Removing the offset between female and male selectivity caused the negative log-likelihood to be worse by 18.1 units, mostly through a worse fit to the length comps but also a worse fit to the conditional age-at-length compositions. The conditional age data was represented independently for each sex, so no sex-ratio information was present in the data, but the growth curves were changed slightly to compensate for the change in fit to the length data, resulting in a less good fit to the age data as well. The scale of the population remained somewhat similar to the base model under both of these sensitivities (Figure 38).

Removing the prior on catchability for the WCGBT Survey had a large change in the estimated scale of the population, with the unfished equilibrium biomass increasing from the 2,224 mt estimated in the base model to 9,932 mt ("Q no prior on WCGBTS" in Figure 38 and Table 8). However, the change in likelihood was relatively small, with the total improving by 0.4 units, of which 0.04 was associated with the prior itself.

Catch and discards

The sensitivity analyses related to discard mortality resulted in little change in the scale of the population for any scenario (Figure 39 and Table 9). Increasing or descring the discard mortality from 0.5 to 0.4 or 0.6 had the least impact, while the two alternative time series of discards caused the population to fall to a lower level around 1990 and increase faster in the recent period. The discards based on 3-yr average analysis simply used the alternative time series of historical discards described above and shown in Figure 4.

The sensitivity analysis in which multipliers on historical discards were estimated made use of the relatively new "catch multiplier" option in Stock Synthesis. Multiplier parameters controling the ratio of the discards removed from the model relative to the input values were estimated for blocks of time covering the periods 1916–1949, 1950–1959, 1960–1969, 1970–1979, 1980–1989, and 1990–1994. These multiplier parameters were bounded to keep the input catch relative to the estimated total within the range 0.5–1.5 and a weak Beta prior distribution spawning this range was applied to the parameters to keep them from hitting the bounds and cause them to remain at 1.0 in the absence of information in the data.

The resulting pattern of historical discards shows a steadily increasing catch, with higher catch relative to the input values in all the blocks up to a peak in the 1980s, followed by an estimated decrease in the estimated catch for the 1990-1994 period (Figures 42 and 41). These changes provide a greater contrast in the catch history, causing the estimated time series of spawning biomass to fall to a lower level and then increase faster from the 1990s onward, thus fitting the WCGBT Survey slightly better (Figures 39 and {fig:Sensitivity_catch2}). However, the improvement in likelihood for the survey was only 0.3 units (Table 9).

Biology and data weighting

The sensitivity analyses related to biology and data weighting included assumptions about natural mortality (M), growth, and data weighting (Figure 43 and Table 10). Allowing separate estimates of female and male natural mortality led to estimates of 0.475 for females and 0.395 for males, which are nearly symmetric around the 0.445 estimate of the shared mortality parameter in the base model. This difference allows more males to be present in the population and therefore better match the skewed sex ratios in the length composition data. The scale of the unfished equilibrium spawning biomass dropped to 61% of the base model estimate due to the smaller fraction of females living to mature with the higher M, but the estimate of total biomass in the unfished population remained at 91% of the base model (Table 10). The improvement in likelihood is 2.2 units, which is modest given the extra parameter estimated. Additional explorations (not shown) indicated that a model with differential M and no sex-specific offsets on the selectivity had much worse fit to the data than either the base model or this sensitivity analysis. Therefore, given that the differential selectivity provided a greater improvement in model fit than the sex-specific M, only the more influential factor was included in the base model.

Removing the prior on M had little impact on the model with M increasing from 0.445 in the base model to 0.448 without the prior.

The use of either von Bertalanffy (1938) or Richards (1959) growth models provided less good fits to both the conditional age-at-length and length data and higher estimated variability in length-at-age (Figure 44). The increase in variability in length-at-age suggests that the model is using this variability to compensate for lack of fit to the mean length-at-age. The Richards model is a generalization of the von Bertalanffy growth model with an additional parameter allowing a more sigmoidal shape. For females, this additional parameter was hitting the lower bound of 0.1 resulting in linear growth up to age 20. This parameter on the bound led to a bad gradient and a non-positive-definite Hessian matrix, indicated that the model had not converged to the maximum likelihood estimates. In theory the additional parameter in the Richards model should allow it to always provide a better likelihood relative to the von Bertallanfy, but further attempts to search for a converged model with Richards growth has not yet been undertaken.

Tuning the sample sizes using the McAllister-Ianelli method had relatively small impact on the model results, with a lower weight given to the fishery lengths than the status-quo Francis tuning method, and a higher weight given to the WCGBT Survey lengths. The lengths from the Triennial Survey were given similar weight. Ages from both the fishery and the WCGBT Survey were increased in weight by a factor of 4.8 and 7.5, respectively. The likelihoods could not be compared due to these changes in the adjusted sample sizes, but the estimated parameters were all relatively similar to those in the base model (Table 10).

5.5.4 Retrospective Analysis

Retrospective analyses, in which the final 5 years of data are successively removed from the model, showed relatively little change in the scale of the estimated population, but the uncertainty about the population size increased (Figure 45). The WCGBT Survey observations were underfit for the final 5 years, so removing these points, combined with a prior on catchability lowers the status of the stock, led to a slightly reduced estimated spawning biomass.

5.5.5 Likelihood Profiles

Likelihood profiles were conducted over $log(R_0)$, stock-recruit steepness (h) and natural mortality (M). Results of these profiles are shown in Figures 47 to 52.

The profile over $log(R_0)$ shows that the change in likelihood over a broad range of values is relatively small compared to models with more contrast in the data, with a total change in likelihood of less than 4 units over a range of 8.2 to 9.6, corresponding to a range in equilibrium recruitment of 3.6 million to 14.8 million (the $log(R_0)$ parameter is the log of R_0 in thousands). Models with $log(R_0) < 8.2$ did not converge. The age data and discard data are best fit at the highest R_0 considered while the index and mean body weight data are best fit at the lowest R_0. Only the priors and the length data are best fit at intermediate values. The length data was best fit at $log(R_0) = 8.6$, while the separate components of the prior likelihood were also best fit at $log(R_0) = 8.6$ in the case of the prior on the catchability of the WCGBT Survey, and at $log(R_0) = 8.2$ in the case of the prior on natural mortality. The base model estimate balancing all these components was $log(R_0) = 8.728$. The spawning biomass estimates from the models in the profile were all relatively similar as a result of the models with higher R_0 also having a higher M estimate, leading to a similar number of fish surviving to maturity (the range was $M = 0.526$ at $log(R_0) = 9.6$ to $M = 0.398$\$ at $log(R_0) = 8.2$).

The profile over steepness of the stock-recruit curve showed less than 0.8 units of likelihood over the range $h = 0.3$ to $h = 0.9$. The best fit occurred at $h = 0.5$, indicating that a model with steepness estimated would have been relatively similar to the base model where h was fixed at 0.4. However, earlier model explorations indicated that models with h estimated sometimes produced unstable results, where small changes in model configuration could cause the parameter to be estimated at either the upper or lower bound of the 0.2–1.0 range on which it's defined for the Beverton-Holt stock-recruit curve.

The profile over natural mortality (M) showed that most of the information in the likelihood about M was from the length and age data, with additional information in the discard rates and the mean body weight data. The prior on M provided relatively little contribution to the total likelihood. The length data had the largest change in likelihood over the 0.25–0.55 range of M considered, and was best fit at 0.45, close to the base model estimate of 0.445.

5.5.6 Reference Points

Reference points were calculated using the estimated selectivities and catch distribution among fleets in the most recent year of the model, (2018). Sustainable total yield (landings plus discards) were 507 mt when using an $SPR_{50\%}$ reference harvest rate and with a 95% confidence interval of 333 mt based on estimates of uncertainty. The spawning biomass equivalent to 40% of the unfished level ($SB_{40\%}$) was 890 mt.

The 2019 spawning biomass relative to unfished equilibrium spawning biomass is above the target of 40% of unfished levels (Figure 34). The relative fishing intensity, $(1 - SPR)/(1 - SPR_{50\%})$, has been below the management target for the entire time series of the model (Table 13).

Table e shows the full suite of estimated reference points for the base model and Figure 53 shows the equilibrium curve based on a steepness value of 0.4.

6 Harvest Projections and Decision Tables

The forecasts of stock abundance and yield were developed using the final base model, with the forecasted projections of the OFL presented in Table g.

The forecasted projections of the OFL for each model are presented in Table h.

7 Regional Management Considerations

Big Skate is not managed to regional specifications.

8 Research Needs

There are a number of areas of research that could improve the stock assessment for Big Skate. Below are issues identified by the STAT team and the STAR panel:

1. **Data!**:
2. **xxxx**:
3. **xxxx**:
4. **xxxx**:
5. **xxxx**:

9 Acknowledgments

The authors gratefully acknowledge the time and effort reviewers John DeVore, Stacey Miller, Jim Hastie and Owen Hamel put into making this a polished document.

We thank the STAR panel Chair, David Sampson, and reviewers Robin Cook and Cody Szulwalski.

The Reconstructions of historical catch were critical to this assessment, and there are many people who contributed, among them

our colleagues at WDFW: Theresa Tsou, Jessi Doerpinghaus and Greg Lippert

our colleagues at ODFW: Ali Whitman and Ted Calavan

our colleagues at the SWFSC: John Field and Rebecca Miller

and others whose knowledge of the fishery provided context: Gerry Richter and Todd Phillips

Our colleagues at NWFWC, including Chantel Wetzel, Kelli Johnson, and John Wallace all provided valuable contributions to the extraction and processing of the survey and fishery data.

Finally, we are deeply grateful to Mellissa Monk of the SWFSC, for creating the RMarkdown template which was used to produce this assessment report.

10 Tables

10.1 Data Tables

Table 2: Landings by source. Landings are reconstructed histories 1916-1995.

Year	CA (mt)	OR (mt)	WA (mt)	Tribal (mt)	Total (mt)
1916	78.30	0.00	0.00	0.00	78.30
1917	80.10	0.00	0.00	0.00	80.10
1918	101.20	0.00	0.00	0.00	101.20
1919	75.20	0.00	0.00	0.00	75.20
1920	122.00	0.00	0.00	0.00	122.00
1921	17.80	0.00	0.00	0.00	17.80
1922	30.80	0.00	0.00	0.00	30.80
1923	34.20	0.00	0.00	0.00	34.20
1924	33.40	0.00	0.00	0.00	33.40
1925	46.70	0.00	0.00	0.00	46.70
1926	59.30	0.00	0.00	0.00	59.30
1927	67.10	0.00	0.00	0.00	67.10
1928	116.70	0.00	0.00	0.00	116.70
1929	107.50	0.00	0.00	0.00	107.50
1930	70.80	0.00	0.00	0.00	70.80
1931	43.60	0.00	0.00	0.00	43.60
1932	73.30	0.00	0.00	0.00	73.30
1933	46.50	0.00	0.00	0.00	46.50
1934	57.40	0.00	0.00	0.00	57.40
1935	70.60	0.00	0.00	0.00	70.60
1936	87.70	0.00	0.00	0.00	87.70
1937	115.40	0.00	0.00	0.00	115.40
1938	99.40	0.00	0.00	0.00	99.40
1939	90.90	0.00	0.00	0.00	90.90
1940	60.30	5.30	0.00	0.00	65.70
1941	53.10	56.40	0.00	0.00	109.40
1942	27.00	34.40	0.00	0.00	61.40
1943	20.40	0.90	0.00	0.00	21.30
1944	7.80	1.60	0.00	0.00	9.50
1945	13.30	0.30	0.00	0.00	13.50
1946	17.10	1.80	0.00	0.00	18.90
1947	24.10	0.00	0.00	0.00	24.10
1948	30.70	5.70	0.00	0.00	36.30
1949	31.90	0.00	7.20	0.00	39.10
1950	32.20	2.10	2.10	0.00	36.40
1951	21.70	4.70	3.90	0.00	30.30

Continued on next page

Table 2: Landings by source. Landings are reconstructed histories 1916-1995.

Year	CA (mt)	OR (mt)	WA (mt)	Tribal (mt)	Total (mt)
1952	39.10	0.10	7.80	0.00	46.90
1953	124.90	1.20	1.60	0.00	127.60
1954	38.80	2.30	1.20	0.00	42.40
1955	45.70	35.60	1.60	0.00	82.90
1956	40.40	2.60	3.10	0.00	46.10
1957	49.50	0.00	2.50	0.00	52.00
1958	38.80	0.00	0.20	0.00	38.90
1959	46.50	0.00	0.80	0.00	47.30
1960	39.20	0.00	0.70	0.00	39.80
1961	54.40	40.90	4.60	0.00	99.80
1962	44.40	27.90	5.20	0.00	77.60
1963	53.20	30.40	2.10	0.00	85.70
1964	49.90	28.30	2.70	0.00	80.90
1965	34.30	12.80	3.50	0.00	50.60
1966	36.40	20.10	0.60	0.00	57.00
1967	53.30	15.60	6.60	0.00	75.50
1968	55.30	45.40	8.80	0.00	109.50
1969	32.50	33.80	6.60	0.00	72.90
1970	16.30	11.90	0.10	0.00	28.20
1971	18.50	3.10	0.00	0.00	21.60
1972	33.50	2.00	0.10	0.00	35.60
1973	40.70	0.90	0.00	0.00	41.70
1974	21.90	5.90	0.10	0.00	27.80
1975	39.80	2.00	0.00	0.00	41.80
1976	20.70	31.30	0.20	0.00	52.20
1977	32.80	31.50	0.60	0.00	64.90
1978	67.70	77.30	4.00	0.00	149.10
1979	90.50	75.50	30.40	0.00	196.40
1980	17.60	34.10	5.20	0.00	56.90
1981	138.00	14.80	6.50	0.00	159.30
1982	78.30	5.20	14.60	0.00	98.10
1983	55.30	14.20	8.90	0.00	78.40
1984	26.20	4.90	1.60	0.00	32.70
1985	60.30	0.40	4.90	0.00	65.60
1986	27.20	1.60	8.90	0.00	37.80
1987	22.60	1.90	18.40	1.00	43.90
1988	15.30	0.30	10.90	1.20	27.60
1989	18.90	0.20	6.20	0.00	25.30
1990	25.10	0.00	9.60	0.10	34.90
1991	22.80	0.20	21.50	0.10	44.60
1992	24.60	0.30	11.20	0.00	36.10

Continued on next page

Table 2: Landings by source. Landings are reconstructed histories 1916-1995.

Year	CA (mt)	OR (mt)	WA (mt)	Tribal (mt)	Total (mt)
1993	29.00	0.20	21.00	0.60	50.70
1994	27.70	2.50	20.50	0.10	50.70
1995	43.00	41.20	21.80	0.10	106.00
1996	146.70	138.50	22.80	0.10	308.10
1997	228.40	215.40	84.00	0.20	528.00
1998	120.50	51.40	22.70	0.20	194.90
1999	109.50	131.30	41.40	0.40	282.60
2000	69.40	193.60	97.70	0.30	361.00
2001	75.30	115.10	26.70	0.40	217.50
2002	34.70	102.80	70.80	4.80	213.10
2003	48.80	223.00	65.70	5.40	342.80
2004	45.20	105.90	98.00	4.60	253.80
2005	33.40	151.30	113.10	15.70	313.40
2006	102.40	206.60	66.20	24.90	400.00
2007	35.50	190.40	29.10	19.90	274.90
2008	46.00	280.10	36.80	3.20	366.00
2009	9.60	162.00	16.50	17.50	205.70
2010	1.20	157.50	25.00	12.50	196.20
2011	0.50	231.50	10.00	26.40	268.40
2012	6.80	216.30	5.00	41.60	269.60
2013	20.90	92.30	13.00	8.80	135.00
2014	41.00	286.00	16.80	28.60	372.40
2015	35.20	218.80	1.00	76.60	331.50
2016	15.00	317.50	1.20	77.80	411.50
2017	28.00	188.00	1.40	60.20	277.60
2018	23.80	115.80	2.40	30.60	172.60

Table 3: Index inputs.

	WCGBTS		Triennial		IPHC	
Year	Obs	se_log	Obs	se_log	Obs	se_log
1980			467.83	0.53		
1983			911.85	0.30		
1986			996.75	0.29		
1989			1431.65	0.22		
1992			2426.18	0.20		
1995			497.24	0.26		
1998			2437.75	0.20		
1999					0.00	0.17
2001			1669.73	0.23	0.00	0.29
2002					0.00	0.53
2003	8170.51	0.20			0.00	0.43
2004	14349.00	0.18	3674.14	0.19	0.00	0.20
2005	12122.52	0.16			0.00	0.18
2006	9273.79	0.18			0.00	0.64
2007	8137.47	0.18			0.00	0.34
2008	5494.76	0.21			0.00	0.81
2009	10721.30	0.17			0.00	0.48
2010	11475.29	0.14			0.00	0.24
2011	8029.69	0.16			0.00	0.20
2012	11593.79	0.16			0.00	0.61
2013	11521.85	0.17			0.00	0.20
2014	19855.79	0.13			0.00	0.19
2015	19251.41	0.13			0.00	0.16
2016	17141.95	0.15			0.00	0.17
2017	13237.37	0.14			0.00	0.18
2018	14568.79	0.14			0.00	0.26

Table 4: PacFIN Samples.

	CA		OR		WA		All Landings		Discards	
Year	Ntows	Nfish	Ntows	Nfish	Ntows	Nfish	Ntows	Nfish	Ntows	Nfish
Lengths										
1995			6	55			6	55		
1996			3	8			3	8		
1997			1	14			1	14		
1998			1	2			1	2		
1999			1	8			1	8		
2000										
2001			3	43			3	43		
2002			6	199			6	199		
2003			9	202			9	202		
2004			2	27	2	12	4	39		
2005			7	123	6	87	13	210		
2006			13	310	15	191	28	501		
2007	1	1	10	128	9	172	20	301		
2008			10	94	8	94	18	188		
2009	8	32	17	234	1	18	26	284		
2010	2	8	15	186			17	194	149	349
2011	2	2	29	418	4	9	35	429	554	1518
2012	3	43	24	477	3	38	30	558	544	1405
2013	11	201	11	252	8	168	30	621	443	987
2014	15	217	11	237	5	249	31	703	676	1625
2015	25	237	21	411	2	5	48	653	688	1557
2016	14	181	34	444	7	98	55	723	652	1456
2017	14	239	50	668	12	47	76	954	508	1248
2018	15	133	46	552	14	98	75	783		
Ages										
2004					2	11	2	11		
2008			8	80			8	80		
2009			10	87	8	65	18	152		
2010			10	102			10	102		
2011			21	202			21	202		
2012			12	120			12	120		
2018			6	39	13	93	19	132		

Table 5: Samples from the surveys.

	Triennial		WCGBTS		IPHC	
Year	Ntows	Nfish	Ntows	Nfish	Nsets	Nfish
Lengths						
2001	41	81				
2003			60	197		
2004	39	100	81	262		
2005			99	328		
2006			67	154		
2007			76	192		
2008			53	159		
2009			82	305		
2010			130	466		
2011			99	360		
2012			104	395		
2013			84	316		
2014			149	552	14	54
2015			134	546		
2016			105	422		
2017			125	496		
2018			123	331		
Ages						
2009			77	230		
2010			124	333		
2016			100	138		
2017			110	164		
2018			118	169		

10.2 Model Results Tables

Table 6: Time-series of population estimates from the base-case model. Relative exploitation rate is $(1 - SPR)/(1 - SPR_{50\%})$.

Year	Total biomass (mt)	Spawning biomass (mt)	%Unfished	Age-0 recruits	Total catch (mt)	Relative exploitation rate	SPR
1916	25232	2224	1.000	6176	0	0.00	1.00
1917	25232	2224	1.000	6176	12	0.00	0.99
1918	25221	2223	0.999	6175	25	0.00	0.99
1919	25199	2220	0.998	6172	37	0.00	0.98
1920	25169	2217	0.997	6168	49	0.00	0.98
1921	25131	2212	0.995	6164	62	0.00	0.97
1922	25087	2206	0.992	6157	74	0.00	0.97
1923	25037	2200	0.989	6150	86	0.00	0.96
1924	24981	2192	0.985	6142	99	0.00	0.96
1925	24920	2183	0.981	6132	111	0.00	0.96
1926	24854	2173	0.977	6122	123	0.01	0.95
1927	24783	2163	0.973	6111	136	0.01	0.94
1928	24707	2153	0.968	6100	148	0.01	0.94
1929	24627	2142	0.963	6088	160	0.01	0.93
1930	24544	2130	0.958	6076	172	0.01	0.93
1931	24456	2118	0.953	6063	185	0.01	0.92
1932	24365	2106	0.947	6049	197	0.01	0.92
1933	24271	2094	0.941	6035	210	0.01	0.91
1934	24174	2081	0.936	6020	222	0.01	0.91
1935	24074	2067	0.929	6005	234	0.01	0.90
1936	23971	2053	0.923	5989	246	0.01	0.90
1937	23866	2039	0.917	5973	259	0.01	0.89
1938	23758	2025	0.910	5956	271	0.01	0.89
1939	23648	2010	0.904	5939	329	0.01	0.87
1940	23494	1991	0.895	5916	329	0.02	0.86
1941	23353	1972	0.887	5894	363	0.02	0.85
1942	23193	1952	0.878	5869	351	0.02	0.85
1943	23059	1933	0.869	5846	343	0.02	0.86
1944	22943	1917	0.862	5826	350	0.02	0.85
1945	22829	1900	0.854	5805	364	0.02	0.85
1946	22708	1884	0.847	5784	379	0.02	0.84
1947	22581	1868	0.840	5763	394	0.02	0.83
1948	22447	1851	0.832	5742	412	0.02	0.83

Table 6: Time-series of population estimates from the base-case model. Relative exploitation rate is $(1 - SPR)/(1 - SPR_{50\%})$.

Year	Total biomass (mt)	Spawning biomass (mt)

1949	22306	1834	0.825	5720	426	0.02	0.82
1950	22162	1818	0.817	5698	424	0.02	0.82
1951	22032	1801	0.810	5677	418	0.02	0.82
1952	21917	1786	0.803	5656	434	0.02	0.81
1953	21794	1771	0.796	5635	515	0.03	0.78
1954	21603	1748	0.786	5604	430	0.02	0.81
1955	21507	1734	0.780	5584	470	0.02	0.80
1956	21377	1718	0.772	5561	434	0.02	0.81
1957	21290	1706	0.767	5544	439	0.02	0.81
1958	21201	1694	0.762	5527	426	0.02	0.81
1959	21126	1685	0.757	5514	435	0.02	0.81
1960	21045	1675	0.753	5500	427	0.02	0.81
1961	20974	1667	0.750	5489	487	0.03	0.78
1962	20849	1655	0.744	5471	465	0.02	0.79
1963	20754	1645	0.740	5456	473	0.02	0.79
1964	20658	1635	0.735	5440	468	0.02	0.79
1965	20575	1624	0.730	5425	438	0.02	0.80
1966	20525	1616	0.727	5413	444	0.02	0.80
1967	20470	1608	0.723	5401	463	0.02	0.79
1968	20399	1599	0.719	5387	497	0.03	0.78
1969	20299	1588	0.714	5369	460	0.02	0.79
1970	20238	1581	0.711	5358	416	0.02	0.81
1971	20223	1578	0.710	5354	409	0.02	0.81
1972	20211	1577	0.709	5352	423	0.02	0.80
1973	20184	1574	0.708	5348	429	0.02	0.80
1974	20150	1571	0.706	5343	415	0.02	0.81
1975	20130	1570	0.706	5341	429	0.02	0.80
1976	20097	1567	0.705	5337	440	0.02	0.80
1977	20057	1564	0.703	5331	452	0.02	0.79
1978	20010	1559	0.701	5324	536	0.03	0.76
1979	19887	1546	0.695	5304	584	0.03	0.74
1980	19732	1529	0.688	5277	444	0.02	0.79
1981	19724	1524	0.685	5268	547	0.03	0.75
1982	19618	1510	0.679	5246	486	0.03	0.77
1983	19576	1502	0.676	5233	466	0.03	0.78
1984	19551	1497	0.673	5224	420	0.02	0.80
1985	19565	1497	0.673	5224	453	0.03	0.79
1986	19541	1495	0.672	5221	425	0.02	0.80
1987	19539	1497	0.673	5224	431	0.02	0.79
1988	19529	1499	0.674	5228	415	0.02	0.80
1989	19534	1502	0.676	5233	413	0.02	0.80

Table 6: Time-series of population estimates from the base-case model. Relative exploitation rate is $(1 - SPR)/(1 - SPR_{50\%})$.

Year	Total biomass (mt)	Spawning biomass (mt)

1990	19541	1506	0.677	5238	422	0.02	0.80
1991	19540	1507	0.678	5240	432	0.02	0.79
1992	19531	1506	0.677	5239	424	0.02	0.80
1993	19534	1505	0.677	5238	438	0.02	0.79
1994	19524	1503	0.676	5234	438	0.02	0.79
1995	19515	1500	0.675	5230	120	0.01	0.94
1996	19808	1525	0.686	5269	348	0.02	0.83
1997	19858	1529	0.688	5277	596	0.03	0.73
1998	19673	1512	0.680	5250	220	0.01	0.89
1999	19862	1529	0.688	5277	319	0.02	0.85
2000	19941	1538	0.692	5291	408	0.02	0.81
2001	19931	1539	0.692	5292	245	0.01	0.88
2002	20076	1554	0.699	5316	240	0.01	0.88
2003	20212	1569	0.706	5340	386	0.02	0.82
2004	20197	1571	0.707	5344	286	0.02	0.86
2005	20281	1582	0.711	5361	347	0.02	0.84
2006	20304	1588	0.714	5369	429	0.02	0.80
2007	20254	1585	0.713	5365	292	0.02	0.86
2008	20344	1593	0.716	5377	387	0.02	0.82
2009	20342	1591	0.715	5374	217	0.01	0.90
2010	20501	1604	0.721	5394	207	0.01	0.90
2011	20652	1618	0.727	5415	282	0.01	0.87
2012	20714	1626	0.731	5427	282	0.01	0.87
2013	20769	1635	0.735	5441	144	0.01	0.93
2014	20947	1657	0.745	5474	397	0.02	0.82
2015	20874	1657	0.745	5474	351	0.02	0.84
2016	20859	1660	0.746	5478	441	0.02	0.80
2017	20770	1652	0.743	5466	297	0.02	0.86
2018	20833	1655	0.744	5471	185	0.01	0.91
2019	0	1667	0.750	5488			

Table 7: List of parameters used in the base model, including estimated values and standard deviations (SD), bounds (minimum and maximum), estimation phase (negative values indicate not estimated), status (indicates if parameters are near bounds, and prior type information (mean, SD).

No.	Parameter	Value	Phase	Bounds	Status	SD	Prior (Exp.Val, SD)
1	NatM_p_1_Fem_GP_1	0.445	3	(0.1, 0.6)	OK	0.030	Log_Norm (-1.02165, 0.438)
2	L_at_Amin_Fem_GP_1	20.094	2	(10, 40)	OK	1.033	None
3	Linf_Fem_GP_1	175.671	2	(100, 300)	OK	4.012	None
4	VonBert_K_Fem_GP_1	12.137	1	(0.005, 30)	OK	0.359	None
5	Cessation_Fem_GP_1	5.652	3	(0.1, 10)	OK	12.041	None
6	SD_young_Fem_GP_1	5.706	5	(1, 20)	OK	0.903	None
7	SD_old_Fem_GP_1	7.085	5	(1, 20)	OK	0.921	None
8	Wtlen_1_Fem_GP_1	0.000	-3	(0, 3)			None
9	Wtlen_2_Fem_GP_1	2.993	-3	(2, 4)			None
10	Mat50%_Fem_GP_1	148.245	-3	(10, 140)			None
11	Mat_slope_Fem_GP_1	-0.132	-3	(-0.09, -0.05)			None
12	Eggs/kg_inter_Fem_GP_1	1.000	-3	(-3, 3)			None
13	Eggs/kg_slope_wt_Fem_GP_1	0.000	-3	(-3, 3)			None
14	NatM_p_1_Mal_GP_1	0.000	-2	(-3, 3)			None
15	L_at_Amin_Mal_GP_1	0.000	-2	(-1, 1)			None
16	Linf_Mal_GP_1	-0.373	2	(-1, 1)	OK	0.025	None
17	VonBert_K_Mal_GP_1	0.101	3	(-10, 20)	OK	0.034	None
18	Cessation_Mal_GP_1	0.200	-3	(-3, 3)			None
19	SD_young_Mal_GP_1	0.000	-5	(-1, 1)			None
20	SD_old_Mal_GP_1	0.000	-5	(-1, 1)			None
21	Wtlen_1_Mal_GP_1	0.000	-3	(0, 3)			None
22	Wtlen_2_Mal_GP_1	2.993	-3	(2, 4)			None
23	CohortGrowDev	1.000	-5	(0, 2)			None
24	FracFemale_GP_1	0.500	-99	(0.001, 0.999)			None
25	SR_LN(R0)	8.728	3	(5, 15)	OK	0.282	None
26	SR_BH_steep	0.400	-3	(0.2, 1)			None

Continued on next page

Table 7: List of parameters used in the base model, including estimated values and standard deviations (SD), bounds (minimum and maximum), estimation phase (negative values indicate not estimated), status (indicates if parameters are near bounds, and prior type information (mean, SD).

No.	Parameter	Value	Phase	Bounds	Status	SD	Prior (Exp.Val, SD)
27	SR_sigmaR	0.300	-2	(0, 0.4)			None
28	SR_regime	0.000	-1	(-2, 2)			None
29	SR_autocorr	0.000	-99	(0, 0)			None
78	LnQ_base_WCGBTS(5)	-0.209	1	(-2, 2)	OK	0.184	Normal (-0.188, 0.187)
79	Q_extraSD_WCGBTS(5)	0.162	1	(0, 2)	OK	0.057	None
80	LnQ_base_Triennial(6)	-1.046	1	(-10, 2)	OK	0.694	None
81	Q_extraSD_Triennial(6)	0.365	1	(0, 2)	OK	0.146	None
82	LnQ_base_Triennial(6)__1995	-0.731	1	(-7, 0)	OK	0.693	None
83	Size_DblN_peak_(1)	94.092	4	(80, 150)	OK	4.912	None
84	Size_DblN_top_logit_(1)	-15.000	-5	(-15, 4)			None
85	Size_DblN_ascend_se_(1)	7.156	4	(-1, 9)	OK	0.118	None
86	Size_DblN_descend_se_(1)	20.000	-5	(-1, 20)			None
87	Size_DblN_start_logit_(1)	-999.000	-4	(-999, 9)			None
88	Size_DblN_end_logit_(1)	-999.000	-5	(-999, 9)			None
89	Retain_L_infl_(1)	66.219	2	(15, 150)	OK	0.671	None
90	Retain_L_width_(1)	4.876	2	(0.1, 10)	OK	0.354	None
91	Retain_L_asymptote_logit_(1)	2.048	3	(-10, 20)	OK	0.359	None
92	Retain_L_maleoffset_(1)	0.000	-3	(0, 0)			None
93	DiscMort_L_infl_(1)	5.000	-4	(5, 15)			None
94	DiscMort_L_width_(1)	0.000	-4	(0.001, 10)			None
95	DiscMort_L_level_old_(1)	0.500	-5	(0, 1)			None
96	DiscMort_L_male_offset_(1)	0.000	-5	(0, 0)			None
97	SzSel_Fem_Peak_(1)	-5.537	4	(-50, 50)	OK	2.174	None
98	SzSel_Fem_Ascend_(1)	0.000	-4	(-5, 5)			None
99	SzSel_Fem_Descend_(1)	0.000	-4	(-5, 5)			None
100	SzSel_Fem_Final_(1)	0.000	-4	(-5, 5)			None
101	SzSel_Fem_Scale_(1)	0.744	4	(0.5, 1.5)	OK	0.095	None

Continued on next page

Table 7: List of parameters used in the base model, including estimated values and standard deviations (SD), bounds (minimum and maximum), estimation phase (negative values indicate not estimated), status (indicates if parameters are near bounds, and prior type information (mean, SD).

No.	Parameter	Value	Phase	Bounds	Status	SD	Prior (Exp.Val, SD)
102	Size_DblN_peak_WCGBTS(5)	76.187	4	(50, 150)	OK	6.668	None
103	Size_DblN_top_logit_WCGBTS(5)	-15.000	-5	(-15, 4)			None
104	Size_DblN_ascend_se_WCGBTS(5)	6.503	4	(-1, 9)	OK	0.371	None
105	Size_DblN_descend_se_WCGBTS(5)	16.488	5	(-1, 20)	OK	56.568	None
106	Size_DblN_start_logit_WCGBTS(5)	-5.000	-4	(-999, 9)			None
107	Size_DblN_end_logit_WCGBTS(5)	-999.000	-5	(-999, 9)			None
108	SzSel_Fem_Peak_WCGBTS(5)	-8.052	4	(-50, 50)	OK	4.166	None
109	SzSel_Fem_Ascend_WCGBTS(5)	0.000	-4	(-5, 5)			None
110	SzSel_Fem_Descend_WCGBTS(5)	0.000	-4	(-5, 5)			None
111	SzSel_Fem_Final_WCGBTS(5)	0.000	-4	(-5, 5)			None
112	SzSel_Fem_Scale_WCGBTS(5)	0.696	4	(0.5, 1.5)	OK	0.125	None
113	Size_DblN_peak_Triennial(6)	187.722	4	(50, 200)	OK	34.761	None
114	Size_DblN_top_logit_Triennial(6)	-15.000	-5	(-15, 4)			None
115	Size_DblN_ascend_se_Triennial(6)	8.474	4	(-1, 9)	OK	0.422	None
116	Size_DblN_descend_se_Triennial(6)	20.000	-5	(-1, 20)			None
117	Size_DblN_start_logit_Triennial(6)	-4.789	4	(-15, 9)	OK	0.786	None
118	Size_DblN_end_logit_Triennial(6)	-999.000	-5	(-999, 9)			None
119	SzSel_Fem_Peak_Triennial(6)	0.000	-4	(-50, 50)			None
120	SzSel_Fem_Ascend_Triennial(6)	0.000	-4	(-5, 5)			None
121	SzSel_Fem_Descend_Triennial(6)	0.000	-4	(-5, 5)			None
122	SzSel_Fem_Final_Triennial(6)	0.000	-4	(-5, 5)			None
123	SzSel_Fem_Scale_Triennial(6)	0.604	4	(0.5, 1.5)	OK	0.130	None
124	Retain_L_asymptote_logit__2005	2.299	4	(-10, 20)	OK	0.566	None
125	Retain_L_asymptote_logit__2006	3.304	4	(-10, 20)	OK	1.305	None
126	Retain_L_asymptote_logit__2007	3.962	4	(-10, 20)	OK	1.982	None
127	Retain_L_asymptote_logit__2008	11.091	4	(-10, 20)	OK	111.895	None

Continued on next page

Table 7: List of parameters used in the base model, including estimated values and standard deviations (SD), bounds (minimum and maximum), estimation phase (negative values indicate not estimated), status (indicates if parameters are near bounds, and prior type information (mean, SD).

No.	Parameter	Value	Phase	Bounds	Status	SD	Prior (Exp.Val, SD)
128	Retain_L_asymptote_logit__2009	4.917	4	(-10, 20)	OK	3.735	None
129	Retain_L_asymptote_logit__2010	13.242	4	(-10, 20)	OK	88.124	None
130	Retain_L_asymptote_logit__2011	14.640	4	(-10, 20)	OK	74.025	None
131	Retain_L_asymptote_logit__2012	13.890	4	(-10, 20)	OK	81.550	None
132	Retain_L_asymptote_logit__2013	3.454	4	(-10, 20)	OK	0.333	None
133	Retain_L_asymptote_logit__2014	3.619	4	(-10, 20)	OK	0.276	None
134	Retain_L_asymptote_logit__2015	3.404	4	(-10, 20)	OK	0.261	None
135	Retain_L_asymptote_logit__2016	2.885	4	(-10, 20)	OK	0.192	None
136	Retain_L_asymptote_logit__2017	2.819	4	(-10, 20)	OK	0.193	None

Table 8: Sensitivity of the base model to assumptions about selectivity and catchability.

Label	Base model	Sel all domed	Sel no sex offset	Q no prior on WCGBTS	Q no offset on triennial
TOTAL likelihood	402.12	401.21	420.24	401.67	402.95
Survey likelihood	-9.72	-9.72	-9.84	-9.31	-9.38
Length comp likelihood	341.44	340.27	356.65	340.46	342.01
Age comp likelihood	97.14	97.44	100.57	97.08	96.99
Discard likelihood	-22.45	-22.80	-22.80	-22.14	-22.64
Mean body wt likelihood	-4.42	-4.05	-4.44	-4.60	-4.27
Parm priors likelihood	0.12	0.06	0.10	0.17	0.23
Recr Virgin millions	6.18	5.05	5.43	34.78	5.94
log(R0)	8.73	8.53	8.60	10.46	8.69
NatM Female	0.45	0.41	0.43	0.46	0.45
NatM Male	0.45	0.41	0.43	0.46	0.45
Linf Female	175.67	176.82	177.04	175.61	175.40
Linf Male	120.97	120.85	120.73	120.95	121.01
Q WCGBTS	0.81	0.81	0.81	0.14	0.90
SSB Virgin thousand mt	2.22	2.81	1.94	9.93	1.91
SSB 2019 thousand mt	1.67	2.17	1.27	9.50	1.37
Bratio 2019	0.75	0.77	0.65	0.96	0.72
SPRratio 2018	0.18	0.16	0.24	0.03	0.20
Retained Catch MSY	558.67	595.13	446.62	2793.89	510.57
Dead Catch MSY	603.92	643.94	481.77	3030.18	551.56
Totbio unfished	25232.30	25321.30	23340.10	126562.00	23048.20
OFLCatch 2021	1390.54	1529.09	995.99	8154.10	1231.59

Table 9: Sensitivity of the base model to assumptions about catches.

Label	Base model	Discards based on 3yr averages	Discard mortality 0 4	Discard mortality 0 6	Multiplier on historical discards
TOTAL likelihood	402.12	401.58	401.85	402.36	401.86
Survey likelihood	-9.72	-9.92	-9.98	-9.49	-10.05
Length comp likelihood	341.44	341.12	341.61	341.28	341.25
Age comp likelihood	97.14	97.24	97.14	97.13	97.22
Discard likelihood	-22.45	-22.51	-22.66	-22.26	-22.65
Mean body wt likelihood	-4.42	-4.46	-4.39	-4.45	-4.44
Parm priors likelihood	0.12	0.11	0.11	0.14	0.51
Recr Virgin millions	6.18	6.02	6.19	6.19	6.06
log(R0)	8.73	8.70	8.73	8.73	8.71
NatM Female	0.45	0.44	0.44	0.45	0.44
NatM Male	0.45	0.44	0.44	0.45	0.44
Linf Female	175.67	175.76	175.68	175.66	175.72
Linf Male	120.97	120.95	120.96	120.98	120.96
Q WCGBTS	0.81	0.83	0.82	0.80	0.83
SSB Virgin thousand mt	2.22	2.23	2.29	2.17	2.27
SSB 2019 thousand mt	1.67	1.62	1.67	1.66	1.63
Bratio 2019	0.75	0.73	0.73	0.77	0.72
SPRratio 2018	0.18	0.18	0.18	0.18	0.18
Retained Catch MSY	558.67	551.42	567.17	552.69	558.71
Dead Catch MSY	603.92	595.86	612.92	597.60	603.65
Totbio unfished	25232.30	25021.50	25620.40	24953.00	25329.90
OFLCatch 2021	1390.54	1346.42	1389.18	1394.56	1352.17

Table 10: Sensitivity of the base model to assumptions about biology and data weighting

Label	Base model	Bio separate M by sex	Bio no M prior	Bio von Bertalanffy growth	Bio Richards growth	Misc McAllister Ianelli tuning
TOTAL likelihood	402.12	399.94	402.00	445.19	456.54	1116.89
Survey likelihood	-9.72	-9.88	-9.72	-9.54	-9.73	-9.66
Length comp likelihood	341.44	338.79	341.48	387.56	362.67	564.52
Age comp likelihood	97.14	97.53	97.09	94.06	129.88	591.26
Discard likelihood	-22.45	-22.79	-22.47	-22.39	-21.98	-22.34
Mean body wt likelihood	-4.42	-3.92	-4.41	-5.05	-4.33	-7.13
Parm priors likelihood	0.12	0.21	0.01	0.53	0.01	0.24
Recr Virgin millions	6.18	5.19	6.29	17.80	0.00	7.26
log(R0)	8.73	8.55	8.75	9.79	8.03	8.89
NatM Female	0.45	0.47	0.45	0.57	0.36	0.46
NatM Male	0.45	0.40	0.45	0.57	0.36	0.46
Linf Female	175.67	175.53	175.65	587.20	2595.92	176.97
Linf Male	120.97	120.15	120.99	236.34	136.91	120.50
Q WCGBTS	0.81	0.81	0.81	0.84	0.85	0.77
SSB Virgin thousand mt	2.22	1.37	2.20	1.25	0.00	2.37
SSB 2019 thousand mt	1.67	0.87	1.65	1.02	0.00	1.83
Bratio 2019	0.75	0.63	0.75	0.82	0.00	0.77
SPRratio 2018	0.18	0.26	0.18	0.13	0.89	0.16
Retained Catch MSY	558.67	432.06	561.23	751.54	0.00	601.43
Dead Catch MSY	603.92	465.72	606.68	812.55	0.00	650.09
Totbio unfished	25232.30	23008.60	25327.00	39650.20	0.00	26861.90
OFLCatch 2021	1390.54	942.16	1397.99	1957.73	0.00	1523.66

Table 11: Results from 100 jitters from the base case model.

Description	Value
Returned to base case	51
Found local minimum	49
Found better solution	0
Error in likelihood	0
Total	100

Table 12: Projection of potential OFL, spawning biomass, and depletion for the base case model.

Yr	OFL contribution (mt)	ACL landings (mt)	Age 5+ biomass (mt)	Spawning Biomass (mt)	Depletion
2019	1389.940	313.160	0.000	1667.190	0.750
2020	1390.490	313.160	0.000	1664.770	0.749
2021	1390.540	1136.647	0.000	1662.950	0.748
2022	1327.210	1072.121	0.000	1581.990	0.711
2023	1278.000	1021.539	0.000	1507.590	0.678
2024	1241.120	982.221	0.000	1438.770	0.647
2025	1212.850	950.914	0.000	1374.480	0.618
2026	1189.120	923.817	0.000	1314.410	0.591
2027	1167.280	899.641	0.000	1259.890	0.566
2028	1145.980	875.107	0.000	1213.480	0.546
2029	1124.960	851.041	0.000	1177.730	0.530
2030	1104.190	828.385	0.000	1152.760	0.518

Table 13: Time-series of population estimates from the base-case model. Relative exploitation rate is $(1 - SPR)/(1 - SPR_{50\%})$.

Year	Total biomass (mt)	Spawning biomass (mt)	%Unfished	Age-0 recruits	Total catch (mt)	Relative exploitation rate	SPR
1916	25232	2224	1.000	6176	0	0.00	1.00
1917	25232	2224	1.000	6176	12	0.00	0.99
1918	25221	2223	0.999	6175	25	0.00	0.99
1919	25199	2220	0.998	6172	37	0.00	0.98
1920	25169	2217	0.997	6168	49	0.00	0.98
1921	25131	2212	0.995	6164	62	0.00	0.97
1922	25087	2206	0.992	6157	74	0.00	0.97
1923	25037	2200	0.989	6150	86	0.00	0.96
1924	24981	2192	0.985	6142	99	0.00	0.96
1925	24920	2183	0.981	6132	111	0.00	0.96
1926	24854	2173	0.977	6122	123	0.01	0.95
1927	24783	2163	0.973	6111	136	0.01	0.94
1928	24707	2153	0.968	6100	148	0.01	0.94
1929	24627	2142	0.963	6088	160	0.01	0.93
1930	24544	2130	0.958	6076	172	0.01	0.93
1931	24456	2118	0.953	6063	185	0.01	0.92

Table 13: Time-series of population estimates from the base-case model. Relative exploitation rate is $(1 - SPR)/(1 - SPR_{50\%})$.

Year Total biomass (mt) Spawning biomass (mt)

Year	Total biomass (mt)	Spawning biomass (mt)					
1932	24365	2106	0.947	6049	197	0.01	0.92
1933	24271	2094	0.941	6035	210	0.01	0.91
1934	24174	2081	0.936	6020	222	0.01	0.91
1935	24074	2067	0.929	6005	234	0.01	0.90
1936	23971	2053	0.923	5989	246	0.01	0.90
1937	23866	2039	0.917	5973	259	0.01	0.89
1938	23758	2025	0.910	5956	271	0.01	0.89
1939	23648	2010	0.904	5939	329	0.01	0.87
1940	23494	1991	0.895	5916	329	0.02	0.86
1941	23353	1972	0.887	5894	363	0.02	0.85
1942	23193	1952	0.878	5869	351	0.02	0.85
1943	23059	1933	0.869	5846	343	0.02	0.86
1944	22943	1917	0.862	5826	350	0.02	0.85
1945	22829	1900	0.854	5805	364	0.02	0.85
1946	22708	1884	0.847	5784	379	0.02	0.84
1947	22581	1868	0.840	5763	394	0.02	0.83
1948	22447	1851	0.832	5742	412	0.02	0.83
1949	22306	1834	0.825	5720	426	0.02	0.82
1950	22162	1818	0.817	5698	424	0.02	0.82
1951	22032	1801	0.810	5677	418	0.02	0.82
1952	21917	1786	0.803	5656	434	0.02	0.81
1953	21794	1771	0.796	5635	515	0.03	0.78
1954	21603	1748	0.786	5604	430	0.02	0.81
1955	21507	1734	0.780	5584	470	0.02	0.80
1956	21377	1718	0.772	5561	434	0.02	0.81
1957	21290	1706	0.767	5544	439	0.02	0.81
1958	21201	1694	0.762	5527	426	0.02	0.81
1959	21126	1685	0.757	5514	435	0.02	0.81
1960	21045	1675	0.753	5500	427	0.02	0.81
1961	20974	1667	0.750	5489	487	0.03	0.78
1962	20849	1655	0.744	5471	465	0.02	0.79
1963	20754	1645	0.740	5456	473	0.02	0.79
1964	20658	1635	0.735	5440	468	0.02	0.79
1965	20575	1624	0.730	5425	438	0.02	0.80
1966	20525	1616	0.727	5413	444	0.02	0.80
1967	20470	1608	0.723	5401	463	0.02	0.79
1968	20399	1599	0.719	5387	497	0.03	0.78
1969	20299	1588	0.714	5369	460	0.02	0.79
1970	20238	1581	0.711	5358	416	0.02	0.81
1971	20223	1578	0.710	5354	409	0.02	0.81
1972	20211	1577	0.709	5352	423	0.02	0.80

Table 13: Time-series of population estimates from the base-case model. Relative exploitation rate is $(1 - SPR)/(1 - SPR_{50\%})$.

1973	20184	1574	0.708	5348	429	0.02	0.80
1974	20150	1571	0.706	5343	415	0.02	0.81
1975	20130	1570	0.706	5341	429	0.02	0.80
1976	20097	1567	0.705	5337	440	0.02	0.80
1977	20057	1564	0.703	5331	452	0.02	0.79
1978	20010	1559	0.701	5324	536	0.03	0.76
1979	19887	1546	0.695	5304	584	0.03	0.74
1980	19732	1529	0.688	5277	444	0.02	0.79
1981	19724	1524	0.685	5268	547	0.03	0.75
1982	19618	1510	0.679	5246	486	0.03	0.77
1983	19576	1502	0.676	5233	466	0.03	0.78
1984	19551	1497	0.673	5224	420	0.02	0.80
1985	19565	1497	0.673	5224	453	0.03	0.79
1986	19541	1495	0.672	5221	425	0.02	0.80
1987	19539	1497	0.673	5224	431	0.02	0.79
1988	19529	1499	0.674	5228	415	0.02	0.80
1989	19534	1502	0.676	5233	413	0.02	0.80
1990	19541	1506	0.677	5238	422	0.02	0.80
1991	19540	1507	0.678	5240	432	0.02	0.79
1992	19531	1506	0.677	5239	424	0.02	0.80
1993	19534	1505	0.677	5238	438	0.02	0.79
1994	19524	1503	0.676	5234	438	0.02	0.79
1995	19515	1500	0.675	5230	120	0.01	0.94
1996	19808	1525	0.686	5269	348	0.02	0.83
1997	19858	1529	0.688	5277	596	0.03	0.73
1998	19673	1512	0.680	5250	220	0.01	0.89
1999	19862	1529	0.688	5277	319	0.02	0.85
2000	19941	1538	0.692	5291	408	0.02	0.81
2001	19931	1539	0.692	5292	245	0.01	0.88
2002	20076	1554	0.699	5316	240	0.01	0.88
2003	20212	1569	0.706	5340	386	0.02	0.82
2004	20197	1571	0.707	5344	286	0.02	0.86
2005	20281	1582	0.711	5361	347	0.02	0.84
2006	20304	1588	0.714	5369	429	0.02	0.80
2007	20254	1585	0.713	5365	292	0.02	0.86
2008	20344	1593	0.716	5377	387	0.02	0.82
2009	20342	1591	0.715	5374	217	0.01	0.90
2010	20501	1604	0.721	5394	207	0.01	0.90
2011	20652	1618	0.727	5415	282	0.01	0.87
2012	20714	1626	0.731	5427	282	0.01	0.87
2013	20769	1635	0.735	5441	144	0.01	0.93

Table 13: Time-series of population estimates from the base-case model. Relative exploitation rate is $(1 - SPR)/(1 - SPR_{50\%})$.

Year	Total biomass (mt)	Spawning biomass (mt)

2014	20947	1657	0.745	5474	397	0.02	0.82
2015	20874	1657	0.745	5474	351	0.02	0.84
2016	20859	1660	0.746	5478	441	0.02	0.80
2017	20770	1652	0.743	5466	297	0.02	0.86
2018	20833	1655	0.744	5471	185	0.01	0.91
2019	0	1667	0.750	5488			

11 Figures

11.1 Data Figures

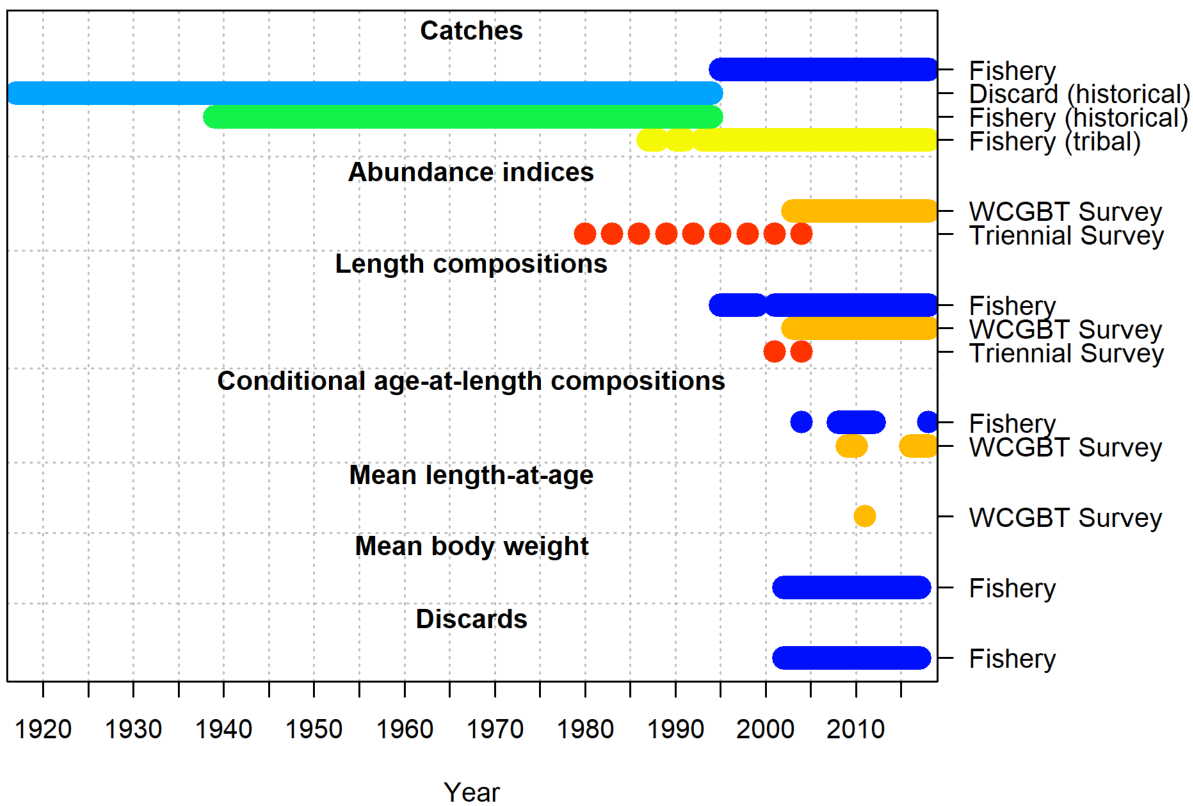

Figure 1: Summary of data sources used in the model.

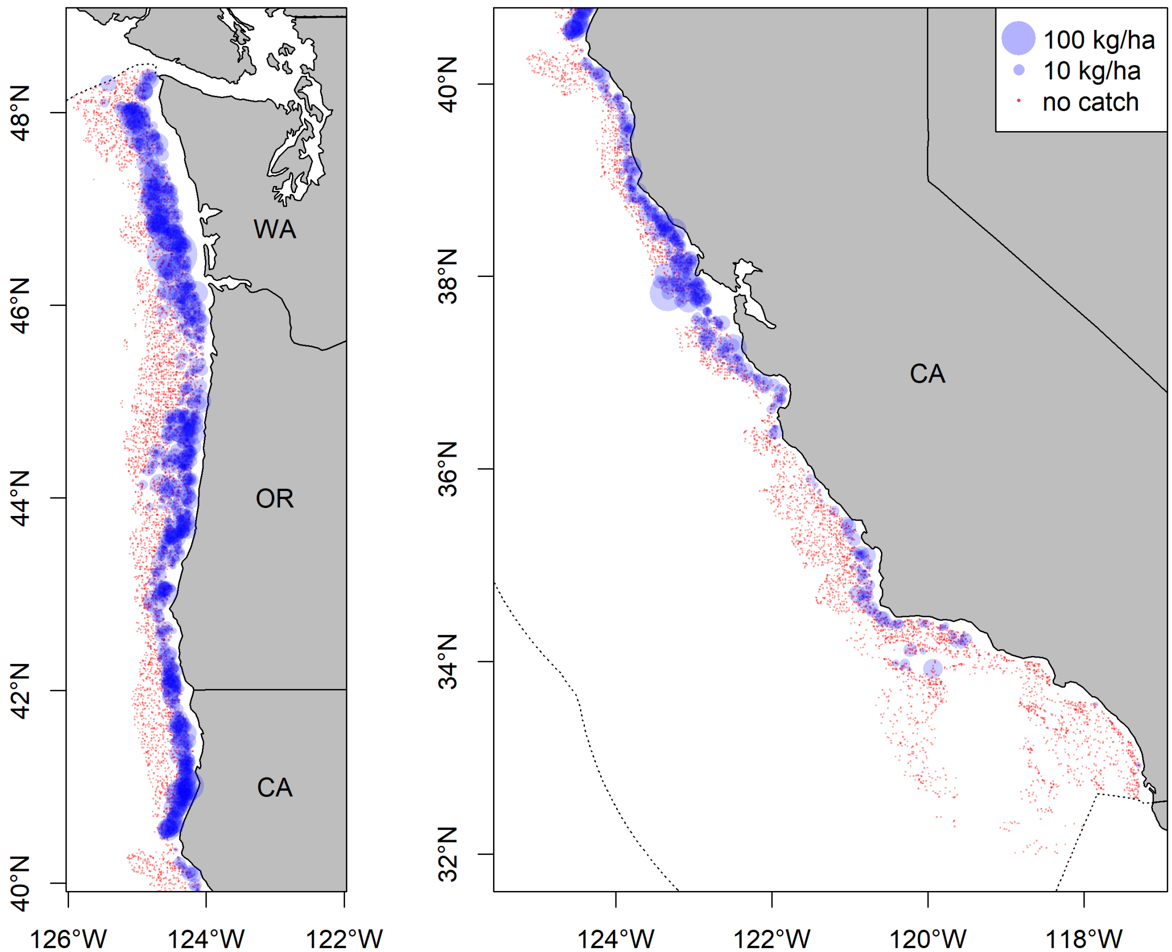

Figure 2: Map showing the distribution of Big Skate within the area covered by the West Coast Groundfish Bottom Trawl Survey aggregated over the years 2003–2018.

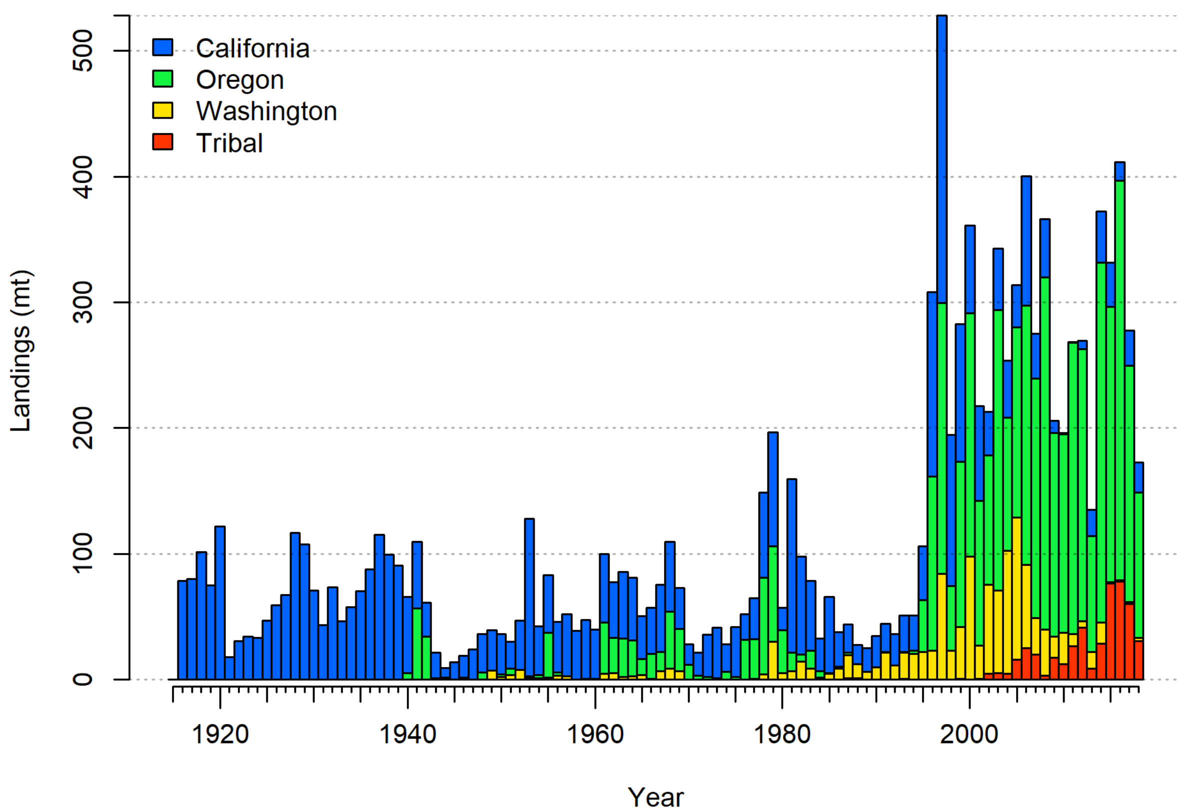

Figure 3: Reconstructed landings by area. Tribal catch was all landed in Washington.

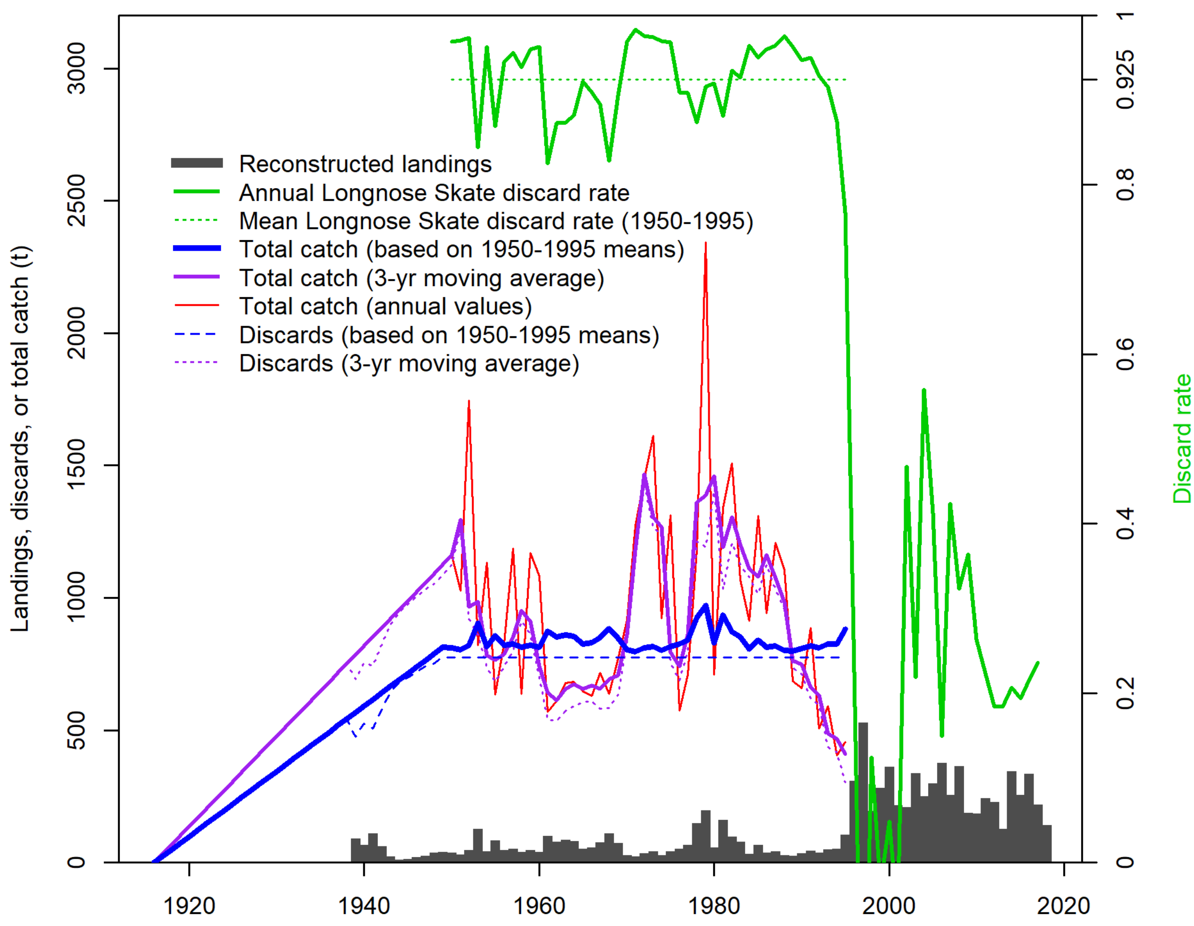

Figure 4: Estimated total catch using different assumptions for discards. The discard rates shown in green lines are relative to the right-hand axis while all other values are relative to the left-hand axis.

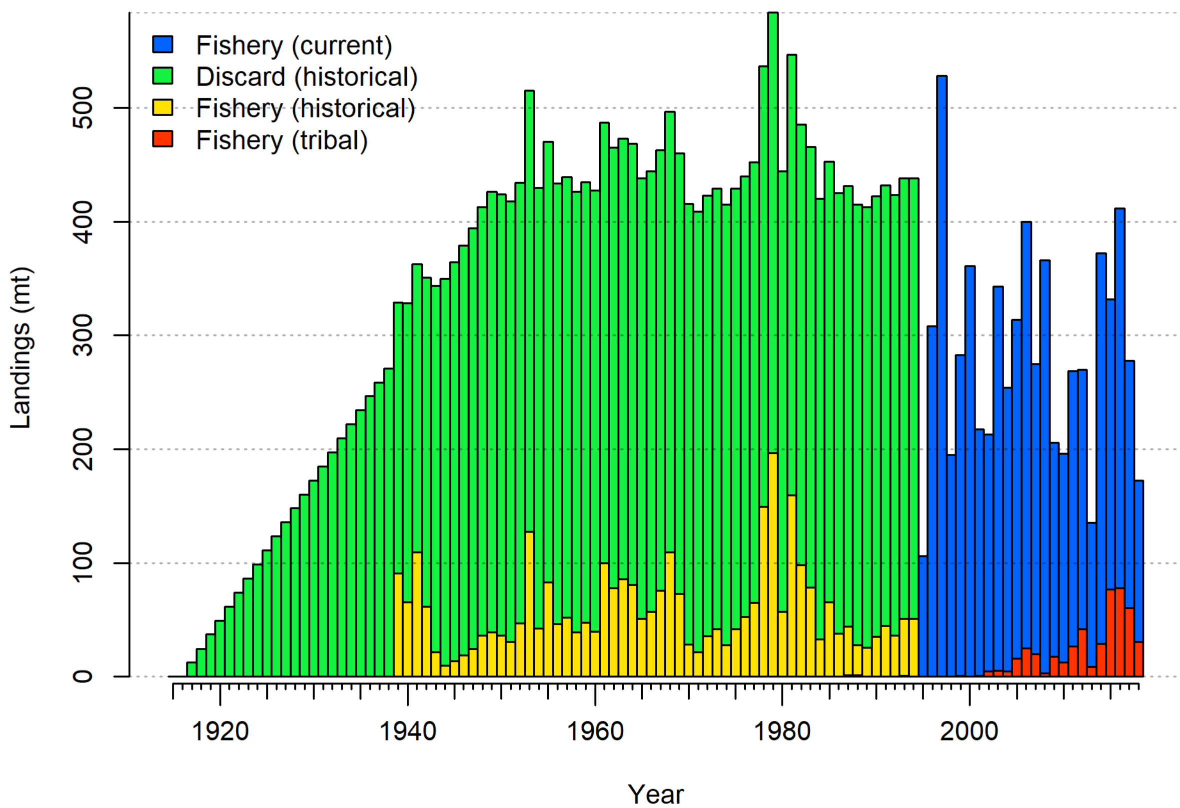

Figure 5: Catch data input to the model under assumed fleet structure. The historical discards shown in green have been scaled to account for an assumed 50% discard mortality. Discards during the period from 1995 onward are not represented here as they are estimated within the model.

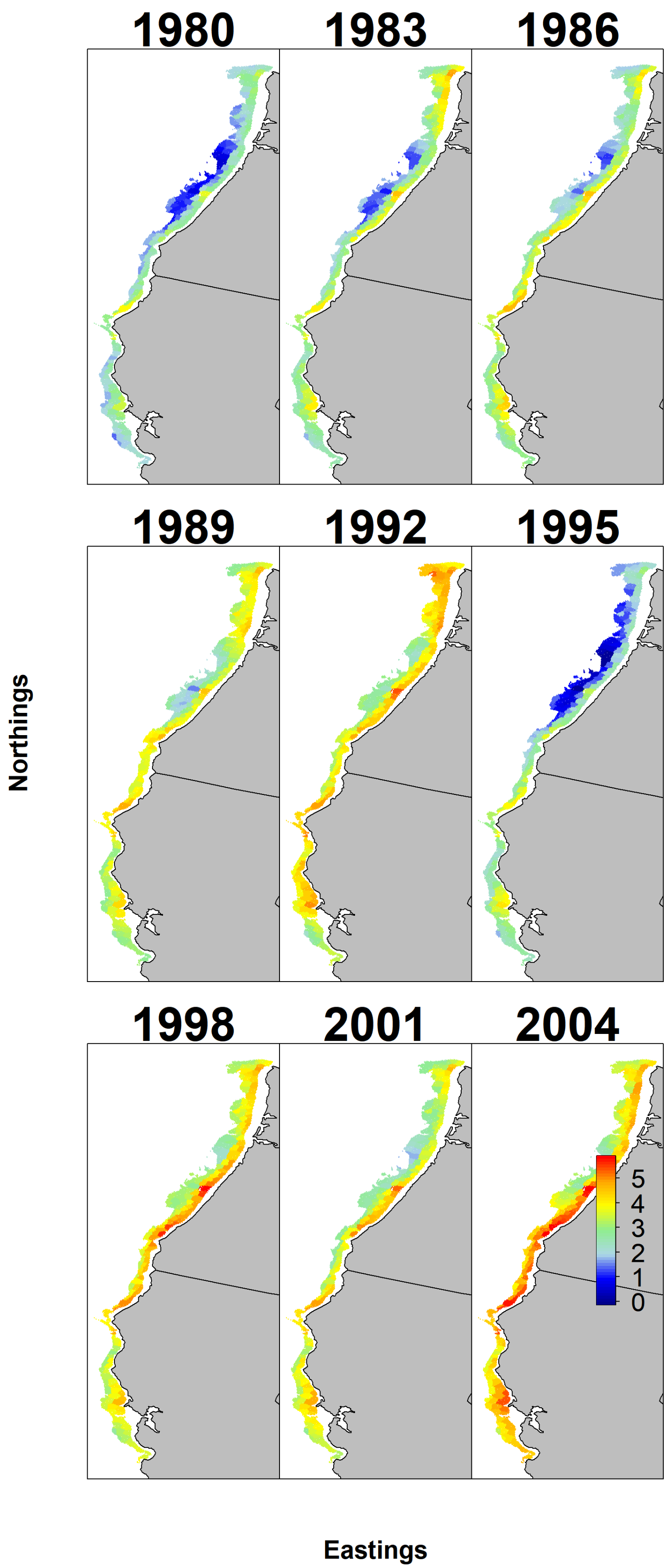

Figure 6: Map of estimated density by year for Big Skate in the Triennial survey.

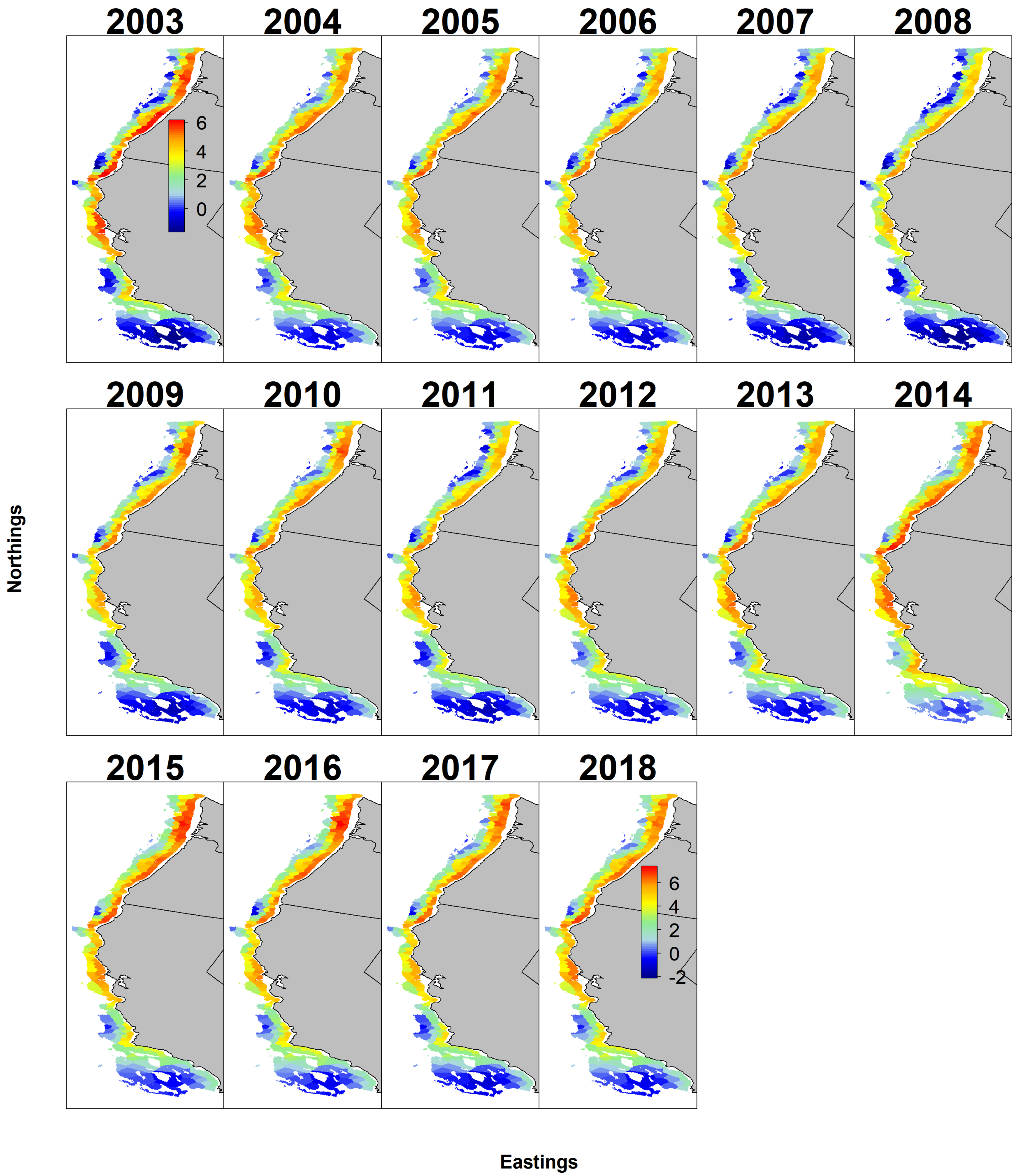

Figure 7: Map of estimated density by year for Big Skate in the WCGBT Survey.

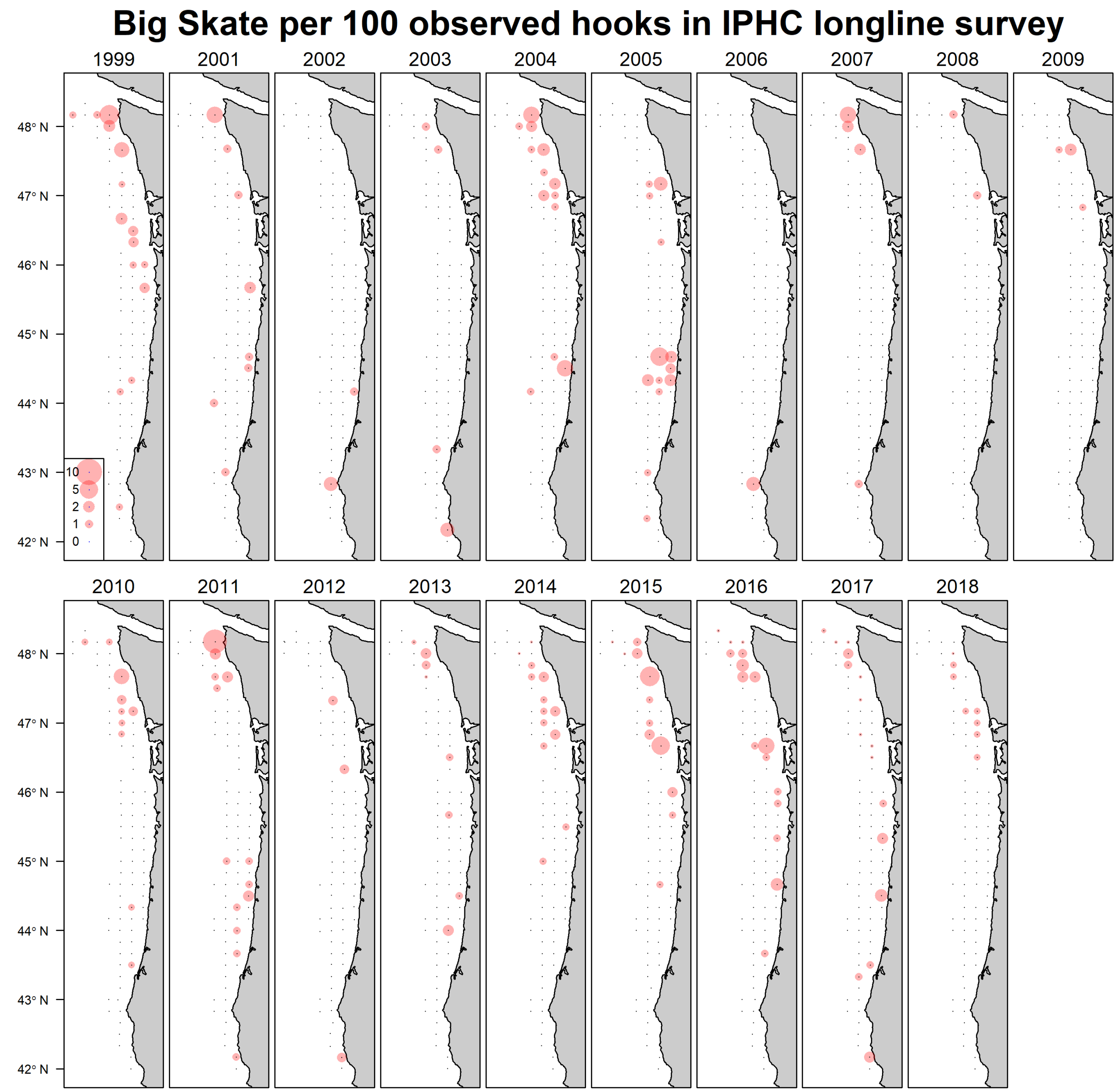

Figure 8: Map of catch rates by year for Big Skate in the International Pacific Halibut Commission longline survey.

11.2 Biology Figures

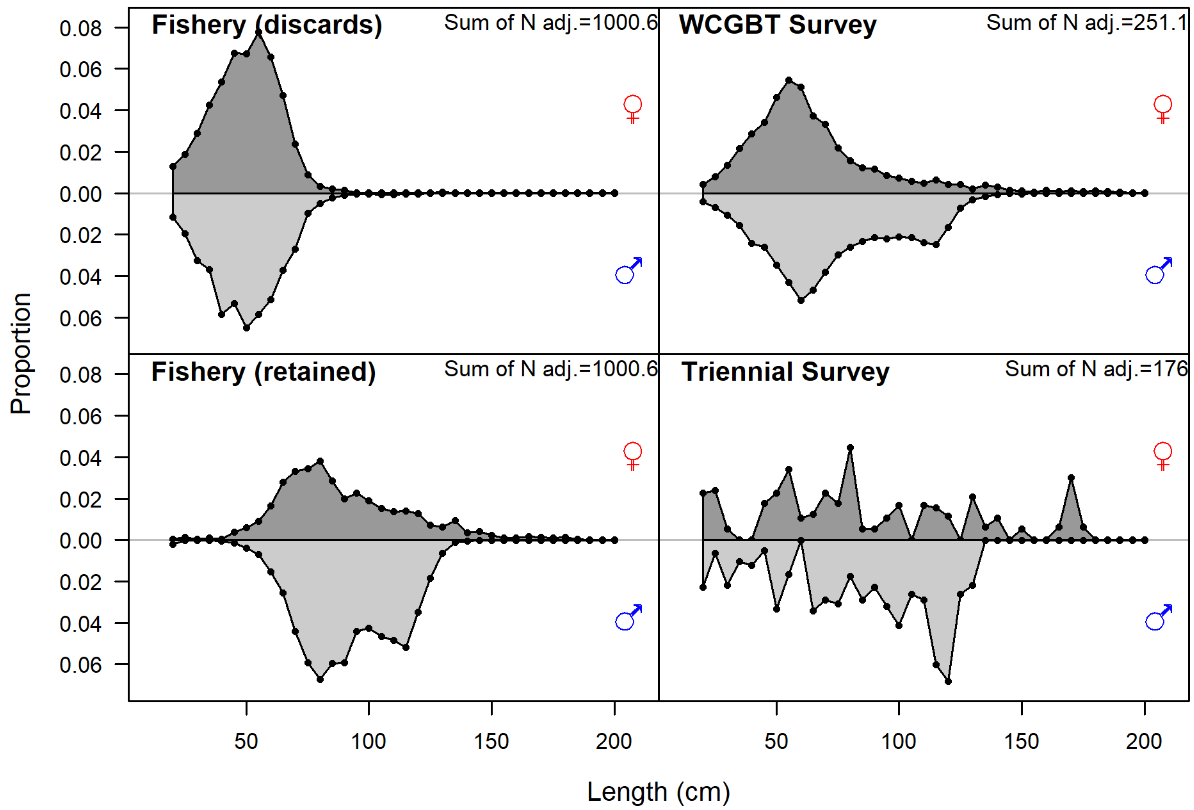

Figure 9: Length comp data, aggregated across time by fleet.

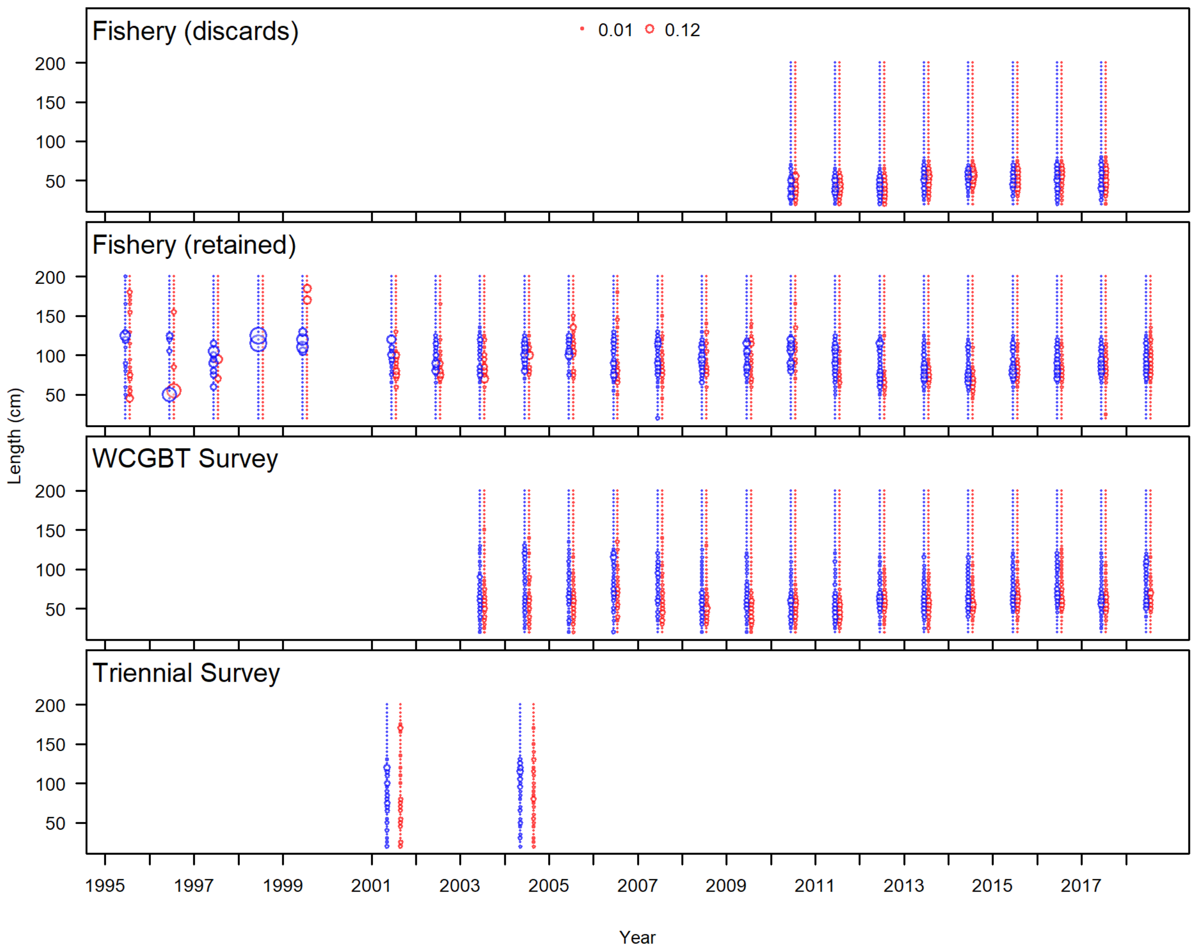

Figure 10: Length comp data for all years and fleets. Bubble size indicates the observed proportions, with females in red and males in blue.

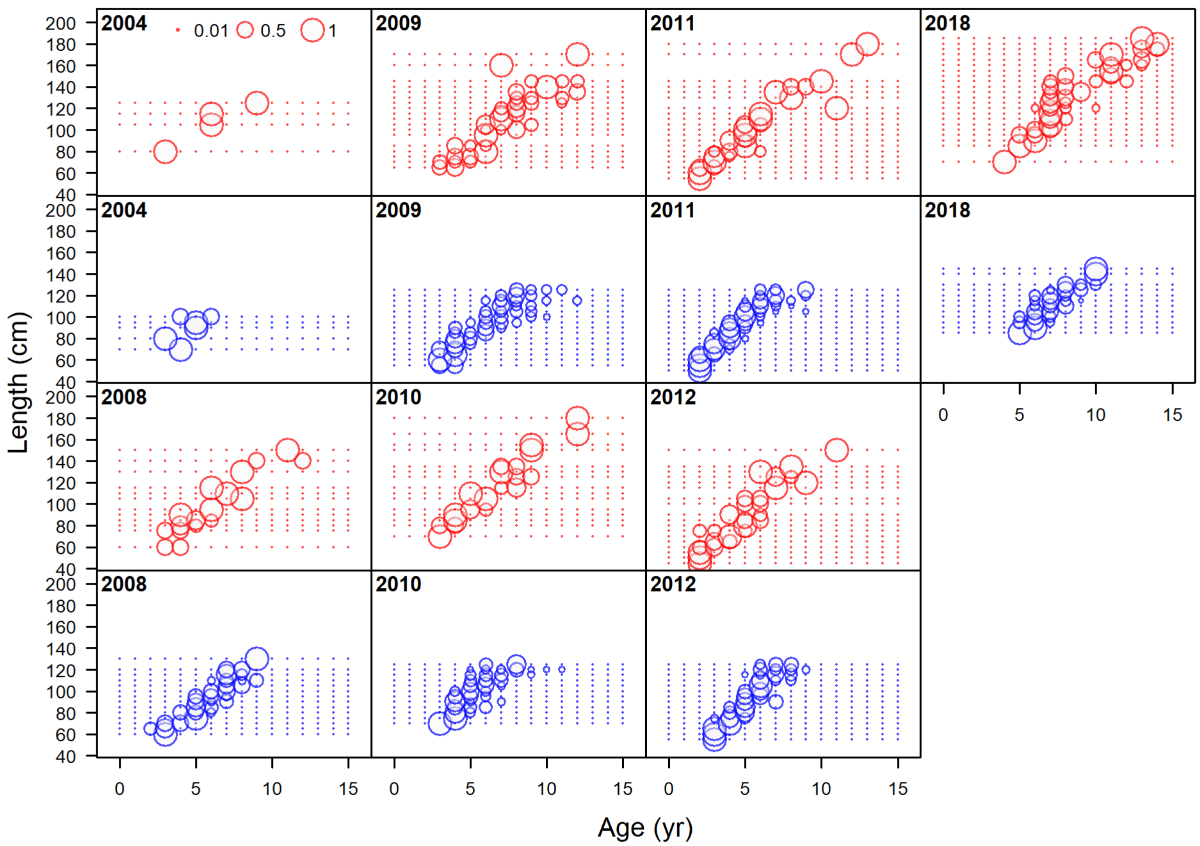

Figure 11: Conditional age-at-length data from the fishery.

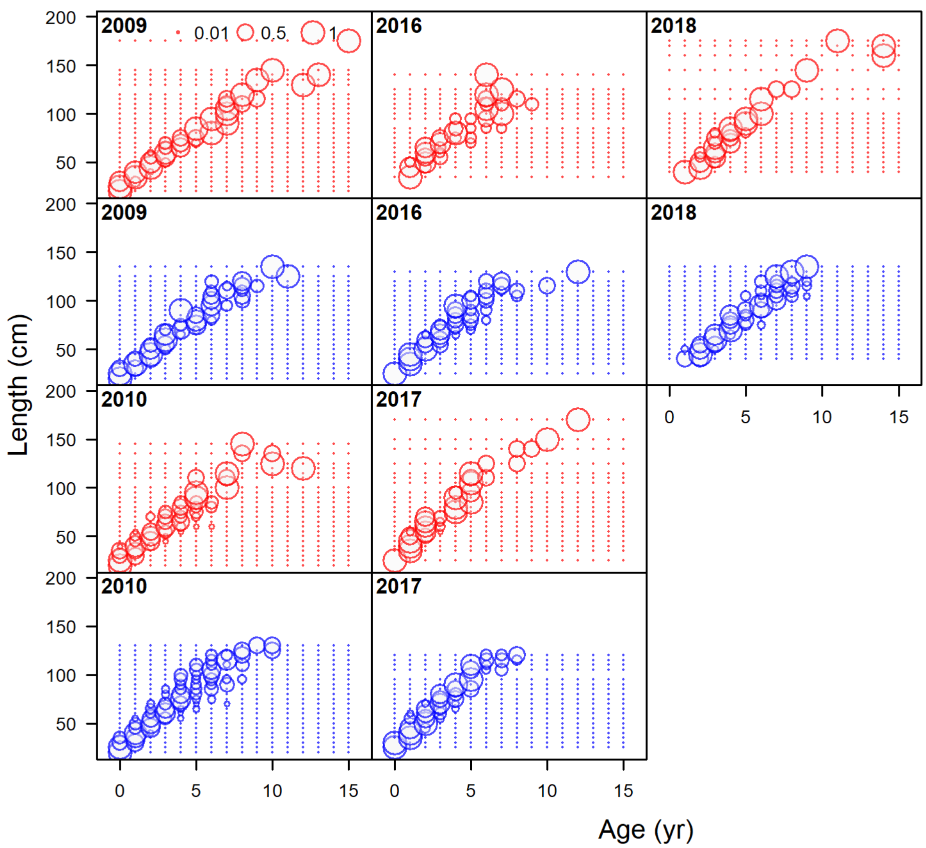

Figure 12: Conditional age-at-length data from the WCGBT Survey.

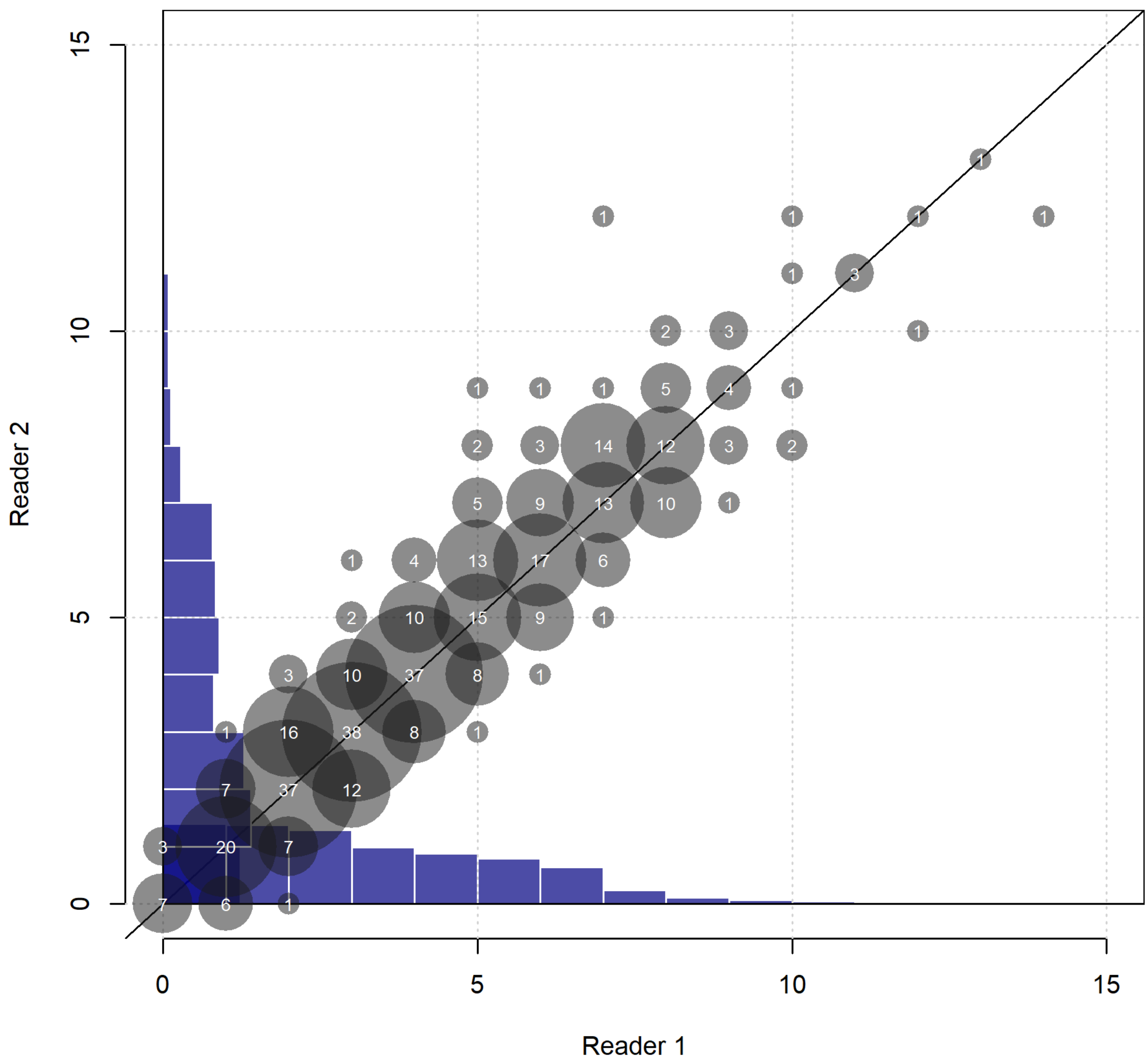

Figure 13: Comparison of reads from each of two age readers for Big Skate. Sample sizes associated with each combination of ages are shown by the size circles and the within them. The blue histograms show the distribution of ages estimated by each reader.

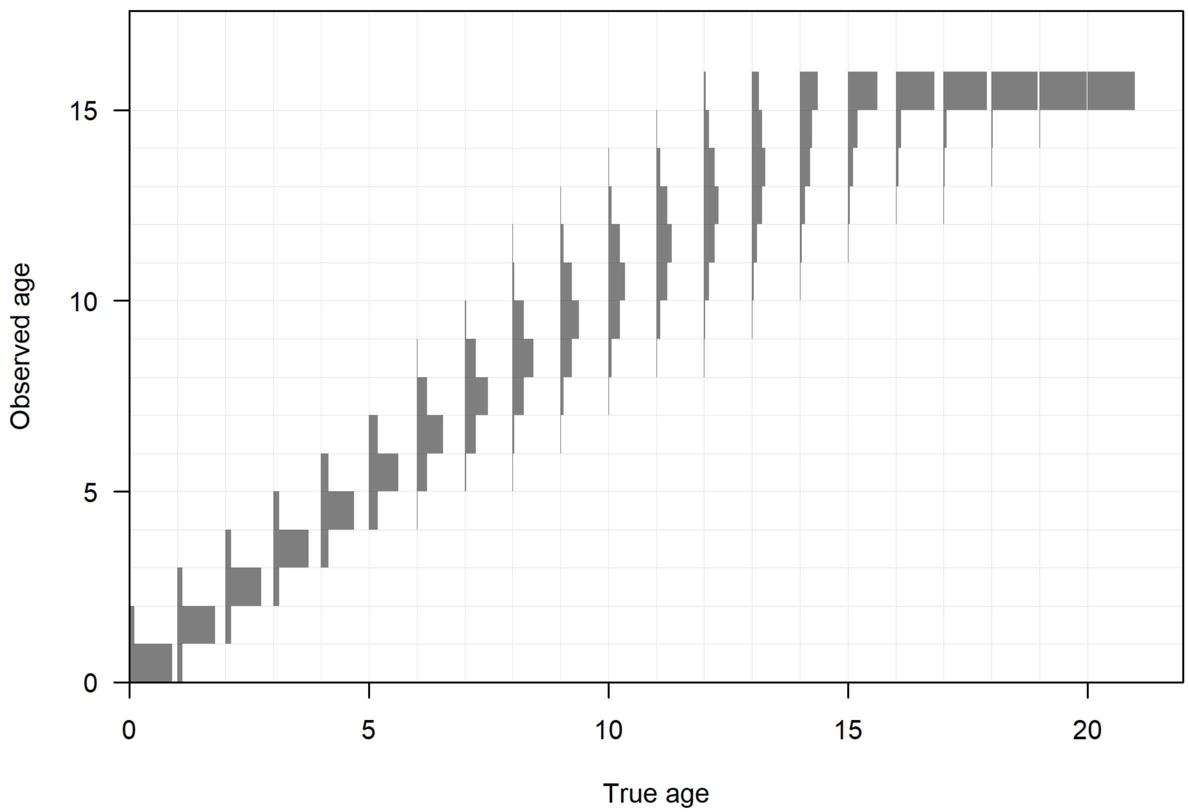

Figure 14: Estimated ageing imprecision.

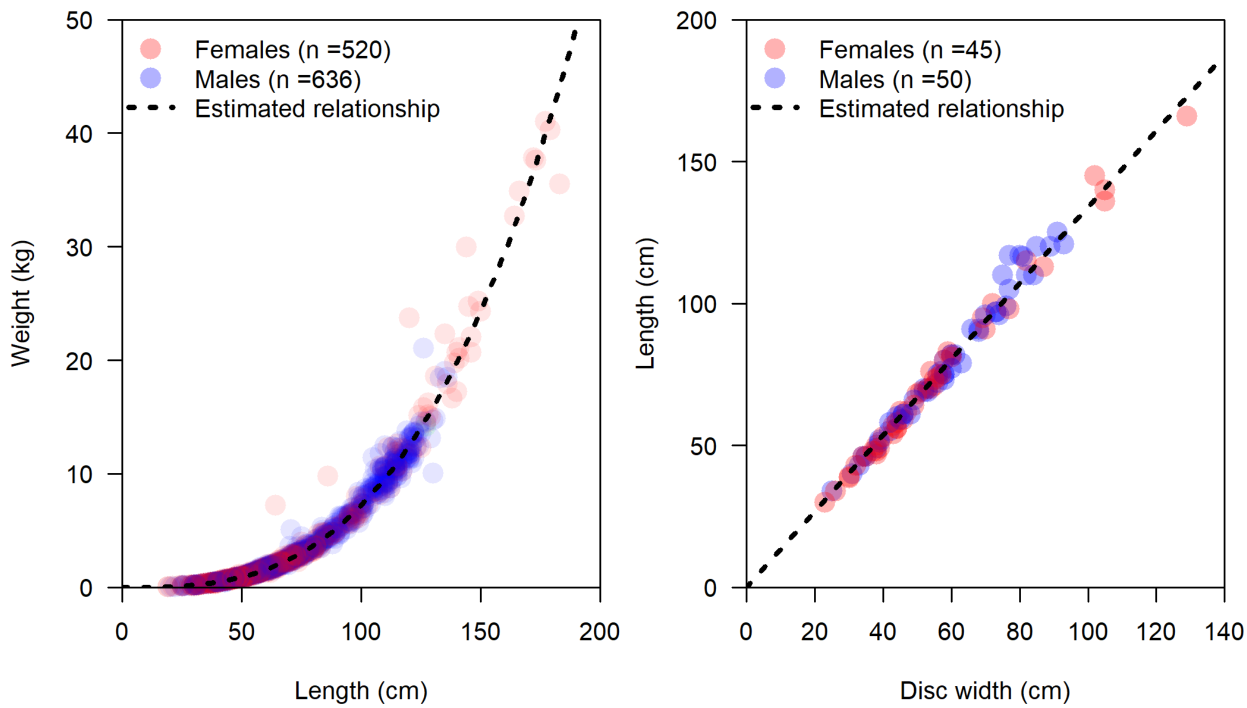

Figure 15: Estimated relationship between length and weight (left) and disc-width and length (right) for Big Skate. Colored points show observed values and the black line indicates the estimated relationship $W = 0.0000074924L^{2.9925}$.

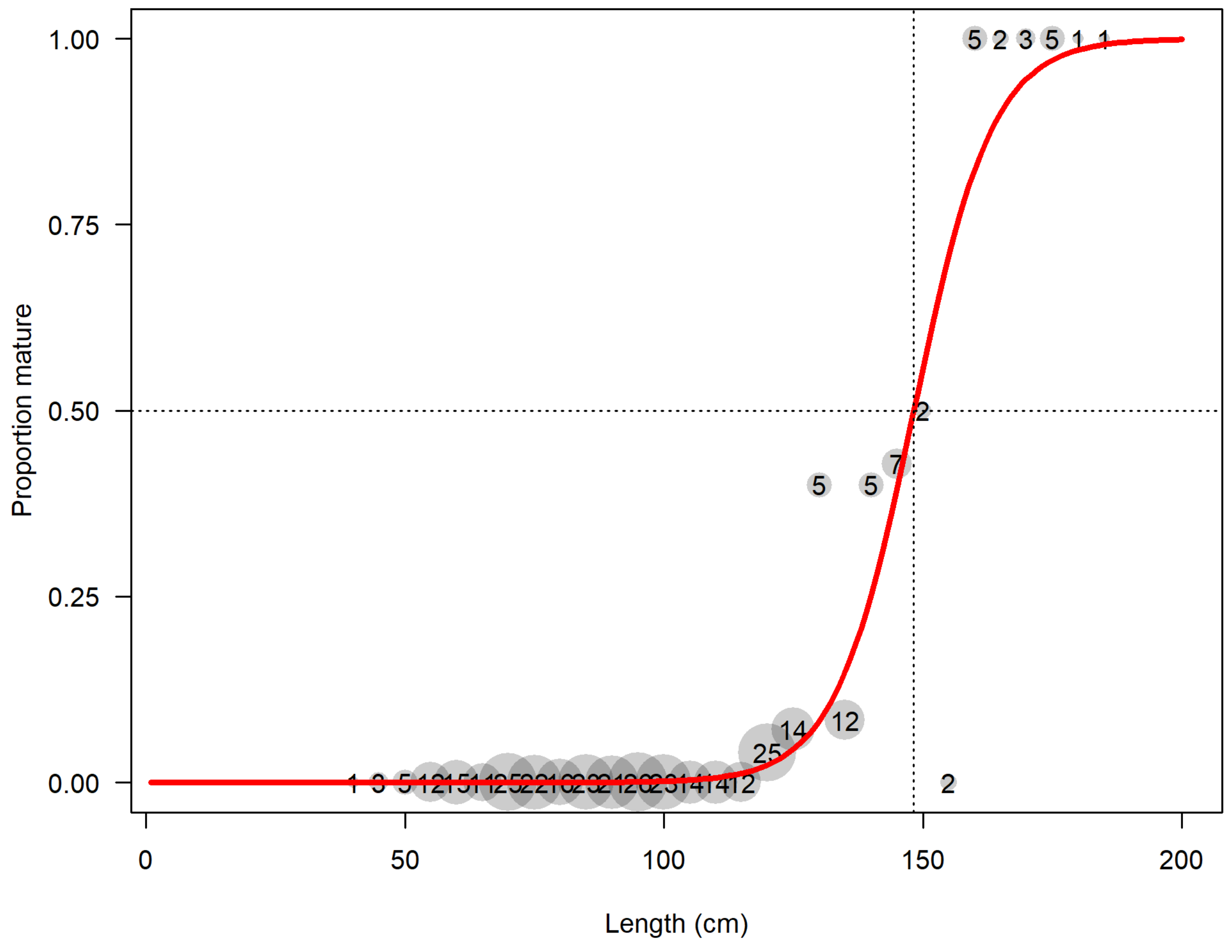

Figure 16: Estimated maturity relationship for female Big Skate. Gray points indicate average observed functional maturity within each length bin with point size proportional to the number of samples (indicated by text within each point).

11.3 Model Results Figures

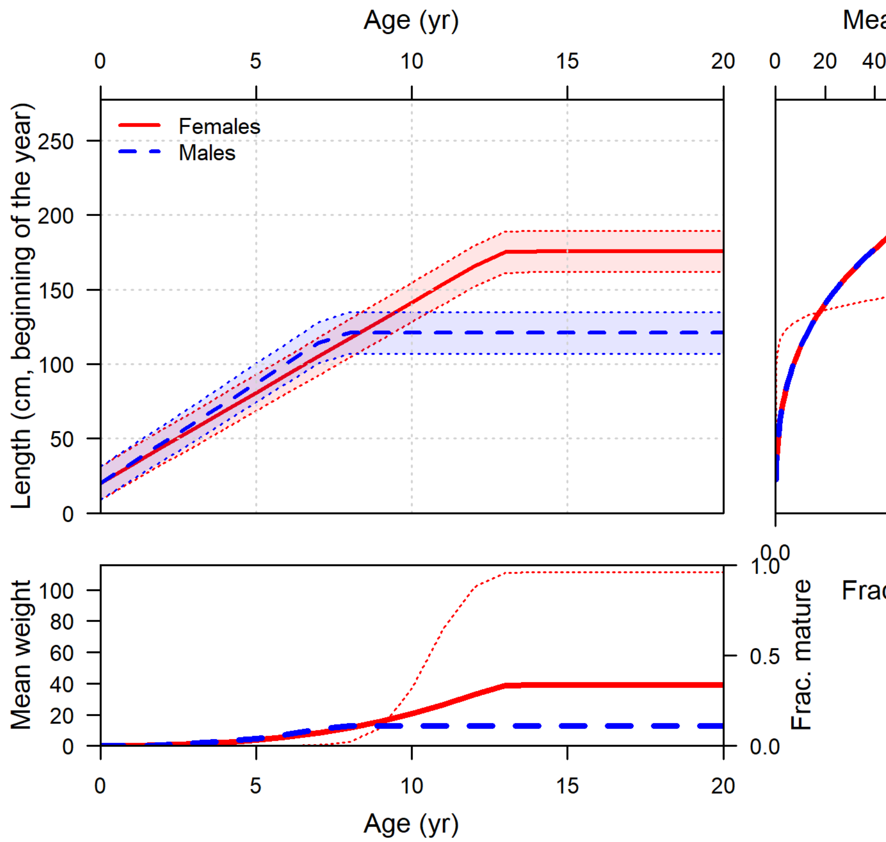

\begin{figure}[H] \begin{centering} \caption{Estimated length-at-age for female and male Big Skate (top left panel). Shaded areas indicate 95% intervals for distribution of lengths at each age. Values represent beginning-of-year growth. Weight (thick line) and maturity (thin line) are shown in the top-right and lower-left panels as a function of length and age, respectively, where the values-at-age are calculated by mapping the length-based relationships through the estimated distribution of length at each age.} \end{centering} \end{figure}

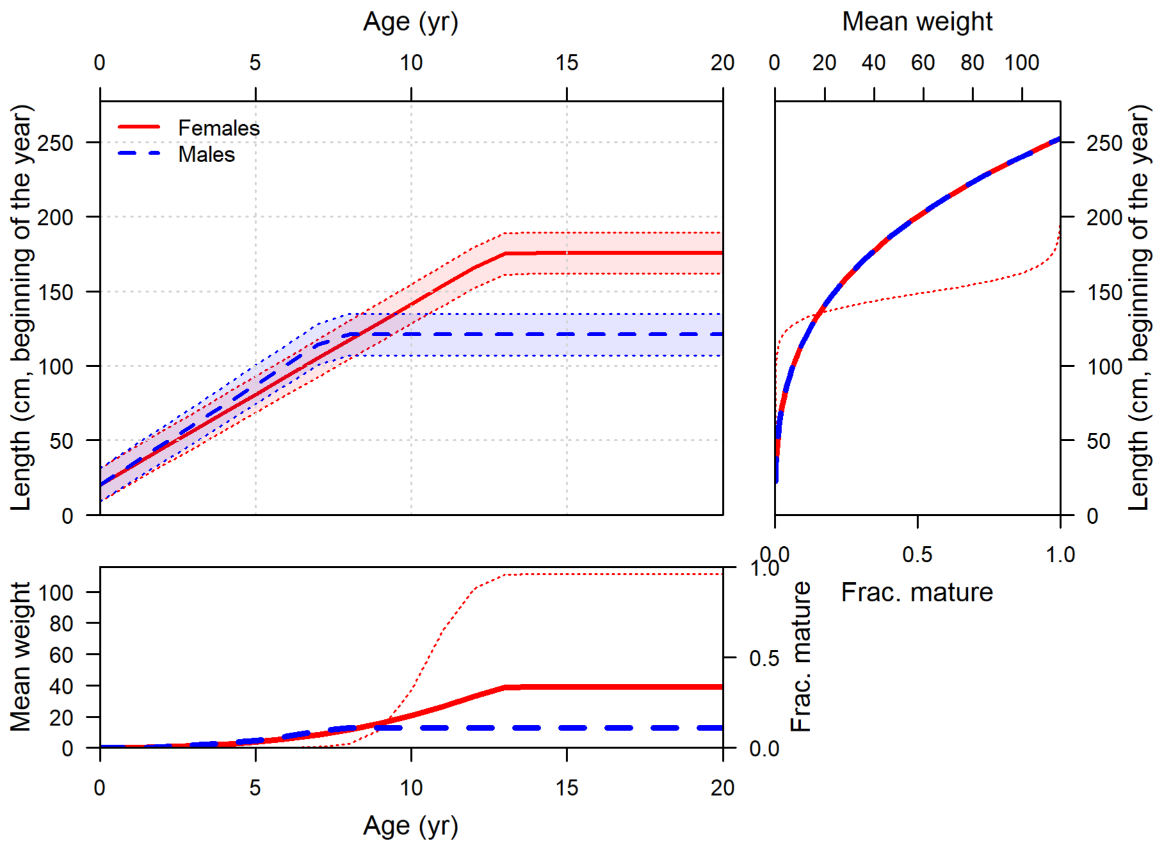

Figure 17: Estimated length-at-age for female and male Big Skate (top left panel). Shaded areas indicate 95% intervals for distribution of lengths at each age. Values represent beginning-of-year growth. Weight (thick line) and maturity (thin line) are shown in the top-right and lower-left panels as a function of length and age, respectively, where the values-at-age are calculated by mapping the length-based relationships through the estimated distribution of length at each age.

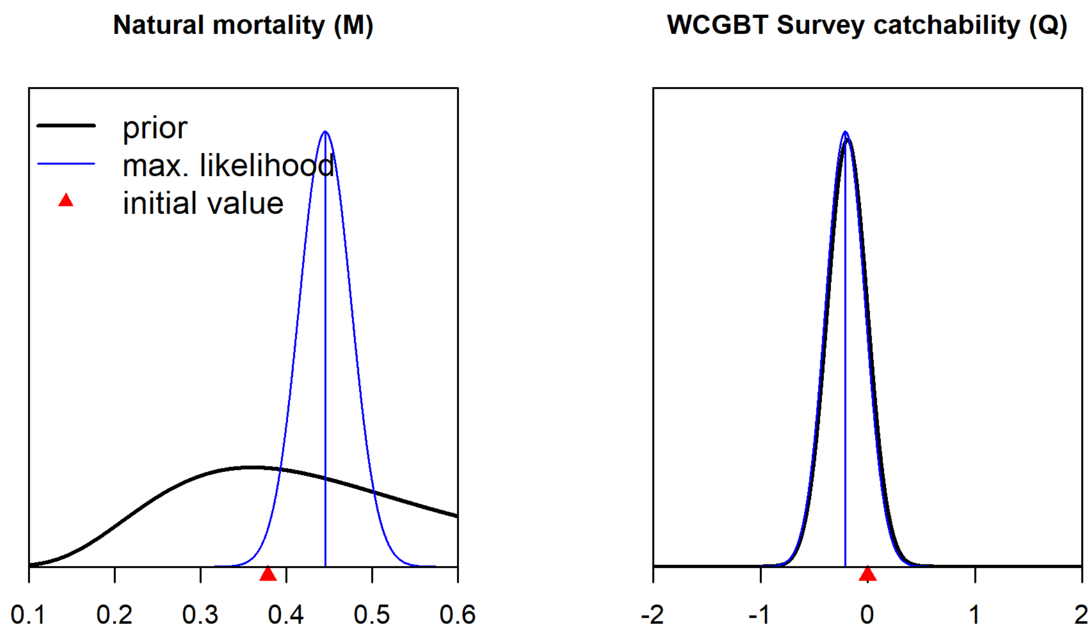

Figure 18: Estimates of natural morality and catchability of the WCGBT Survey with normal approximations to their uncertainty compared to their prior distributions.

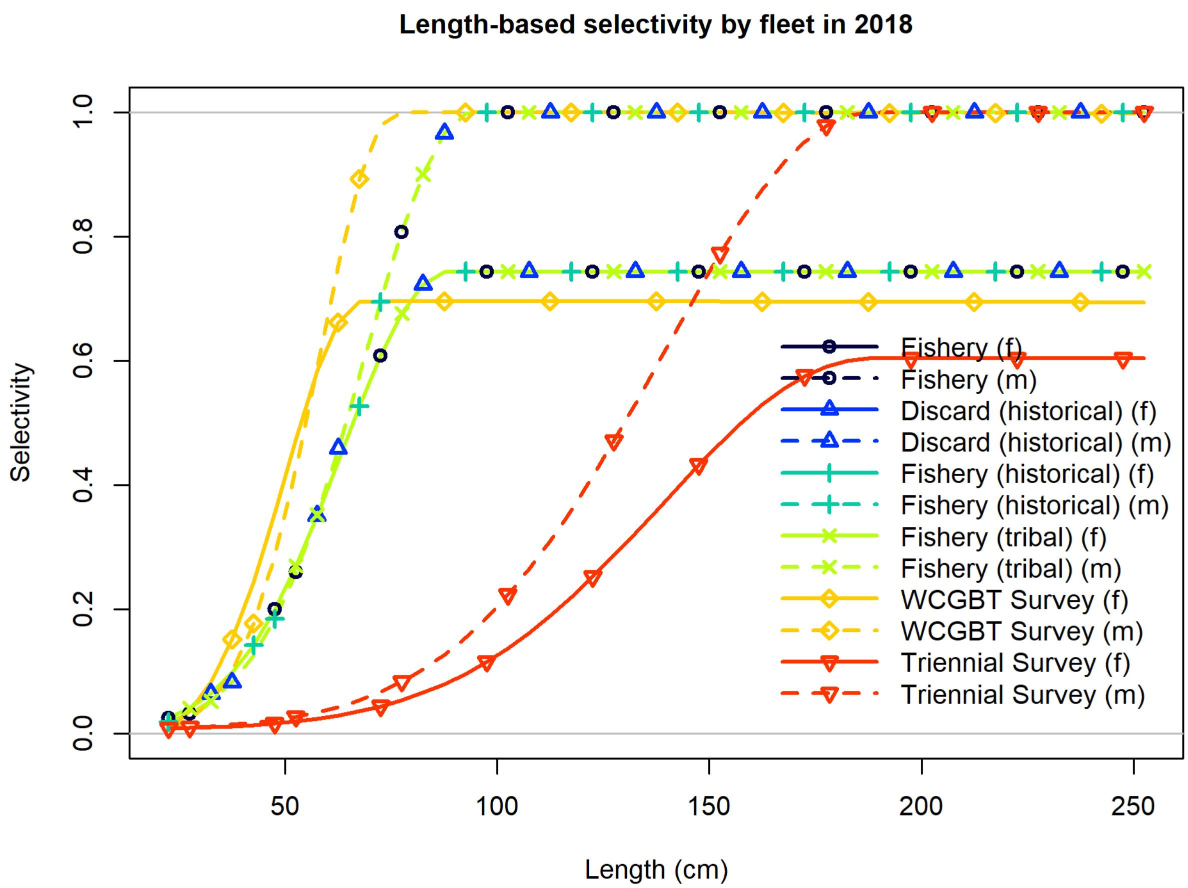

Figure 19: Selectivity at length for all of the fleets in the base model. Female selectivity is shown in the solid lines and males in the dashed lines.

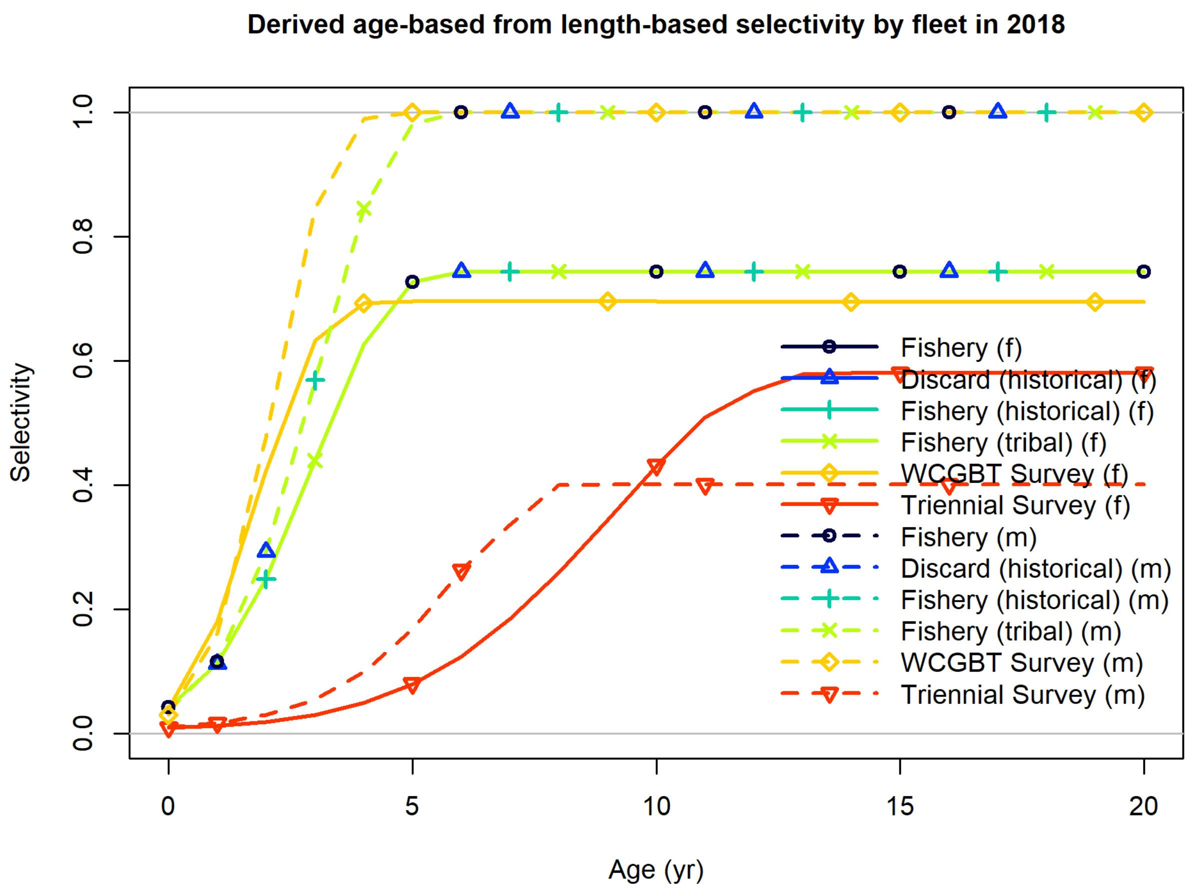

Figure 20: Selectivity at age derived from the combination of selectivity-at-length (shown above) and the estimated distribution of length at each age for all of the fleets in the base model. Female selectivity is shown in the solid lines and males in the dashed lines.

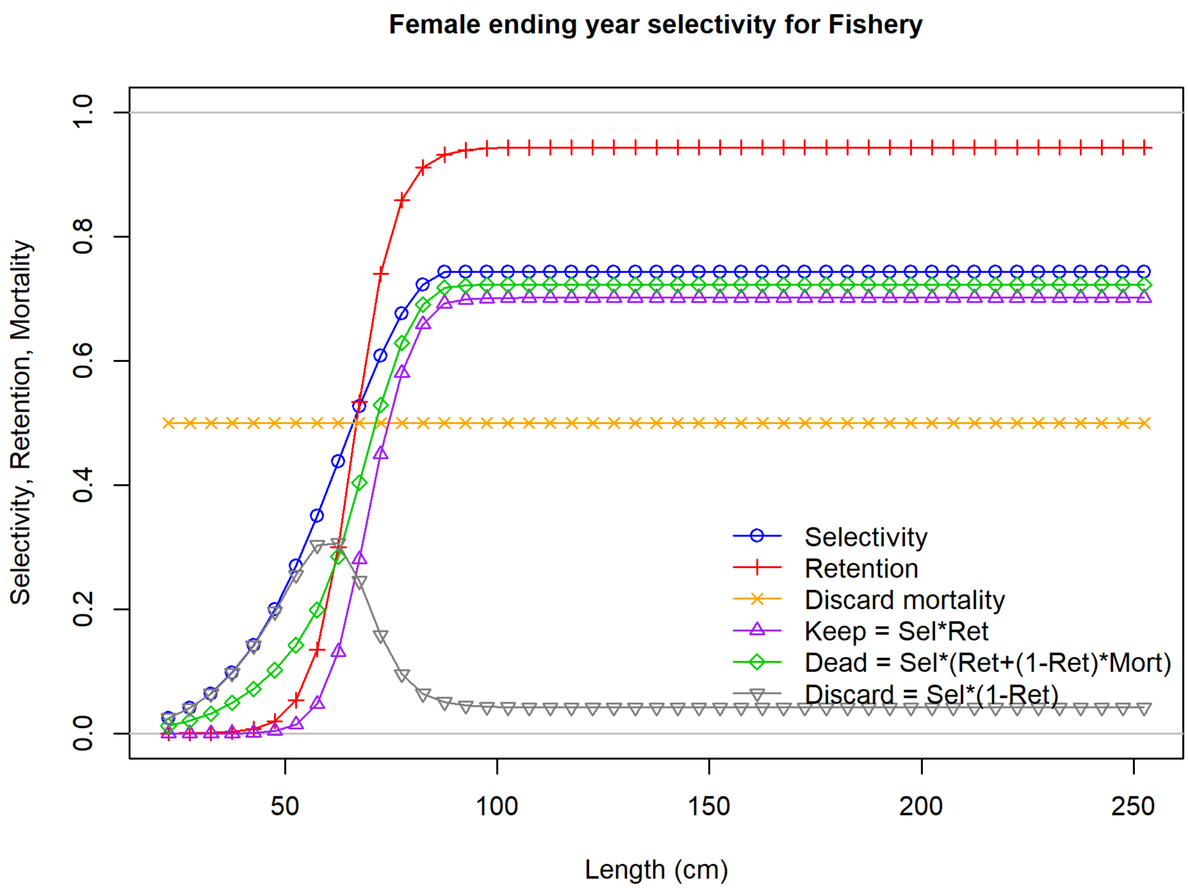

Figure 21: Female fishery selectivity and retention in 2018 with associated derived quantities.

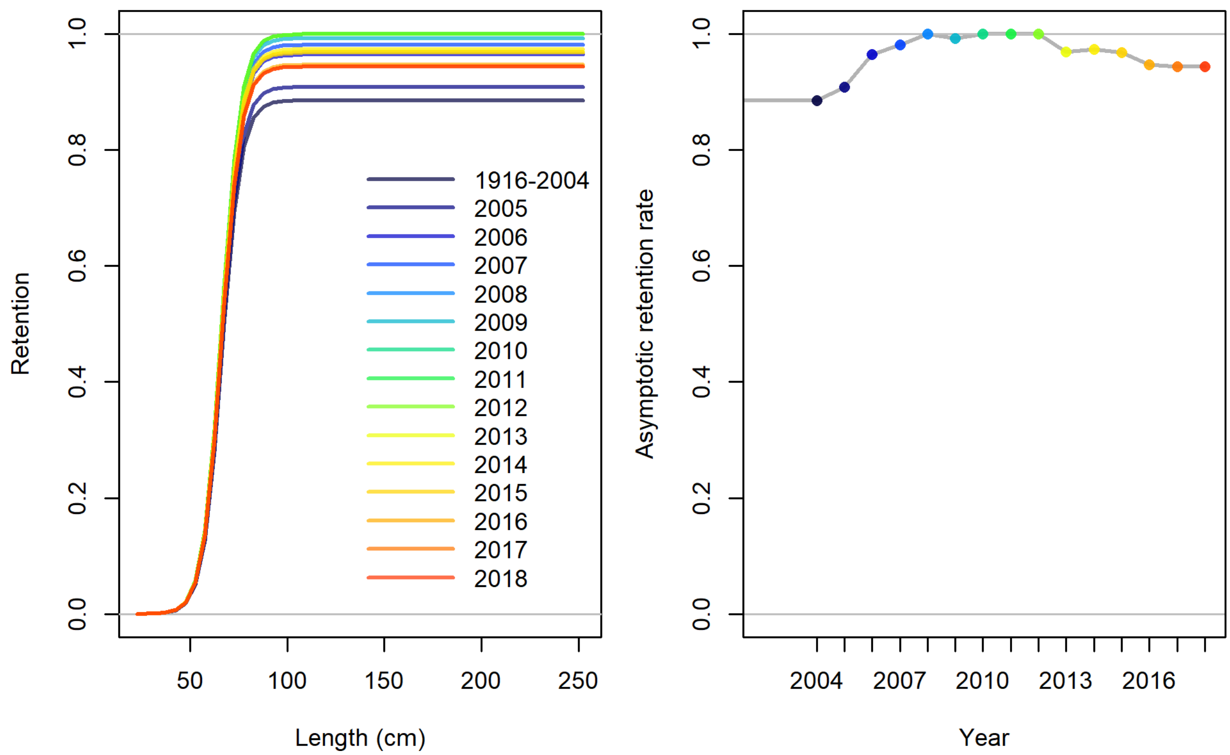

Figure 22: Time-varying retention for the fishery (left) with the time-series of asymptotic retention rates (right).

11.3.1 Fits to the Data

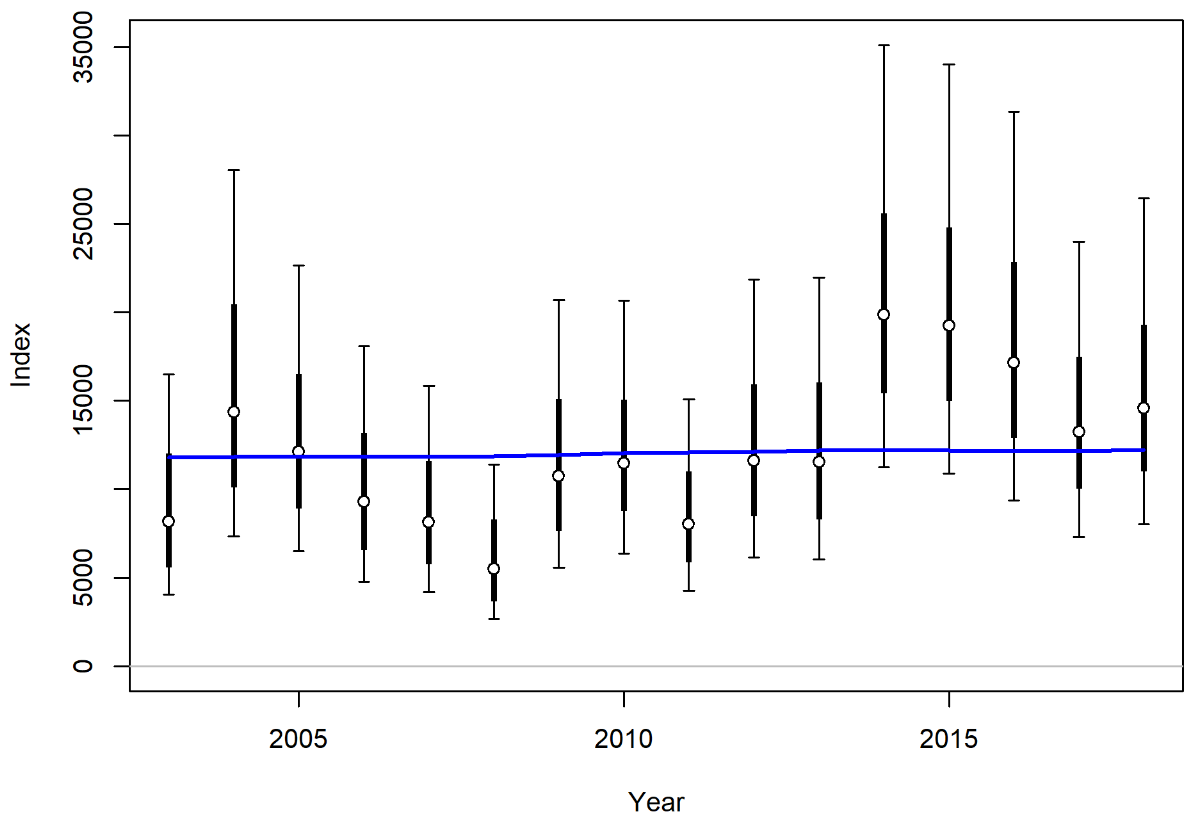

Figure 23: Fit to index data for WCGBT Survey. Lines indicate 95% uncertainty interval around index values. Thicker lines indicate input uncertainty before addition of estimated additional uncertainty parameter. The blue line indicates the model estimate.

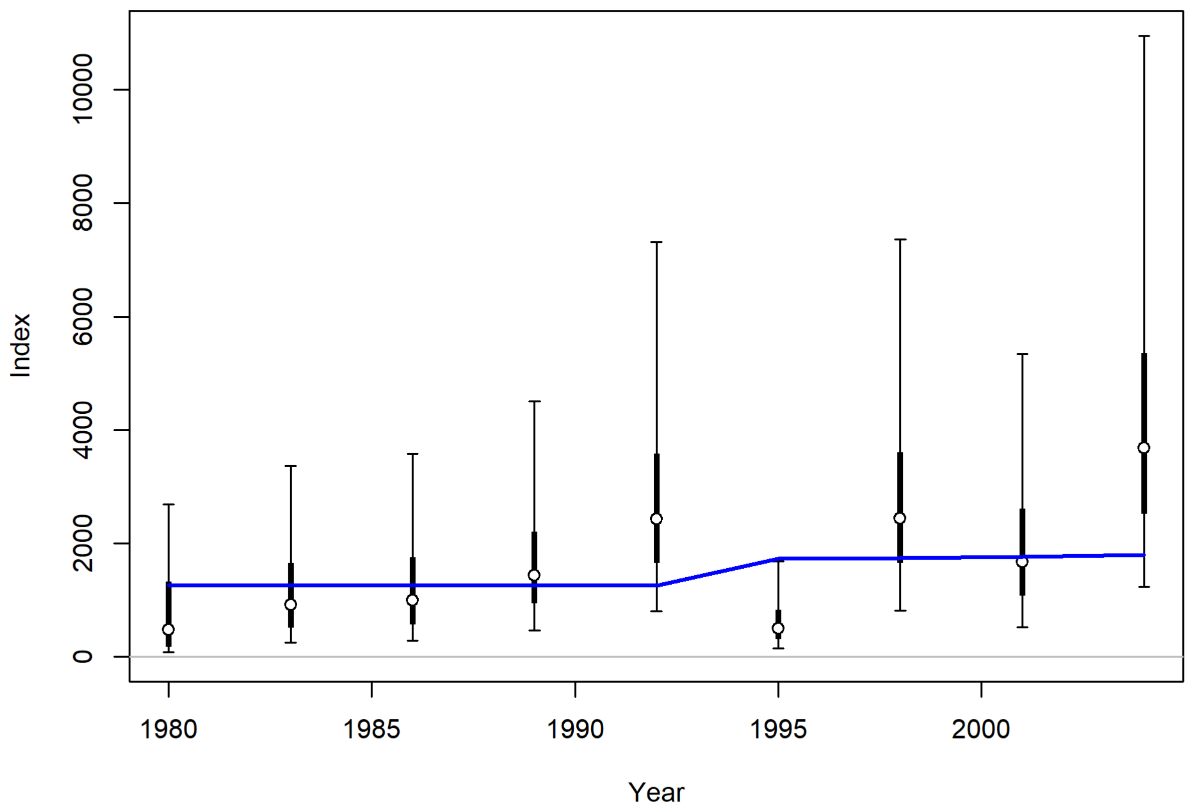

Figure 24: Fit to index data for Triennial Survey. Lines indicate 95% uncertainty interval around index values. Thicker lines indicate input uncertainty before addition of estimated additional uncertainty parameter. The blue line indicates the model estimate with a change between 1992 and 1995 associated with the estimated change in catchability.

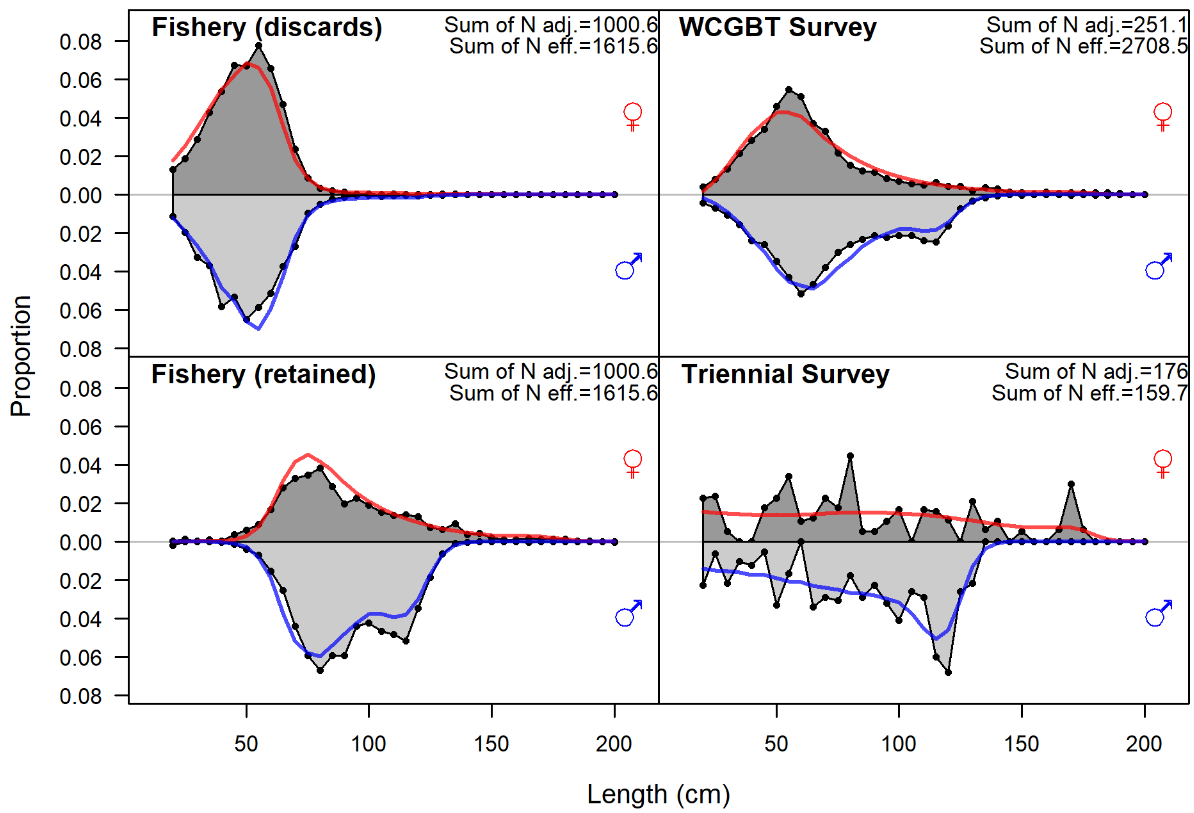

Figure 25: Fits to length comp data, aggregated across time by fleet.

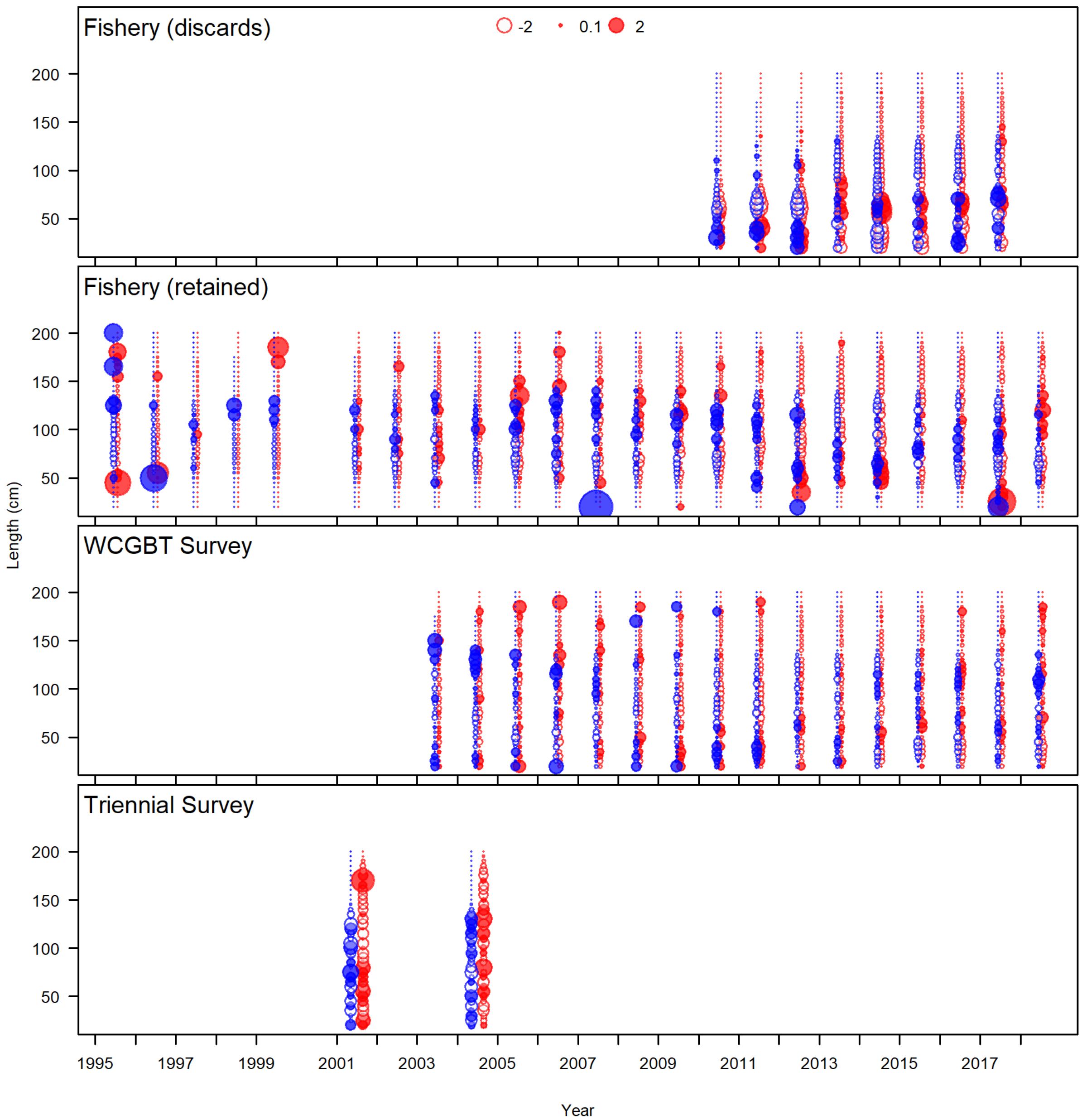

Figure 26: Pearson residuals for length composition data for all years and fleets, with females in red and males in blue. Closed bubbles are positive residuals (observed > expected) and open bubbles are negative residuals (observed < expected).

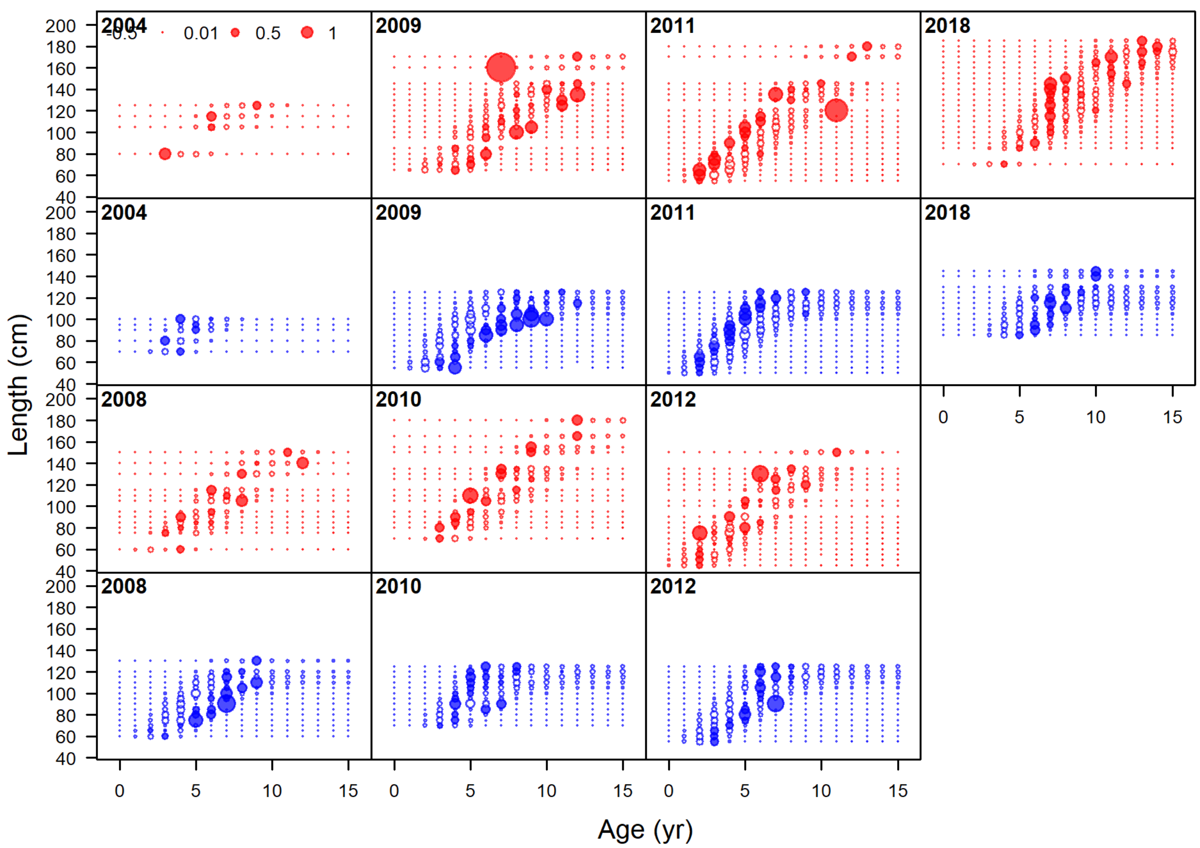

Figure 27: Pearson residuals for the fit to conditional age-at-length data from the fishery. Closed bubbles are positive residuals (observed > expected) and open bubbles are negative residuals (observed < expected).

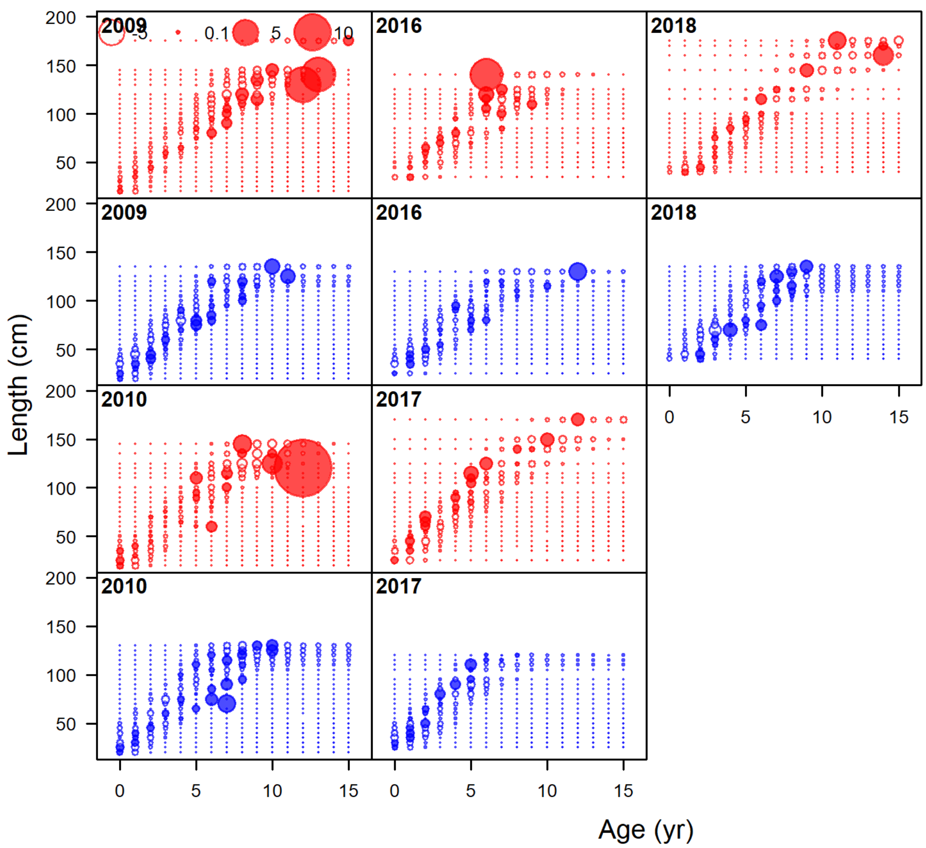

Figure 28: Pearson residuals for the fit to conditional age-at-length data from the WCGBT Survey. Closed bubbles are positive residuals (observed > expected) and open bubbles are negative residuals (observed < expected).

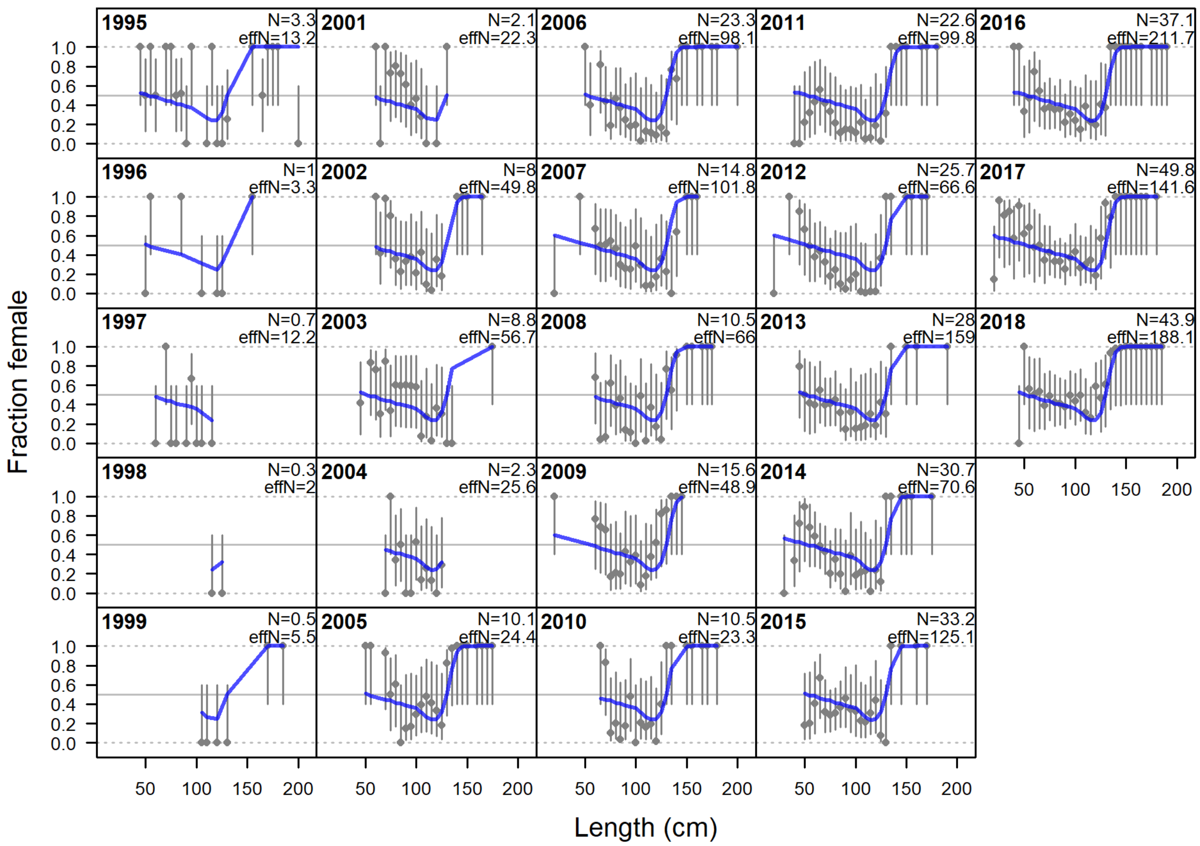

Figure 29: Observed sex ratios (points) from the fishery length comp data with 75% intervals (vertical lines) calculated as a Jeffreys interval based on the adjusted input sample size. The model expectation is shown in the blue line.

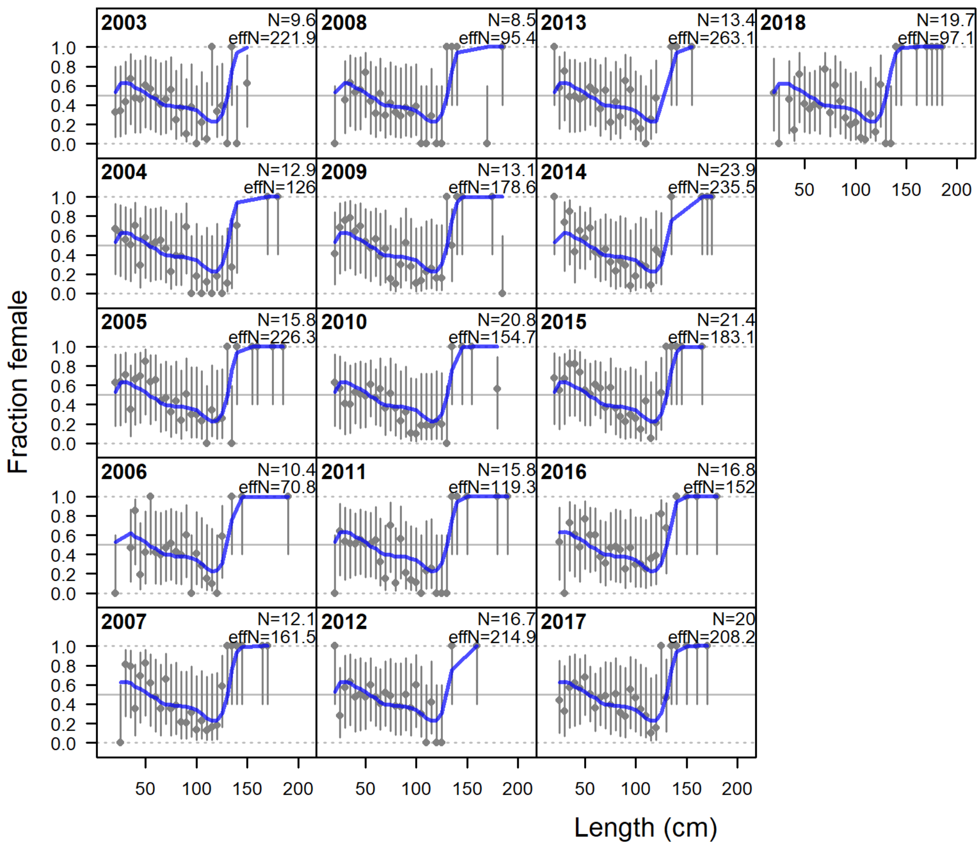

Figure 30: Observed sex ratios (points) from the WCGBT Survey length comp data with 75% intervals (vertical lines) calculated as a Jeffreys interval based on the adjusted input sample size. The model expectation is shown in the blue line.

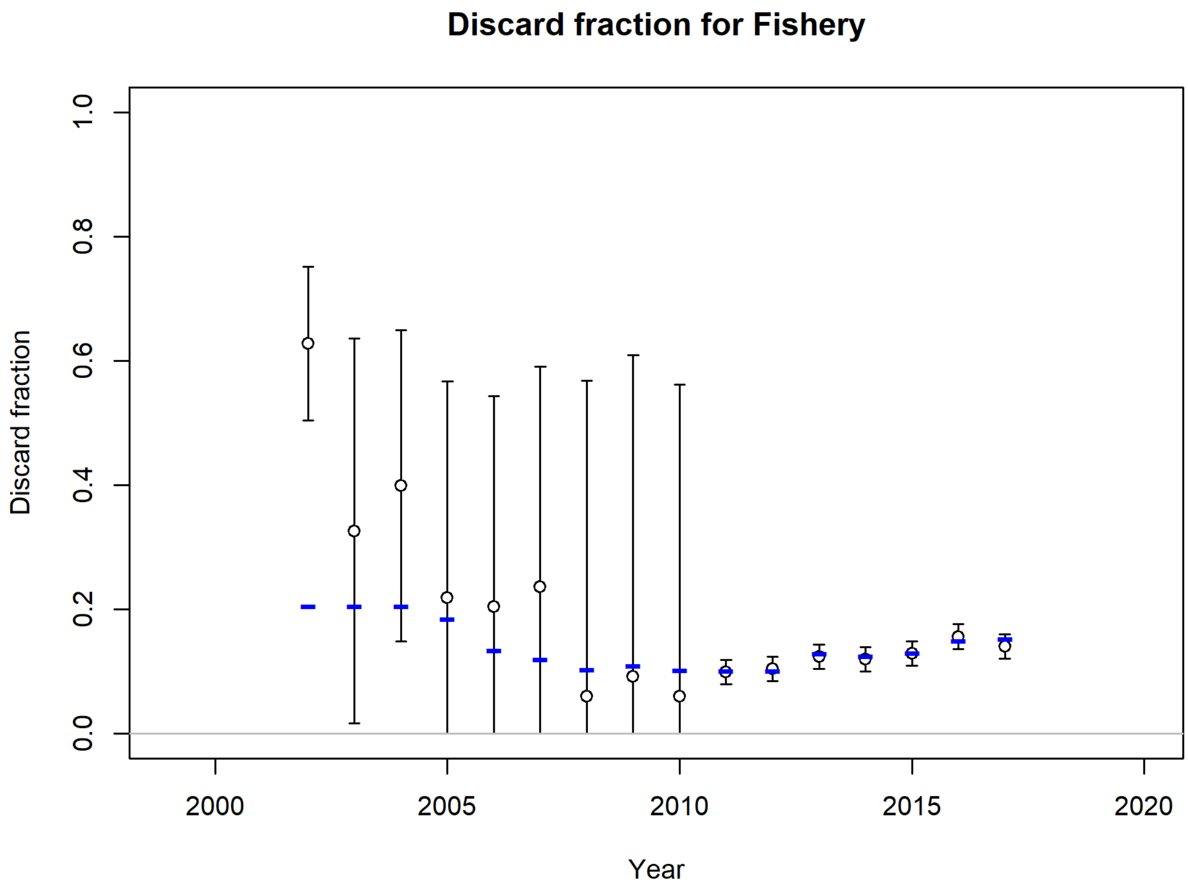

Figure 31: Fit to the discard fraction estimates. Points are model estimates with 95% uncertainty intervals. The model estimate is shown in the blue lines.

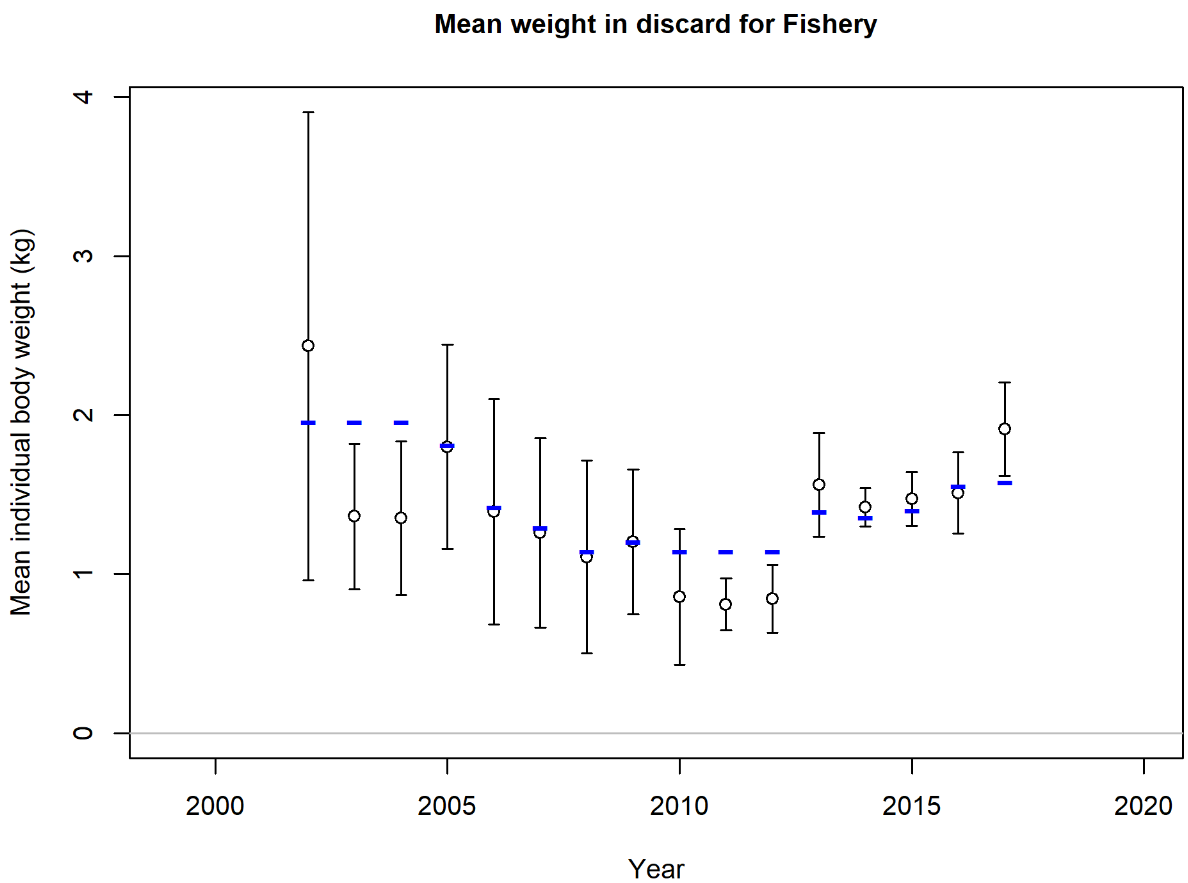

Figure 32: Fit to the mean weight of the discards. Points are model estimates with 95% uncertainty intervals. The model estimate is shown in the blue lines.

11.3.2 Time Series Figures

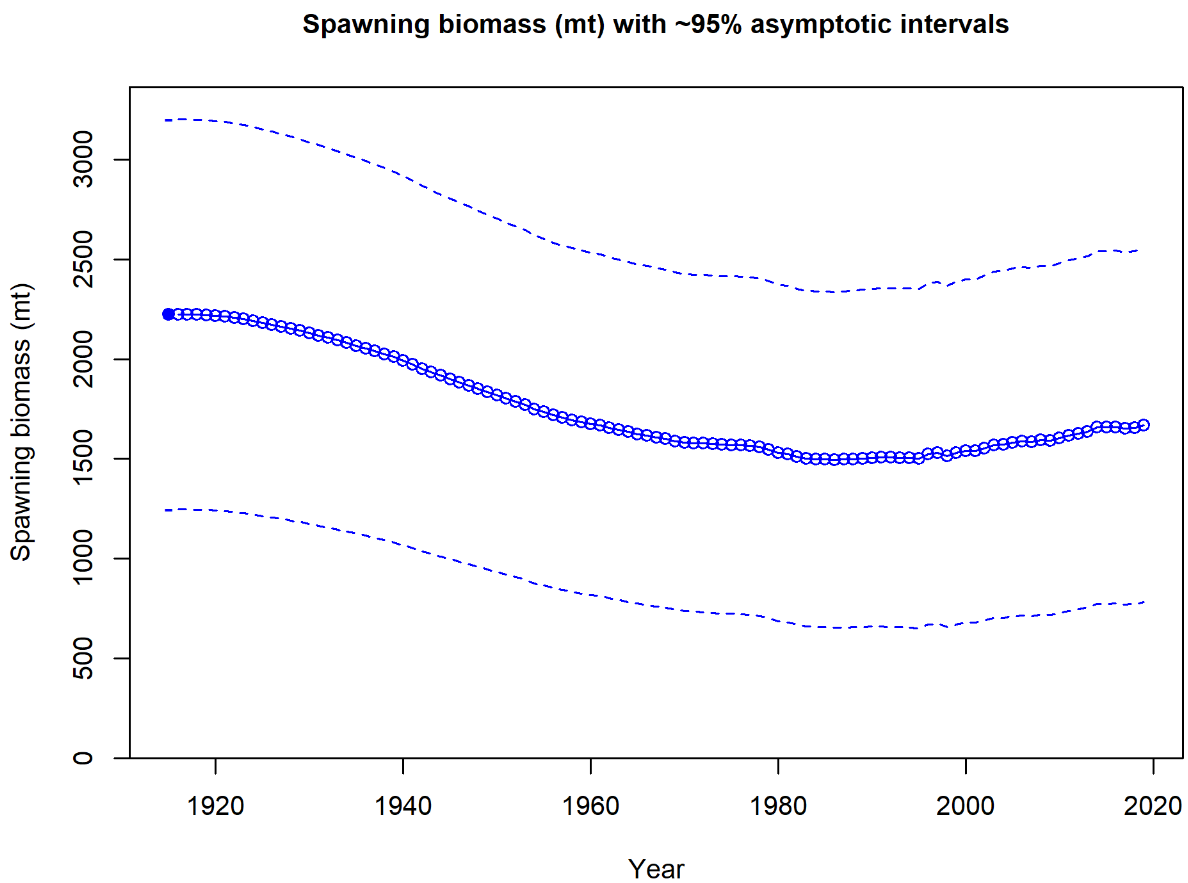

Figure 33: Estimated spawning biomass (mt) with approximate 95% asymptotic intervals.

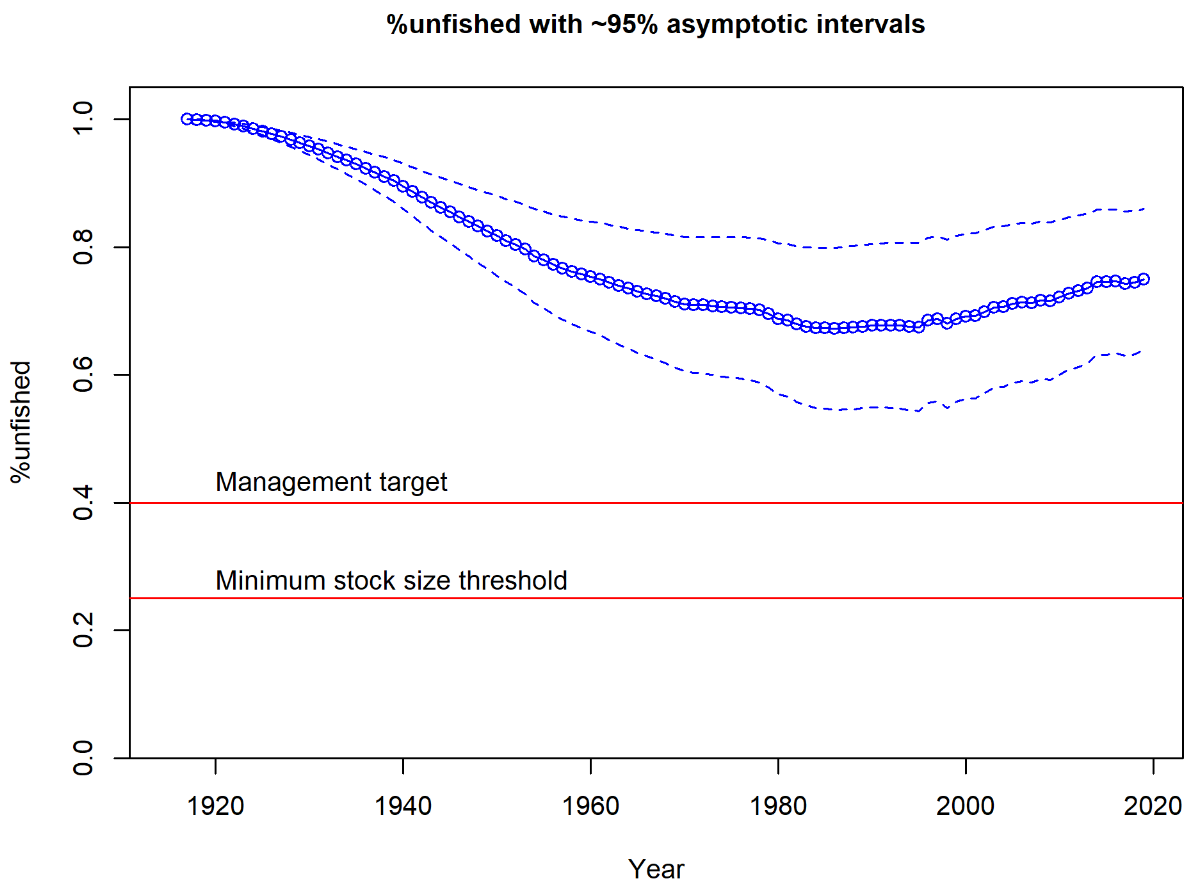

Figure 34: Estimated %unfished with approximate 95% asymptotic intervals.

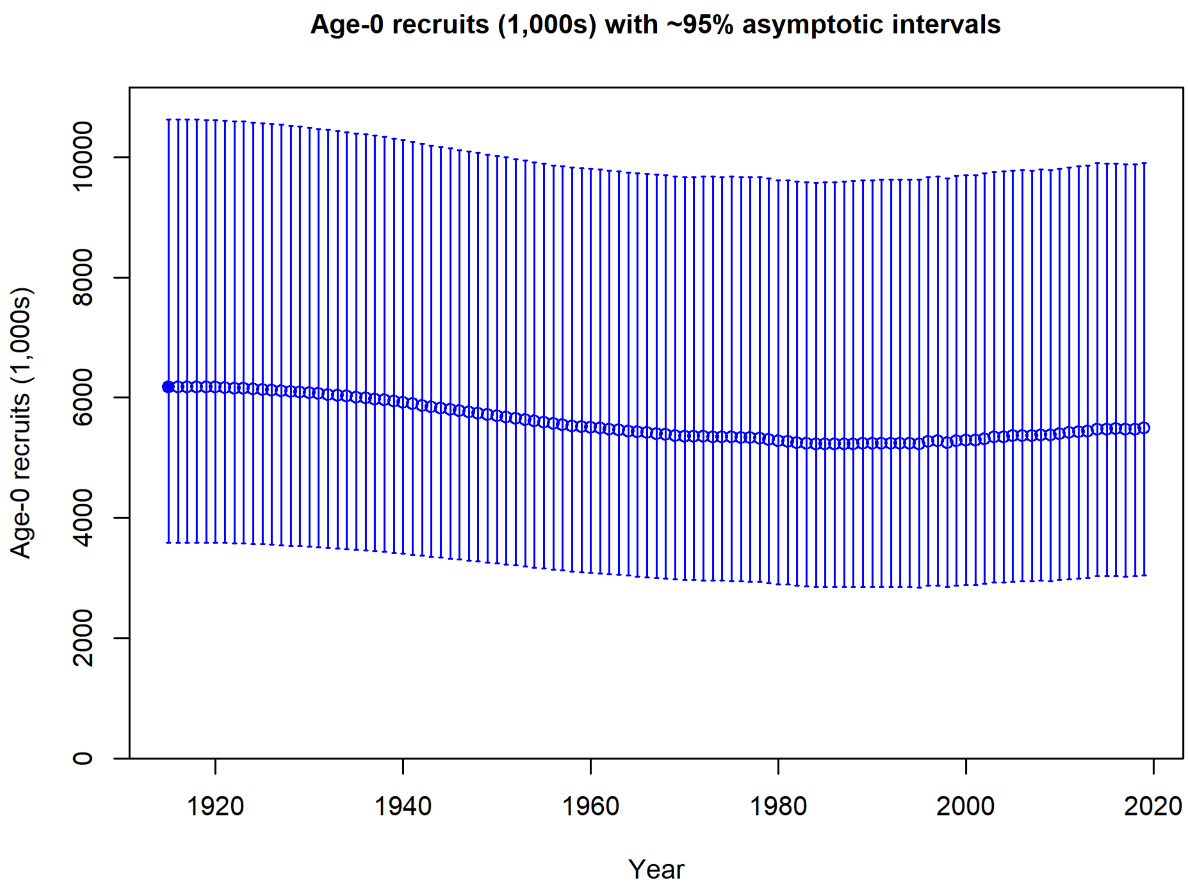

Figure 35: Estimated time-series of recruitment for Big Skate.

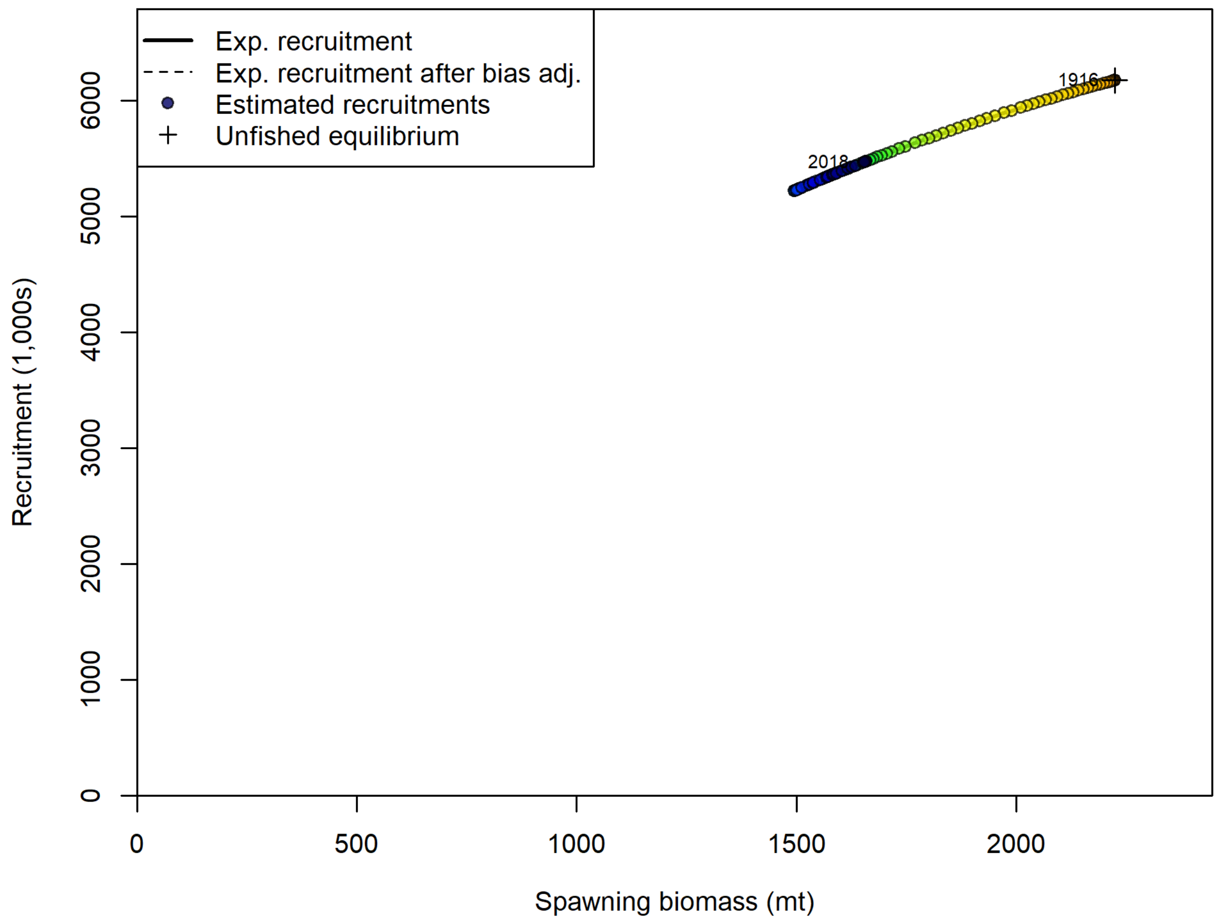

Figure 36: Estimated recruitment and the assumed stock-recruit relationship.

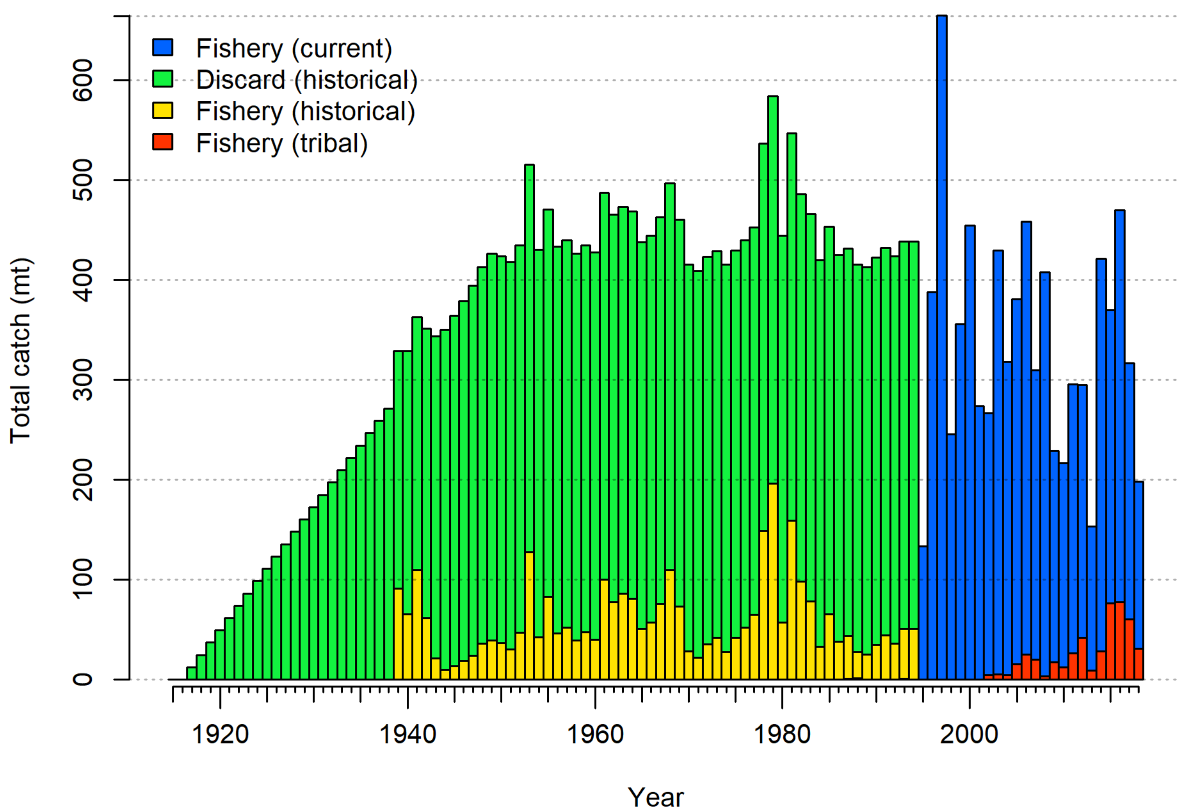

Figure 37: Estimated total catch including discards estimated within the model. The historical discards shown in green have been scaled to account for an assumed 50% discard mortality but the discards in the recent period show both live and dead discards.

1132 ### 11.3.3 Sensitivity Analyses and Retrospectives

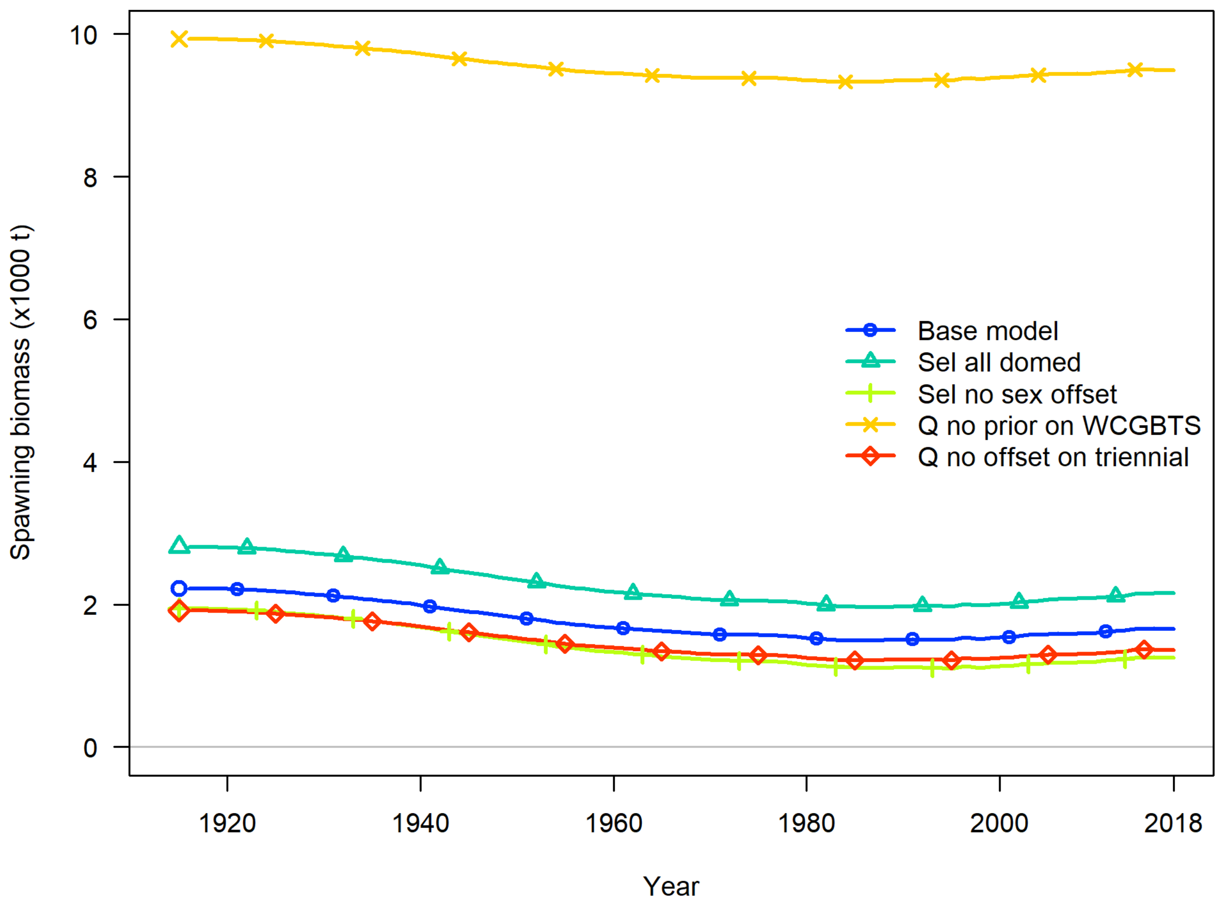

Figure 38: Time series of spawning biomass (mt) estimated in sensitivity analyses related to selectivity and catchability.

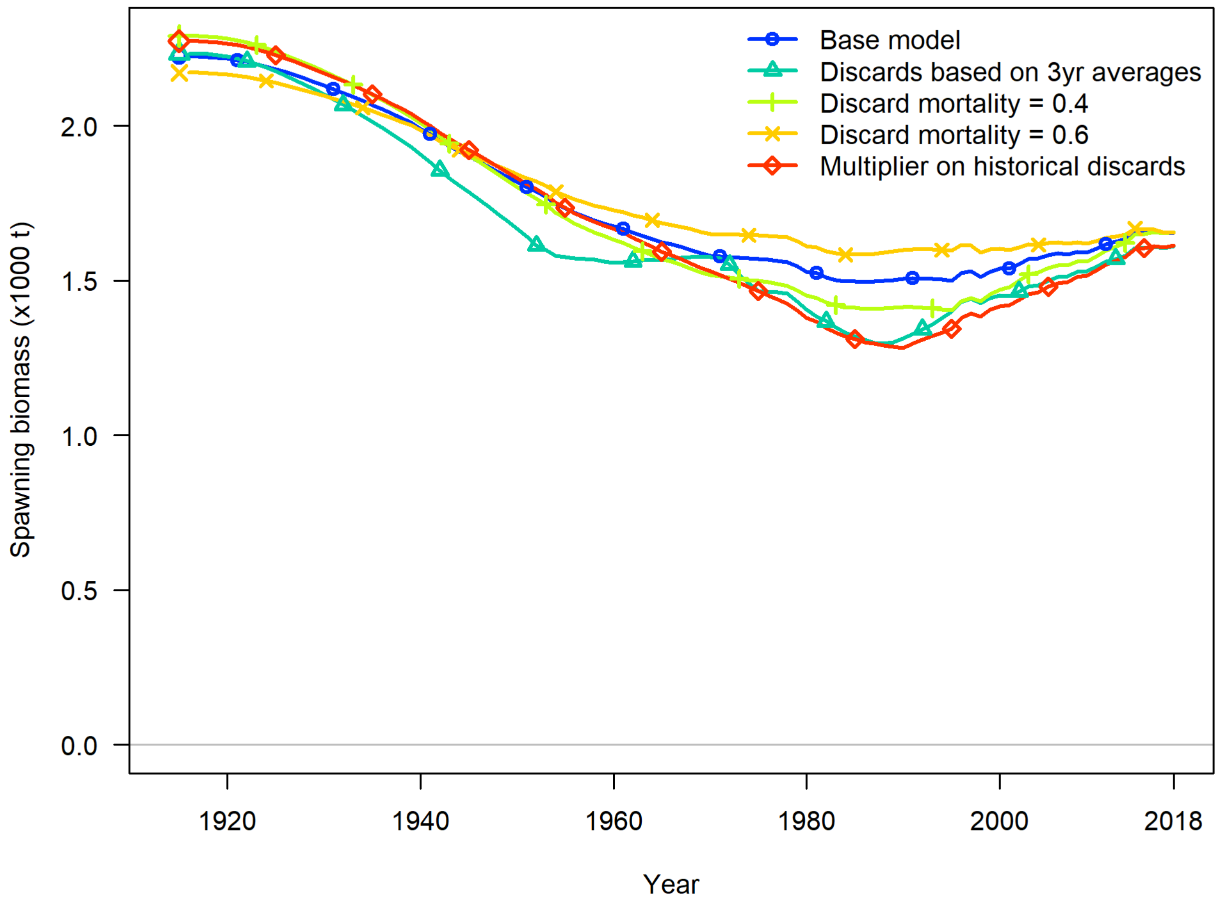

Figure 39: Time series of spawning biomass (mt) estimated in sensitivity analyses related to historic catch and discards.

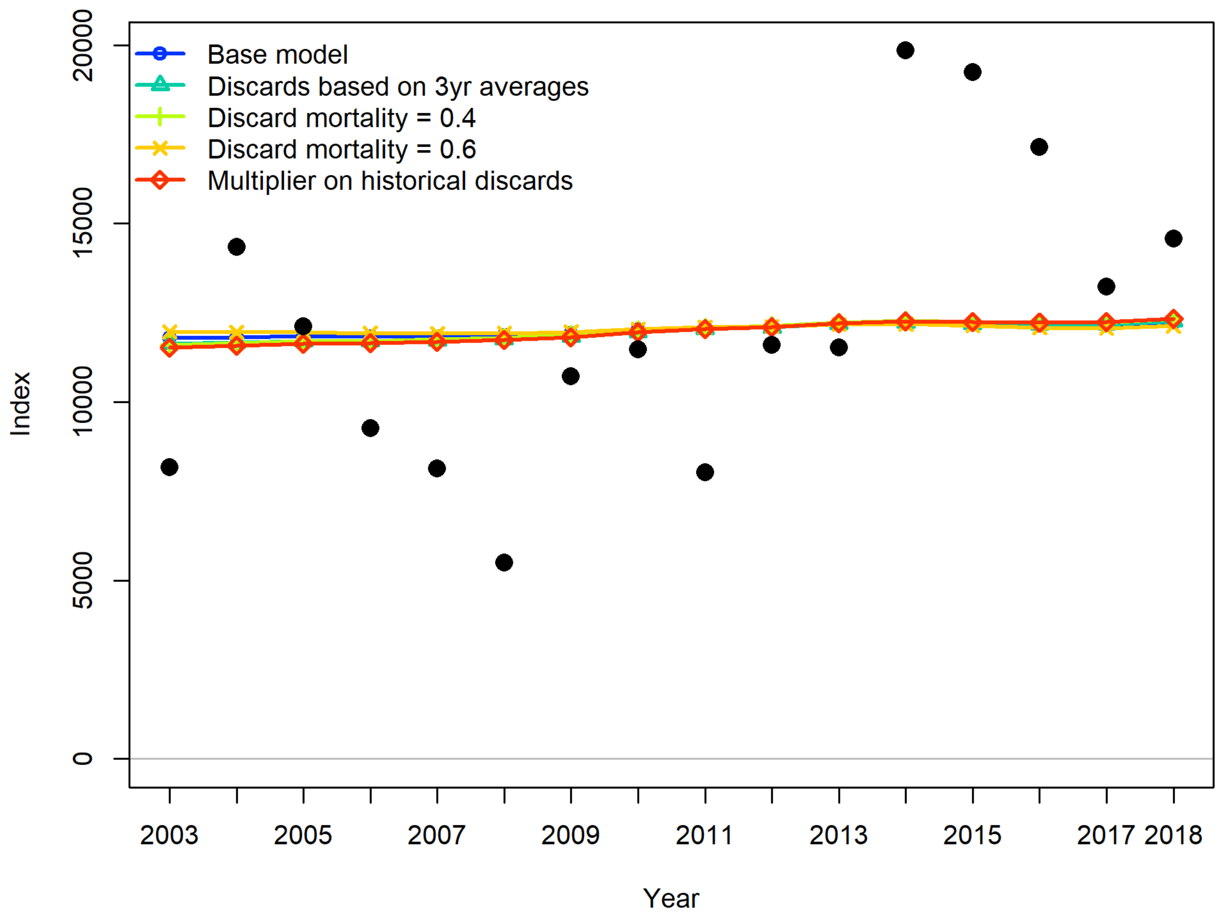

Figure 40: Fit to the WCGBT Survey estimated in the sensitivity analyses related to historic catch and discards.

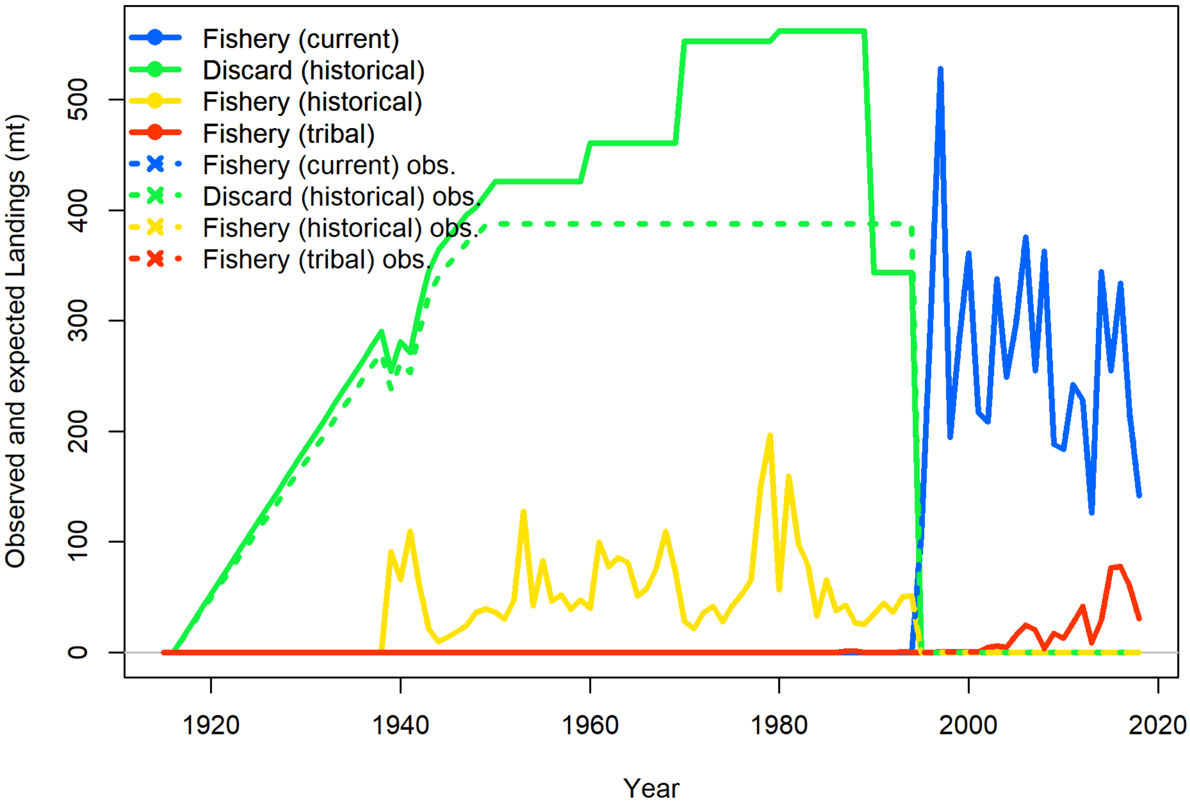

Figure 41: Catch by category for the sensitivity analysis where multipliers on historical discards were estimated. The estimated time series including the multipliers is shown in the solid green line and the input values in the base model are shown in the dashed green line.

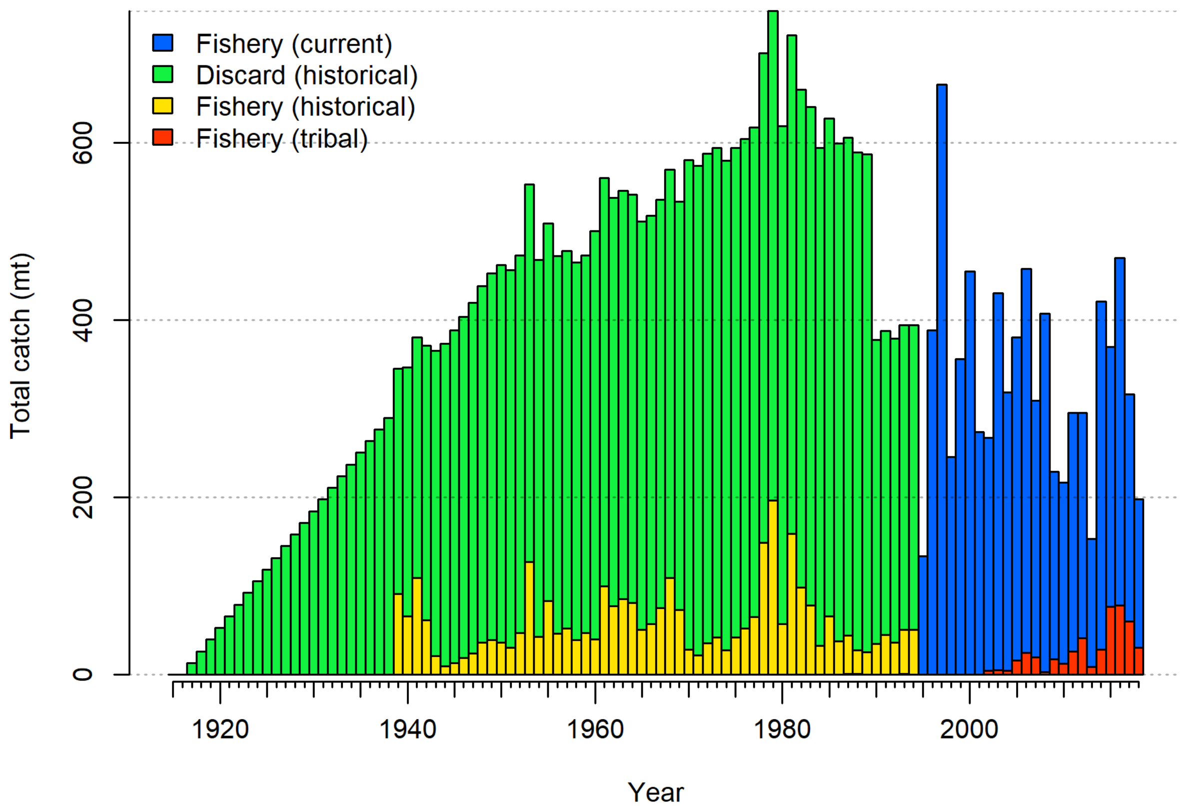

Figure 42: Estimated total catch for the sensitivity analysis where multipliers on historical discards were estimated. The historical discards shown in green have been scaled to account for an assumed 50% discard mortality but the discards in the recent period show both live and dead discards.

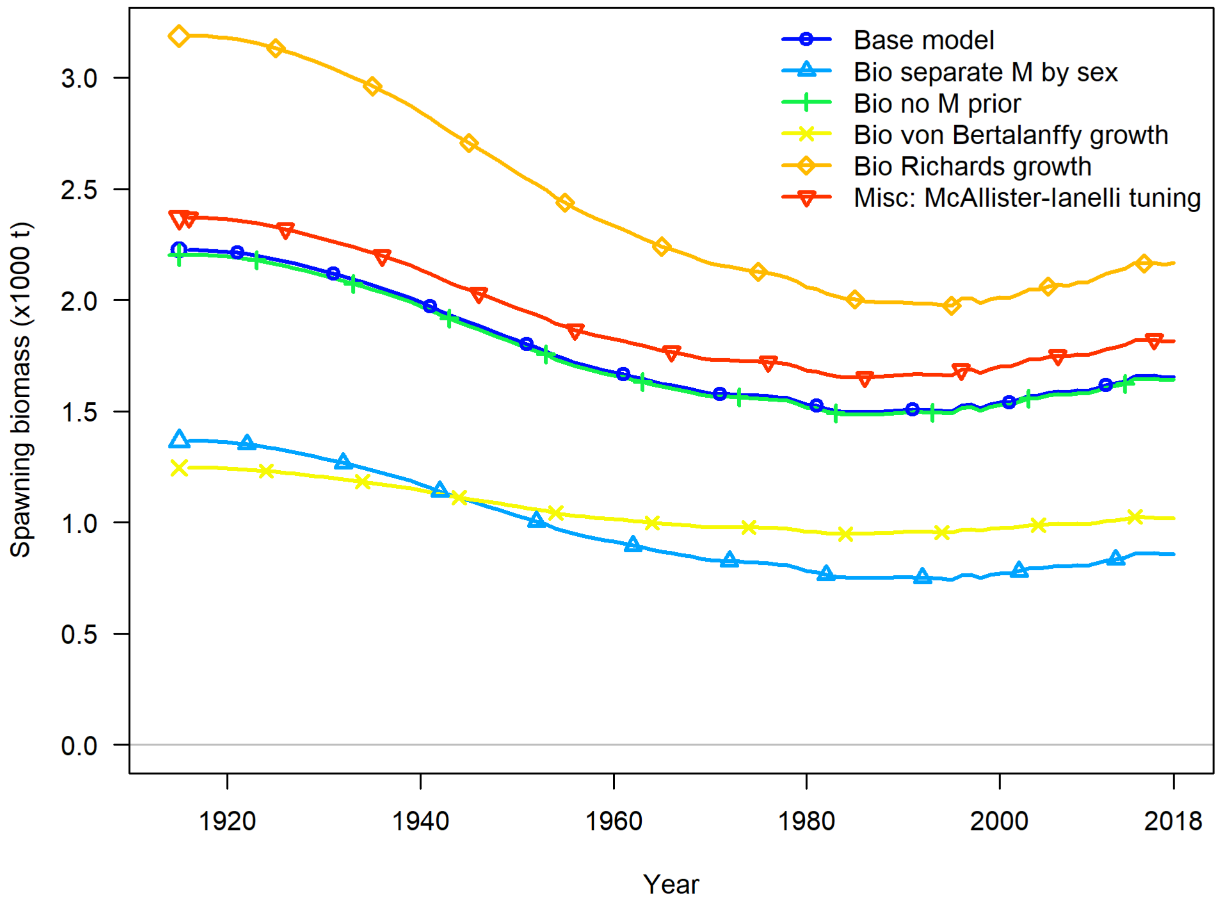

Figure 43: Time series of spawning biomass (mt) estimated in sensitivity analyses related to biology and other assumptions.

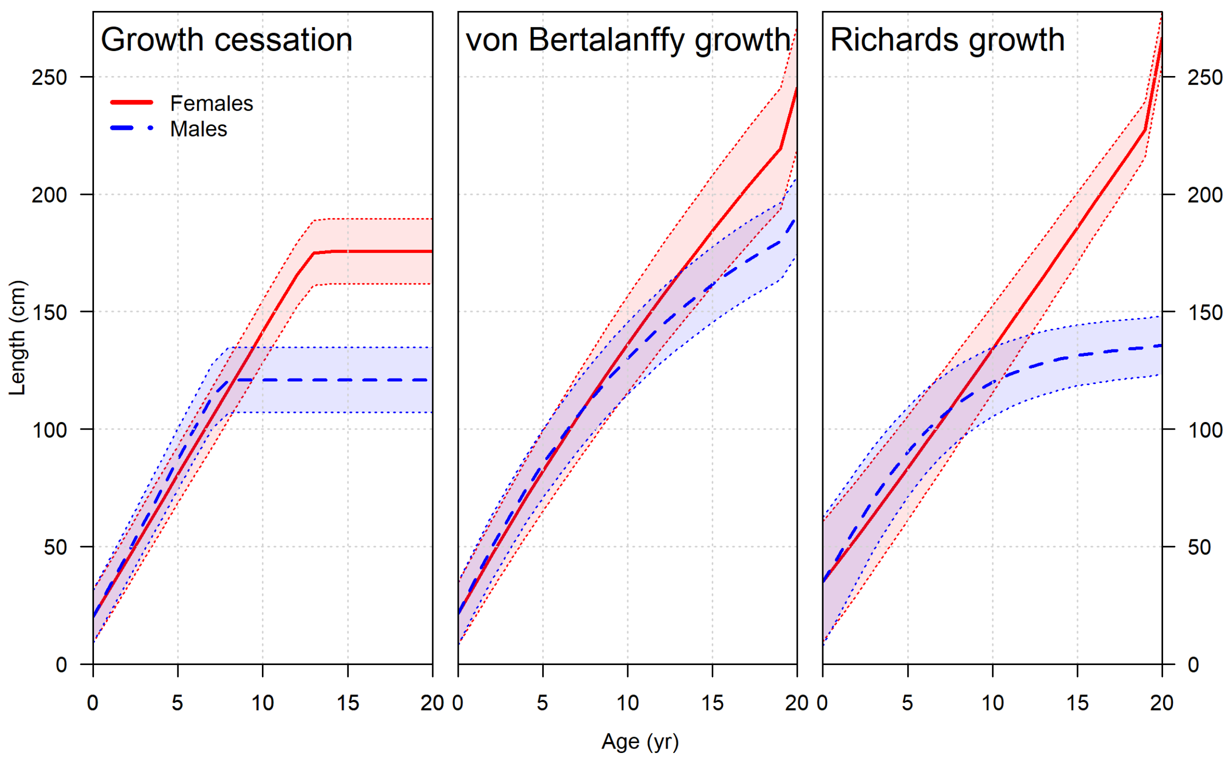

Figure 44: Comparison of the estimated growth curves from the sensitivities analyses. The increase at age 20 in the von Bertalanffy and Richards growth models is an adjustment to account for average size in the plus group based on an assumed exponential decay of the numbers at age beyond age 20.

11.3.4 Likelihood Profiles

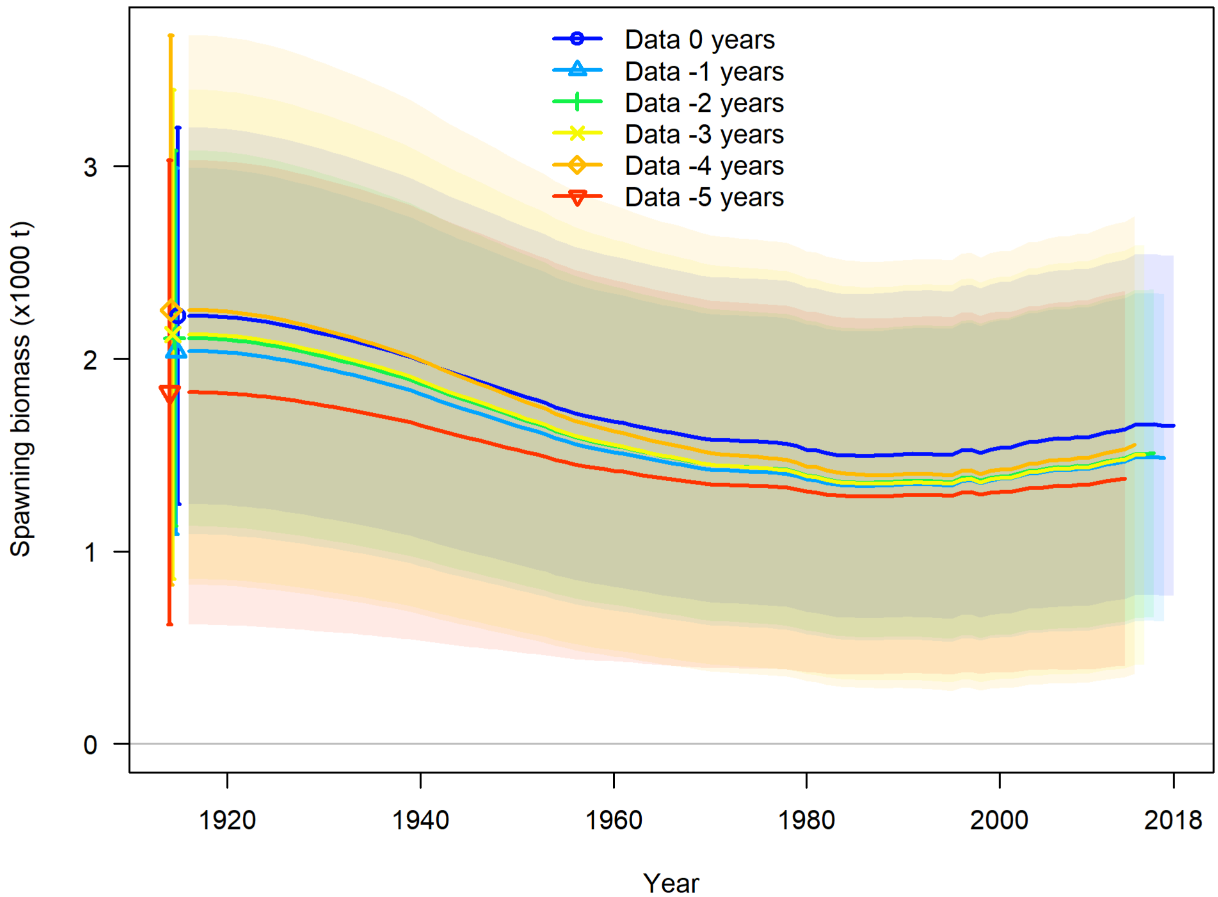

Figure 45: Time series of spawning biomass (mt) with approximate 95% asymptotic intervals estimated in retrospective analyses in which the final 5 years of data are successively removed from the model.

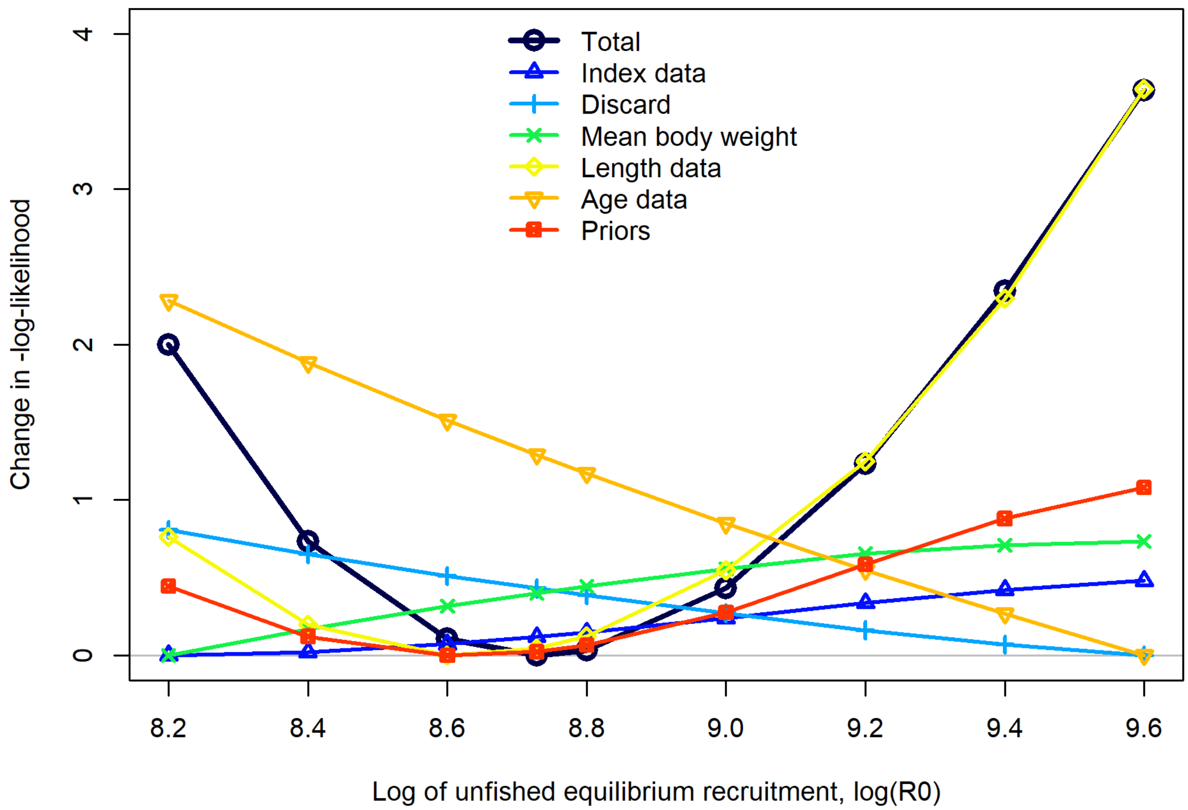

Figure 46: Likelihood profile over the log of equilibrium recruitment (R_0).

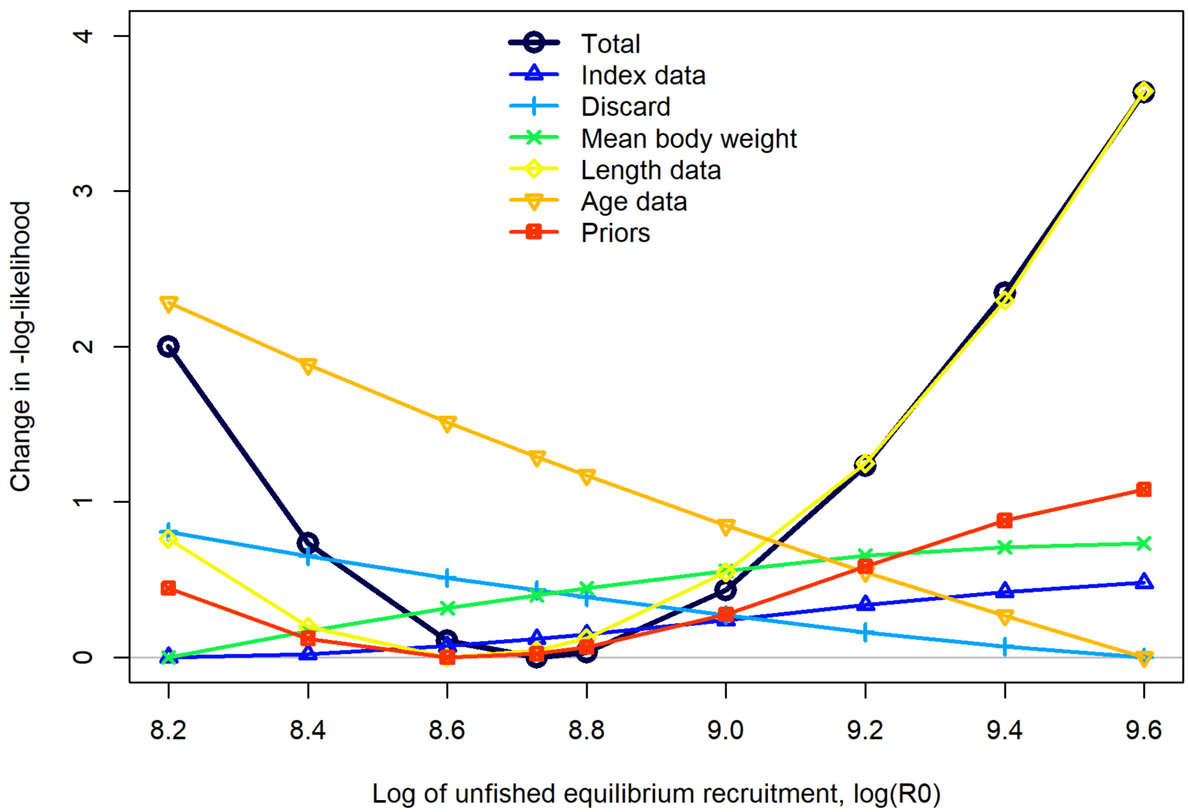

Figure 47: Likelihood profile over the log of equilibrium recruitment (R_0).

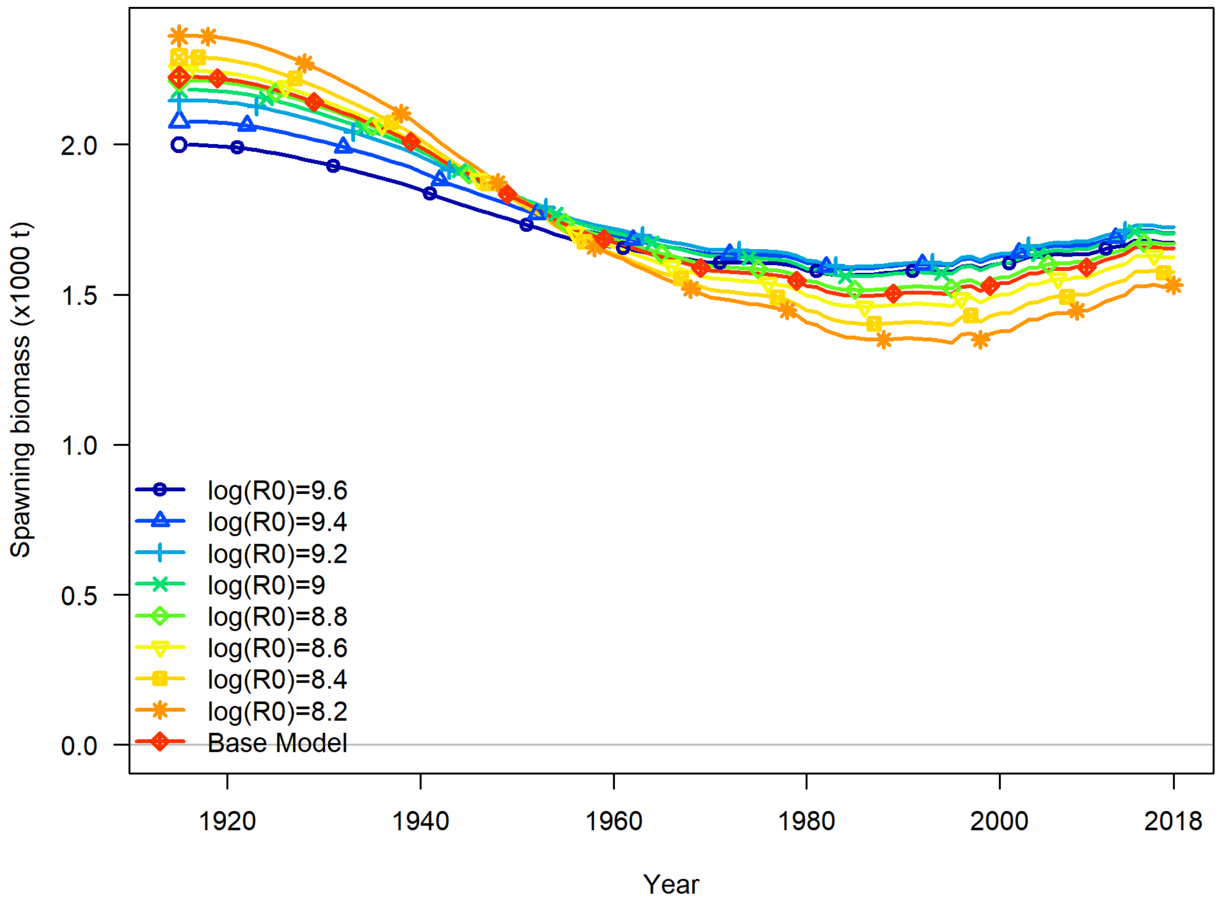

Figure 48: Time series of spawning biomass (mt) estimated for the models included in the profile over the log of equilibrium recruitment (R_0).

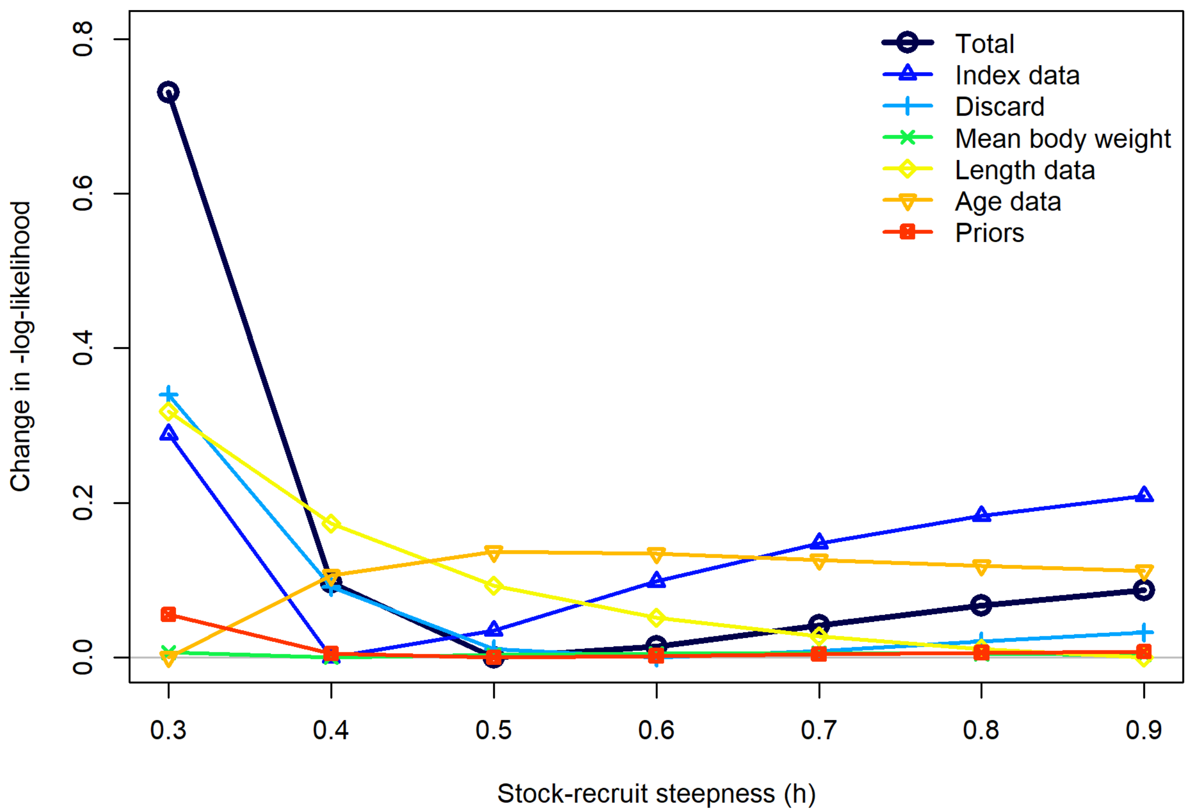

Figure 49: Likelihood profile over stock-recruit steepness (h).

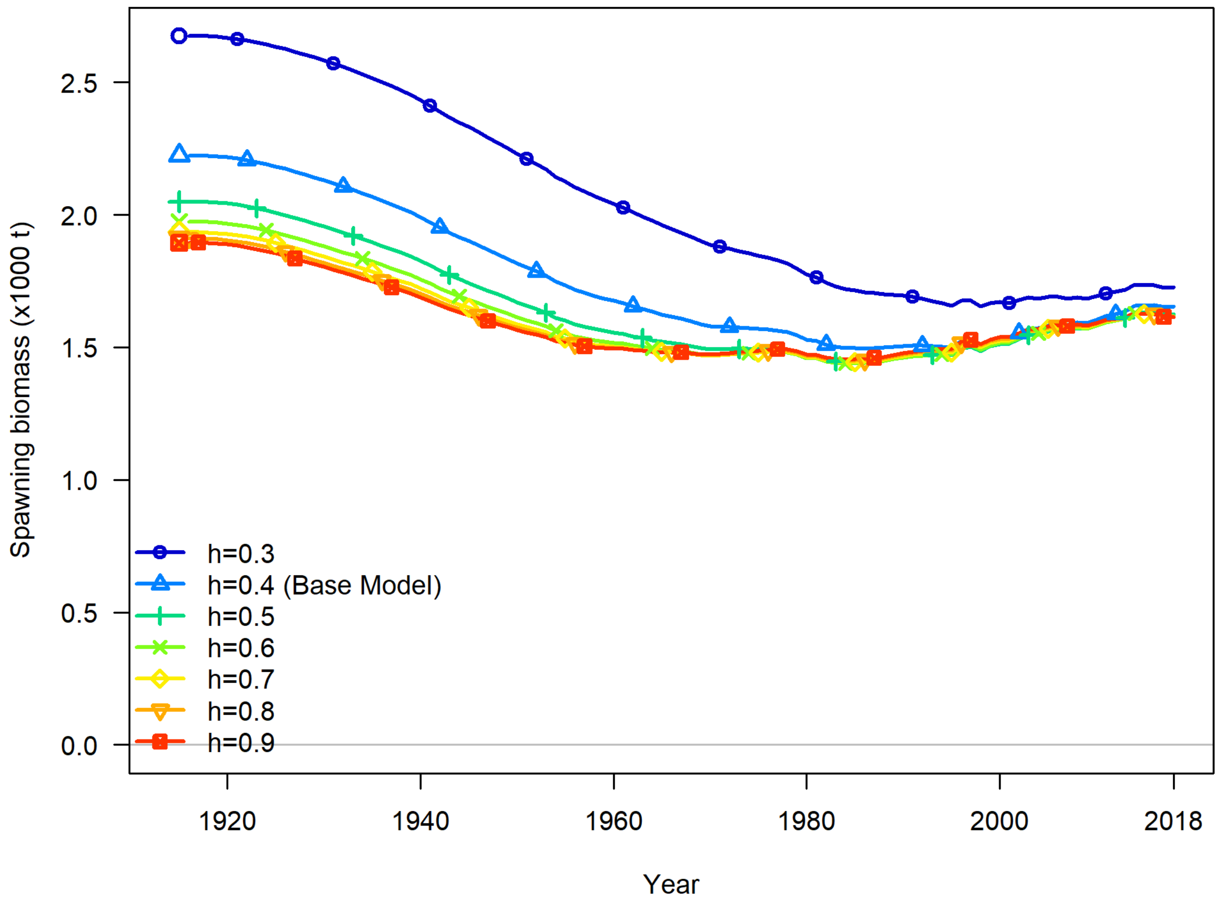

Figure 50: Time series of spawning biomass (mt) estimated for the models included in the profile over stock-recruit steepness (h).

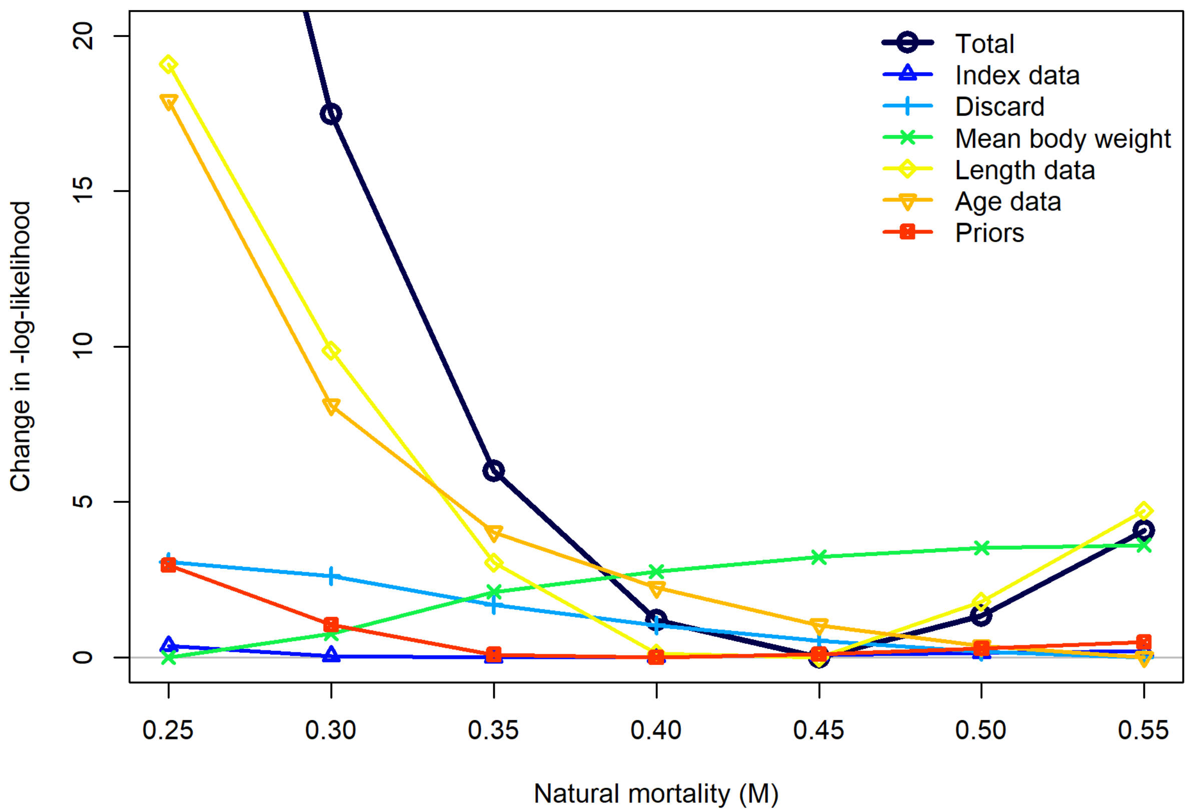

Figure 51: Likelihood profile over natural mortality (M).

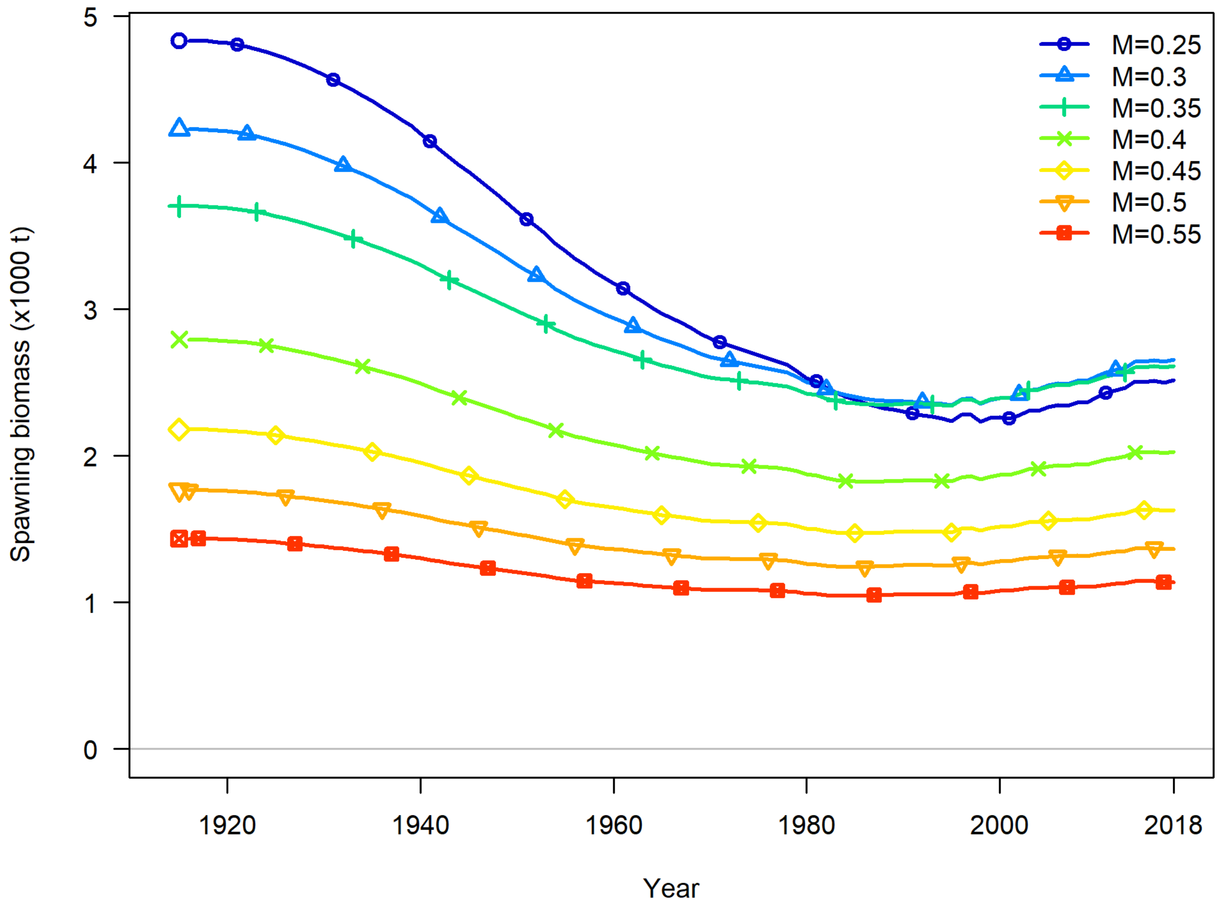

Figure 52: Time series of spawning biomass (mt) estimated for the models included in the profile over natural mortality (M).

1134 ### 11.3.5 Reference Points and Forecasts

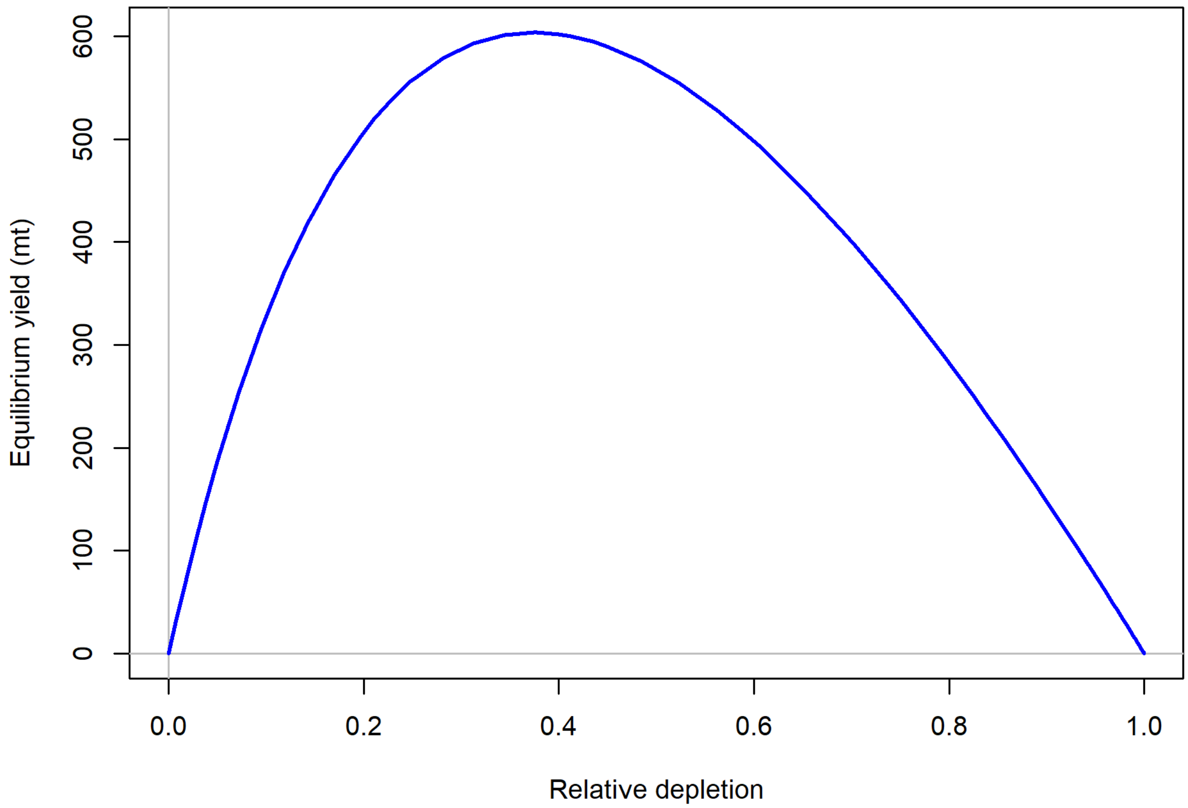

Figure 53: Equilibrium yield curve for the base case model. Values are based on the fishery selectivity and with steepness fixed at 0.4.

Appendix A. Detailed fits to length composition data

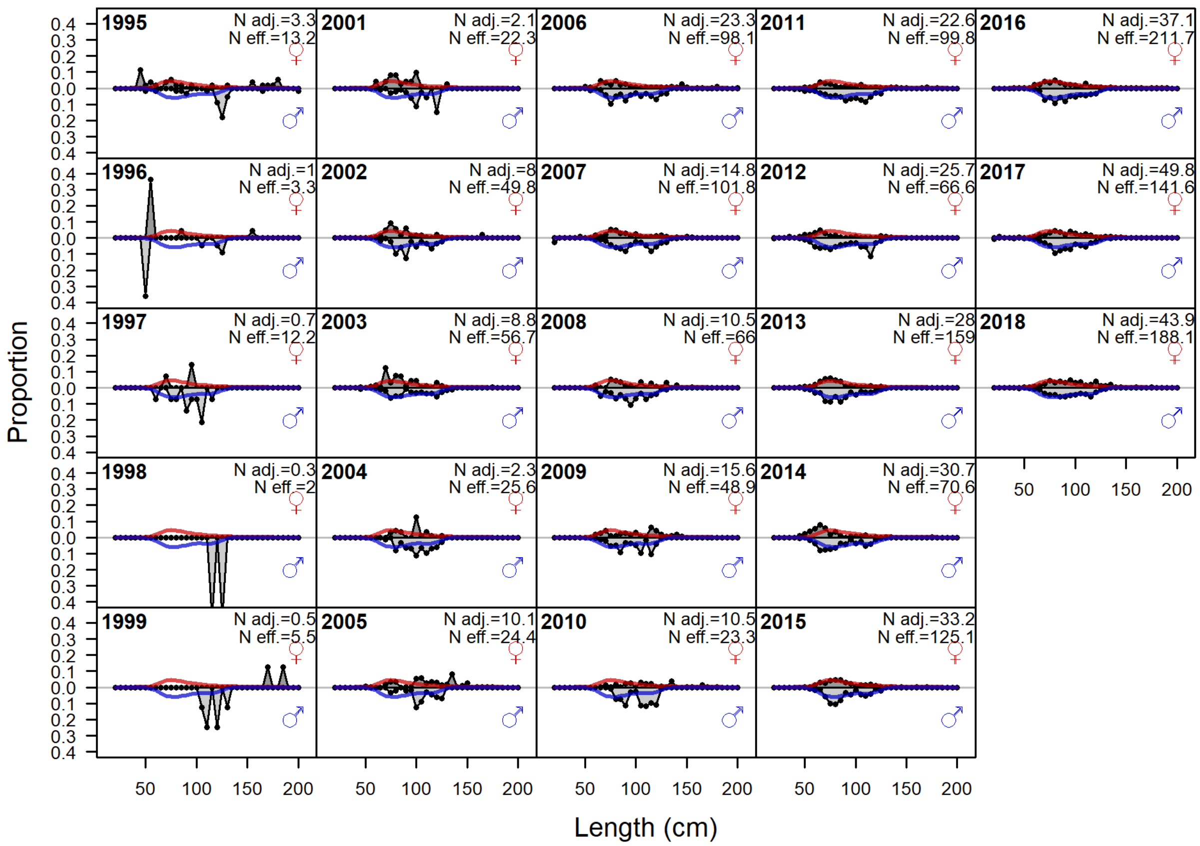

Figure A54: Length comps, retained, Fishery. 'N adj.' is the input sample size after data_weighting adjustment. N eff. is the calculated effective sample size used in the McAllister_Iannelli tuning method.

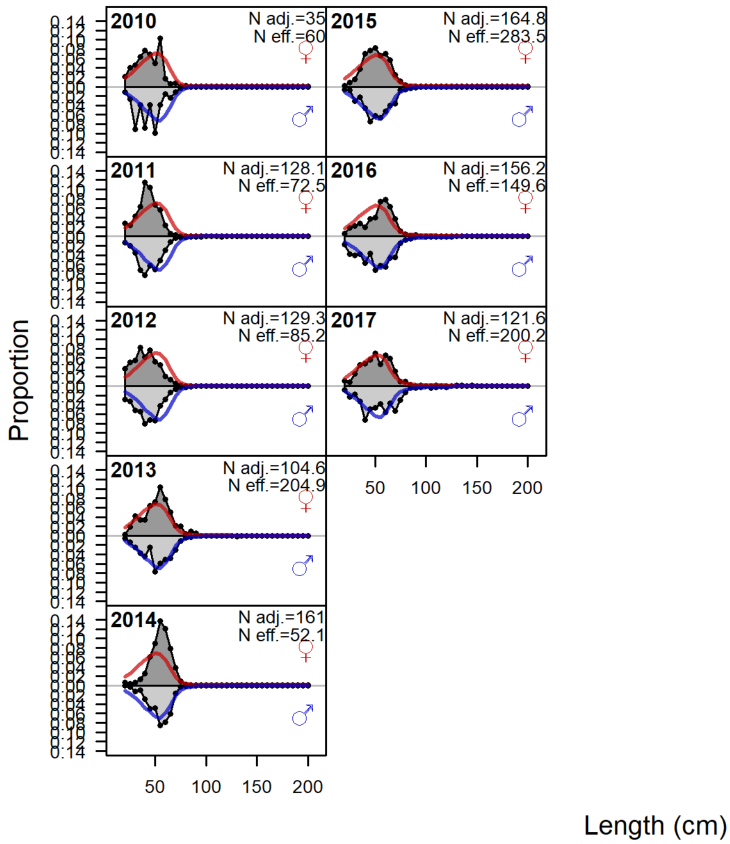

Figure A55: Length comps, discard, Fishery. 'N adj.' is the input sample size after data_weighting adjustment. N eff. is the calculated effective sample size used in the McAllister_Iannelli tuning method.

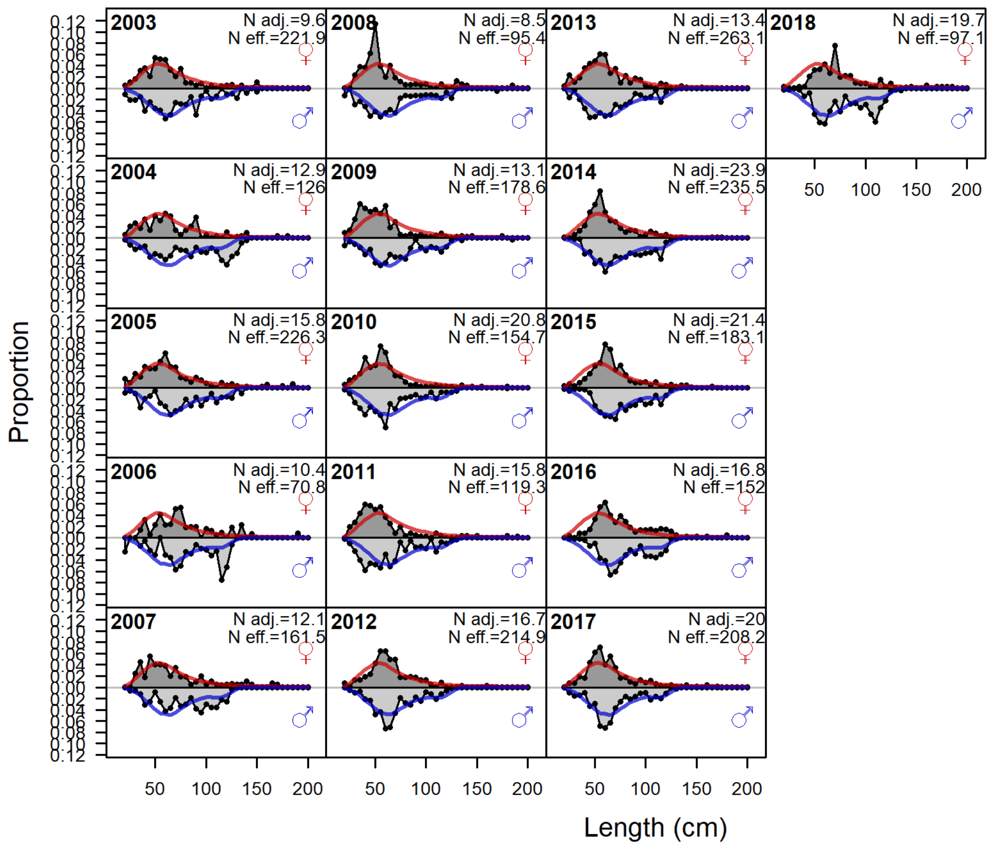

Figure A56: Length comps, whole catch, WCGBT Survey. 'N adj.' is the input sample size after data_weighting adjustment. N eff. is the calculated effective sample size used in the McAllister_Iannelli tuning method.

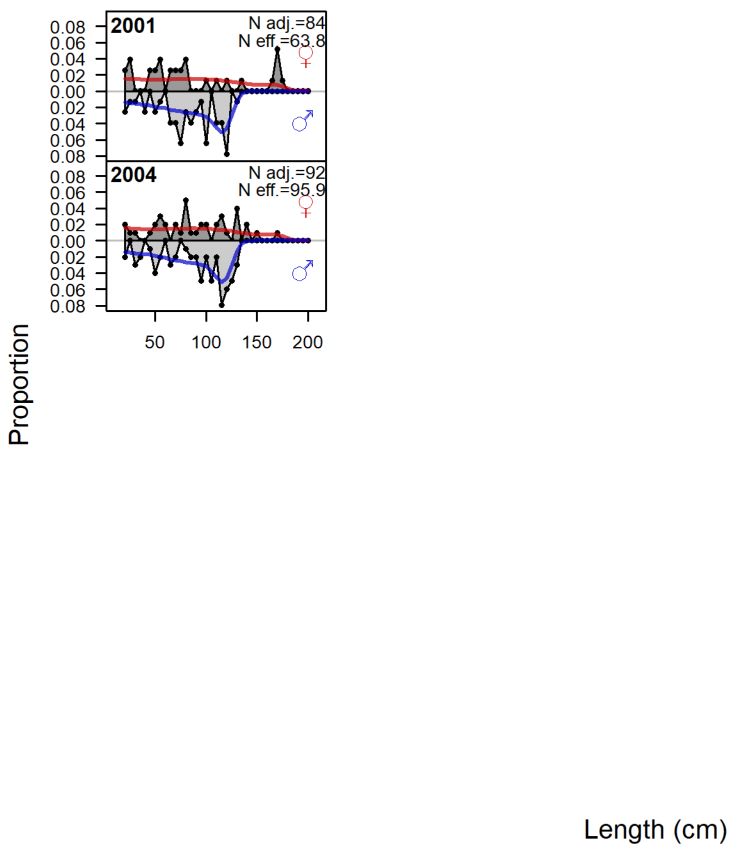

Figure A57: Length comps, whole catch, Triennial Survey. 'N adj.' is the input sample size after data_weighting adjustment. N eff. is the calculated effective sample size used in the McAllister_Iannelli tuning method.

References

Alaska Fisheries Science Center. 2018. Assessment of the skate stock complex in the Gulf of Alaska. Available from {https://www.afsc.noaa.gov/REFM/Docs/2018/GOA/GOAskate.pdf}.

Batdorf, C. 1990. Northwest Native Harvest. Hancock House Publishers Ltd.; Surrey, B.C., Canada.

Bizzarro, J. 2015. Comparative resource utilization of eastern north pacific skates (rajiformes: Rajidae) with applications for ecosystem-based fisheries management. WA: University of Washington.

Bizzarro, J. 2019. Manuscript in preparation.

Bizzarro, JJ and Broms, KM and Logsdon, MG and Ebert, DA and Yoklavich, MM and Kuhnz, LA and Summers, AP. 2014. Spatial segregation in eastern north Pacific skate assemblages. PloS one **9**(10).

Bizzarro, J., Robinson, H., Rinewalt, C., and Ebert, D. 2007. Comparative feeding ecology of four sympatric skate species off central California, USA. *In* Biology of skates. Springer. pp. 91–114.

Bowers, G. M. 1909. Report of The Commissioner For the Year Ending June 30, 1909. Part XXVIII. Washington Printing Office.

Bradburn, M.J. and Keller, A.A and Horness, B.H. 2011. The 2003 to 2008 US West Coast bottom trawl surveys of groundfish resources off Washington, Oregon, and California: estimates of distribution, abundance, length, and age composition. NOAA Technical Memorandum NMFS NOAA-TM-NMFS-NWFSC-114: 323 pp.

Brown, L.D., Cai, T.T., and DasGupta, A. 2001. Interval estimation for a binomial proportion. Statistical science: 101–117. JSTOR.

Calavan, T. 2019. Oregon Department of Fisheries; Wildlife; Personal Communication, Newport, OR, USA.

Castro-Aguirre, J.L., and Pérez, H.E. 1996. Catálogo sistemático de las rayas y especies afines de méxico: Chondrichthyes: Elasmobranchii: Rajiformes: Batoideiomorpha. Unam.

Castro-Aguirre, J., Schmitter, J., Balart, E., and Torres-Orozco, R. 1993. Sobre la distribución geográfica de algunos peces bentónicos de la costa oeste de baja california sur, méxico, con consideraciones ecológicas y evolutivas. *In* Anales de la escuela nacional de ciencias biológicas, méxico. pp. 75–102.

Chapman, W.M. 1944. The Latent Fisheries of Washington and Alaska. Washington State Department of Fisheries.

Chiquillo, Kelcie L and Ebert, David A and Slager, Christina J and Crow, Karen D. 2014. The secret of the mermaid's purse: Phylogenetic affinities within the Rajidae and the evolution of a novel reproductive strategy in skates. Molecular Phylogenetics and Evolution **75**: 245–251. Elsevier.

DeLacy, A.C., and Chapman, W.M. 1935. Notes on some elasmobranchs of puget sound, with descriptions of their egg cases. Copeia **1935**(2): 63–67. JSTOR.

Dorn, M and Cordue, P and Haist, V. 2007. Pacific Fishery Management Council, Portland, OR. Available from {{https://www.pcouncil.org/wp-content/uploads/STARreport_Skate.pdf}}.

Downs, D.E., and Cheng, Y.W. 2013. Length–length and width–length conversion of longnose skate and big skate off the pacific coast: Implications for the choice of alternative measurement units in fisheries stock assessment. North American journal of fisheries management **33**(5): 887–893. Taylor & Francis.

Ebert, D. 2003. Sharks, rays, and chimaeras of california. Univ of California Press.

Ebert, D.A., and Compagno, L.J. 2007. Biodiversity and systematics of skates (chondrichthyes: Rajiformes: Rajoidei). *In* Biology of skates. Springer. pp. 5–18.

Ebert, D.A., Smith, W.D., and Cailliet, G.M. 2008. Reproductive biology of two commercially exploited skates, raja binoculata and r. Rhina, in the western gulf of alaska. Fisheries Research **94**(1): 48–57. Elsevier.

Eschmeyer, W.N., and Herald, E.S. 1983. A field guide to pacific coast fishes: North america. Houghton Mifflin Harcourt.

Farrugia, T.J., Goldman, K.J., Tribuzio, C., and Seitz, A.C. 2016. First use of satellite tags to examine movement and habitat use of big skates beringraja binoculata in the gulf of alaska. Marine Ecology Progress Series **556**: 209–221.

Ford, P. 1971. Differential growth rate in the tail of the pacific big skate, (*Raja binoculata*). Journal of the Fisheries Board of Canada **28**(1): 95–98. NRC Research Press.

Francis, R.I.C.C. 2011. Data weighting in statistical fisheries stock assessment models. Canadian Journal of Fisheries and Aquatic Sciencies **68**: 1124–1138.

Gburski, C.M. and Gaichas, S.K. and Kimura, D.K. 2007. Age and growth of big skate (*Raja binoculata*) and longnose skate (*Raja rhina*) in the Gulf of Alaska. *In* Biology of Skates. Springer, Dordrecht.

Gertseva, V. 2019. Manuscript in preparation.

Gertseva, V and Schrippa, MJ. 2007. Status of the Longnose Skate (*Raja rhina*) off the continental US Pacific Coast in 2007. Pacific Fishery Management Council, Portland, OR. Available from {http://www.pcouncil.org/groundfish/stock-assessments/}.

Gertseva, V., and Taylor, I. 2011. Status of spiny dogfish shark resource off the continental us pacific coast in 2011. PFMC. 2011. Pacific Fishery Management Council, Portland, OR. Available from {http://www.pcouncil.org/groundfish/stock-assessments/}.

Gunderson, Donald Raymond and Sample, Terrance M. 1980. Distribution and abundance of rockfish off Washington, Oregon and California during 1977. Northwest and Alaska Fisheries Center, National Marine Fisheries Service. Available from {http://spo.nmfs.noaa.gov/mfr423-4/mfr423-42.pdf}.

Hamel, Owen S. 2015. A method for calculating a meta-analytical prior for the natural mortality rate using multiple life history correlates. ICES Journal of Marine Science: Journal du Conseil **72**(1): 62–69. doi: {10.1093/icesjms/fsu131}.

Hitz, C.R. 1964. Observations on egg cases of the big skate (raja binoculata girard) found in oregon coastal waters. Journal of the Fisheries Board of Canada **21**(4): 851–854. NRC Research Press.

Hoff, GR. 2009. Skate Bathyraja spp. egg predation in the eastern Bering Sea. J. Fish. Biol. **74**: 250–269.

Ishihara, H., Treloar, M., Bor, P., Senou, H., and Jeong, C. 2012. The comparative morphology of skate egg capsules (Chondrichthyes: Elasmobranchii: Rajiformes). Bulletin of the Kanagawa Prefectural Museum (Natural Science) **41**: 9–25.

Keller, A.A. and Wallace, J.R. and Methot, R.D. 2017. The Northwest Fisheries Science Center's West Coast Groundfish Bottom Trawl Survey: History, Design, and Description. NOAA Technical Memorandum NMFS NOAA-TM-NMFS-NWFSC-136: 38 pp.

King, J., and McFarlane, G. 2009. Biological results of the strait of georgia spiny dogfish (squalus acanthias) longline survey, october 10-22, 2008. Fisheries; Oceans Canada, Science Branch, Pacific Region.

King, J.R., Surry, A.M., Garcia, S., and P.J. Starr. 2015. Big skate (Raja binoculata) and longnose skate (R. rhina) stock assessments for British Columbia. Ottawa : Canadian Science Advisory Secretariat.

King, JR and McFarlane, GA. 2010. Movement patterns and growth estimates of big skate (*Raja binoculata*) based on tag-recapture data. Fish. Res. **101**: 50–59.

Lippert, G. 2019. Washington Department of Fisheries; Wildlife; Personal Communication, Olympia, Washington, USA.

Love, Milton S. 2011. Certainly more than you want to know about the fishes of the Pacific Coast: a postmodern experience. Really Big Press.

Maunder, M.N., Deriso, R.B., Schaefer, K.M., Fuller, D.W., Aires-da-Silva, A.M., Minte-Vera, C.V., and Campana, S.E. 2018. The growth cessation model: A growth model for species showing a near cessation in growth with application to bigeye tuna (thunnus obesus). Marine biology **165**(4): 76. Springer.

McEachran, J., and Miyake, T. 1990. 1990. Zoogeography and bathymetry of skates (chondrichthyes, rajidae). Elasmobranchs as living resources. Advances in biology, Ecology, Systematics and the status of the fisheries: 305–326.

McFarlane GA and King JR. 2006. Age and growth of big skate (*Raja binoculata*) and longnose skate (*Raja rhina*) in British Columbia waters. Fisheries Research **May 1 (2-3)**: 169–78.

Mecklenburg, CW and Mecklenburg, TA and Thorsteinson, LK. 2002. Fishes of Alaska. American Fisheries Society, Bethesda, Maryland.

Methot, RD Jr. and Wetzel, CR and Taylor, IG. 2019. Stock Synthesis User Manual Version 3.30.13. NOAA Fisheries. Seattle, WA. Available from {https://vlab.ncep.noaa.gov/web/stock-synthesis}.

Methot, Richard D. and Wetzel, Chantell R. 2013. Stock synthesis: A biological and statistical framework for fish stock assessment and fishery management. Fisheries Research **142**: 86–99.

Miller, B.S., Cross, J.N., Steinfort, S.N., Fresh, K.L., and Simenstad, C.A. 1980. Nearshore fish and macroinvertebrate assemblages along the strait of juan de fuca including food habits of the common nearshore fish.

Pacific Fishery Management Council. 2018. Status of the Pacific Coast Groundfish Fishery. Available from {http://www.pcouncil.org/wp-content/uploads/2017/02/SAFE_Dec2016_02_2}.

Punt AE and Smith DC and KrusicGolub K and Robertson S. 2008. Quantifying age-reading error for use in fisheries stock assessments, with application to species in Australia's southern and eastern scalefish and shark fishery. Canadian Journal of Fisheries and Aquatic Sciences.

Richards, F. 1959. A flexible growth function for empirical use. Journal of experimental Botany **10**(2): 290–301. Oxford University Press.

Stevenson, DE and Orr, JW and Hoff, GR and McEachran, JD. 2008. Emerging patterns of species richness, diversity, population density, and distribution in the skates (Rajidae) of Alaska. Fish Bull **106**: 24–39.

Stewart, I.J., Wallace, J.R., and McGilliard, C. 2009. Status of the us yelloweye rockfish resource in 2009. *In* Pacific Fishery Management Council, Portland, OR. Available from {http://www.pcouncil.org/groundfish/stock-assessments/}.

Taylor, I.G., Stewart, I.J., Hicks, A.C., Garrison, T.M., Punt, A.E., Wallace, J.R., Wetzel, C.R., Thorson, J.T., Takeuchi, Y., Ono, K., Monnahan, C.C., Stawitz, C.C., A'mar, Z.T., Whitten, A.R., Johnson, K.F., Emmet, R.L., Anderson, S.C., Lambert, G.I., Stachura, M.M., Cooper, A.B., Stephens, A., Klaer, N.L., McGilliard, C.R., Iwasaki, W.M., Doering, K., and Havron, A.M. 2019. R4ss: R code for stock synthesis. Available from https://github.com/r4ss.

Taylor IG and Cope, J and Hamel O and Thorson, J. 2013. Deriving estimates of OFL for species in the "Other Fish" complex or potential alternative complexes. Pacific Fishery Management Council, Portland, OR. Available from {http://www.pcouncil.org/groundfish/stock-assessments/}.

Thorson, James T. and Barnett, Lewis A. K. 2017. Comparing estimates of abundance trends and distribution shifts using single- and multispecies models of fishes and biogenic habitat. ICES Journal of Marine Science: Journal du Conseil: fsw193. doi: {10.1093/icesjms/fsw193}.

Thorson, J. T. and Shelton, A. O. and Ward, E. J. and Skaug, H. J. 2015. Geostatistical delta-generalized linear mixed models improve precision for estimated abundance indices for West Coast groundfishes. ICES Journal of Marine Science **72**(5): 1297–1310. doi: {10.1093/icesjms/fsu243}.

von Bertalanffy, L. 1938. A quantitative theory of organic growth. Human Biology **10**: 181–213.

Zeiner, S.J. and P. Wolf. 1993. Growth characteristics and estimates of age at maturity of two species of skates (*Raja binoculata*) and (*Raja rhina*) from Monterey Bay, California.